MARTIN MARIETTA ENERGY SYSTEMS LIBRARIES

3 4456 0050331 9

CENTRAL RESEARCH LIBRARY
DOCUMENT COLLECTION

ORNL-3858, Vol. I
UC-34 – Physics
TID-4500 (45th ed.)

NEUTRON PHYSICS DIVISION
ANNUAL PROGRESS REPORT
FOR PERIOD ENDING AUGUST 1, 1965

CENTRAL RESEARCH LIBRARY
DOCUMENT COLLECTION
LIBRARY LOAN COPY
DO NOT TRANSFER TO ANOTHER PERSON
If you wish someone else to see this document, send in name with document and the library will arrange a loan.

OAK RIDGE NATIONAL LABORATORY
operated by
UNION CARBIDE CORPORATION
for the
U.S. ATOMIC ENERGY COMMISSION

Printed in USA. Price $3.00. Available from the Clearinghouse for Federal Scientific and Technical Information, National Bureau of Standards, U.S. Department of Commerce, Springfield, Virginia

LEGAL NOTICE

This report was prepared as an account of Government sponsored work. Neither the United States, nor the Commission, nor any person acting on behalf of the Commission:

A. Makes any warranty or representation, expressed or implied, with respect to the accuracy, completeness, or usefulness of the information contained in this report, or that the use of any information, apparatus, method, or process disclosed in this report may not infringe privately owned rights; or

B. Assumes any liabilities with respect to the use of, or for damages resulting from the use of any information, apparatus, method, or process disclosed in this report.

As used in the above, "person acting on behalf of the Commission" includes any employee or contractor of the Commission, or employee of such contractor, to the extent that such employee or contractor of the Commission, or employee of such contractor prepares, disseminates, or provides access to, any information pursuant to his employment or contract with the Commission, or his employment with such contractor.

ORNL-3858, Vol. I

Contract No. W-7405-eng-26

NEUTRON PHYSICS DIVISION

ANNUAL PROGRESS REPORT

For Period Ending August 1, 1965

E. P. Blizard, Director

A. D. Callihan, Associate Director
F. C. Maienschein, Associate Director

Group Leaders

C. E. Clifford, Reactor and Weapons Radiation Shielding
R. G. Alsmiller, Theoretical Space and High-Energy Accelerator Shielding
R. W. Peelle, Experimental Space and High-Energy Accelerator Shielding

NOVEMBER 1965

OAK RIDGE NATIONAL LABORATORY
Oak Ridge, Tennessee
operated by
UNION CARBIDE CORPORATION
for the
U. S. ATOMIC ENERGY COMMISSION

MARTIN MARIETTA ENERGY SYSTEMS LIBRARIES

3 4456 0050331 9

Preface

The Neutron Physics Division is again issuing its annual progress report in two volumes, with the papers describing research performed in the high-energy radiation shielding program collected in Volume II. The Division is also continuing its policy of including only abbreviated papers in the annual report, either summaries of work in progress or abstracts of papers published elsewhere. As was pointed out in last year's preface, this policy was instituted to give authors more time to spend on topical reports and journal articles and its success is evidenced by the 50% increase in the number of papers included in the list of publications beginning on page 65 of this volume.

The reader will notice that for some of the abstracts included here the corresponding papers are not yet published. This is done only for those papers that have progressed to the point that publication is either imminent or at least considered to be not too far in the future. Also, we are including abstracts of papers which cover work that was summarized in last year's annual. This is done to call attention to the fact that topical papers on these particular subjects have now been issued and to help in locating them. As before, work that was performed during the reporting period but not yet described in a separate paper is summarized in this report.

Contents

1. NUCLEAR AND REACTOR PHYSICS 1

1.1 Neutron Scattering Cross Sections for Silicon Determined by Time-of-Flight Technique – J. A. Biggerstaff, J. K. Dickens, M. V. Harlow, Jr., W. E. Kinney, and F. G. Perey 1

1.2 Local-Energy Approximation for Finite Range in Stripping Reactions – J. K. Dickens, R. M. Drisko, F. G. Perey, and G. R. Satchler 2

1.3 Inelastic Scattering of Deuterons from ^{60}Ni and ^{114}Cd – J. K. Dickens, F. G. Perey, and G. R. Satchler 2

1.4 Level Structure of ^{64}Zn – J. K. Dickens, F. G. Perey, and R. J. Silva 3

1.5 Dependence of Proton Optical-Model Parameters upon Experimental Errors – J. K. Dickens 5

1.6 Elastic and Inelastic Scattering of 12.0-Mev Protons from ^{62}Ni, ^{63}Cu, and ^{64}Zn: Tabulated Differential Cross Sections – J. K. Dickens and R. J. Silva 7

1.7 Elastic Scattering of 12.0- and 14.0-Mev Deuterons from ^{90}Zr and the Reaction ^{90}Zr$(d,p)^{91}$Zr: Tabulated Differential Cross Sections – J. K. Dickens, F. G. Perey, and R. J. Silva 7

1.8 Analysis of Elastic and Inelastic Scattering of Neutrons from ^{206}Pb, ^{208}Pb, and ^{209}Bi Below 4.5 Mev – W. R. Smith 7

1.9 Use of Elastic-Scattering Parameters in (d,p) Stripping Calculations – W. R. Smith 8

1.10 DWBA Analysis of the ^{90}Zr$(d,p)^{91}$Zr Reaction at Energies Between 3.5 and 5.5 Mev – W. R. Smith 8

1.11 Regions of Validity of the (d,p) Coulomb-Stripping Approximation – W. R. Smith 8

1.12 Integral Spectra and Dose Conversion Factors for Am-Be, Po-Be, Pu-Be, and Am-B Neutron Sources – S. K. Mehta and W. R. Burrus 8

1.13 Simultaneous Measurements of the Neutron-Capture and Fission Cross Sections of ^{235}U – L. W. Weston, R. Gwin, G. de Saussure, J. E. Russell, R. W. Hockenbury, and R. Ingle 9

1.14 Measurement of α, the Ratio of the Neutron-Capture Cross Section to the Fission Cross Section, for ^{235}U in the Energy Region 3.25 ev to 1.8 kev – G. de Saussure, L. W. Weston, J. E. Russell, R. Gwin, and R. W. Hockenbury 10

1.15 Study of Resonance Parameters of Pu – J. Blons, H. Derrien, A. Michaudon, P. Ribon, and G. de Saussure 10

1.16 Pulsed-Neutron Measurements of Diffusion Parameters in Ordinary Ice as a Function of Temperature by the Method of Time-Dependent Neutron Diffusion – E. G. Silver 10

1.17 Photoneutron Spectra and Cross Sections for ^{12}C and ^{16}O – V. V. Verbinski and J. C. Courtney 11

1.18 Differential Neutron Cross Sections for Several Materials Bombarded by 14-, 18-, and 56-Mev Protons – M. Young, V. V. Verbinski, W. R. Burrus, and J. C. Courtney 11

1.19 Deuteron Polarization from the $^{9}Be(p,d)^{8}Be$ Reaction at 3 to 5 Mev – V. V. Verbinski and M. S. Bokhari 12

2. CRITICAL EXPERIMENTS 13

2.1 Determination of Neutron Flux in Nuclear Reactors by the Uncollided-Flux Estimator Applied to Monte Carlo Collisions – J. W. Webster 13

2.2 Boundary Conditions for the Cylindricalized Cell of Reactor-Lattice Calculations – J. W. Webster 13

2.3 One-Velocity Monte Carlo Calculations of Uranium-Metal Critical Geometries – J. T. Mihalczo 13

2.4 Increased Yield from Fast Burst Reactors: Parts I and II – J. T. Mihalczo 14

2.5 Criticality of a Single Unit of Aqueous Uranyl Fluoride Solution Enriched to 5% in ^{235}U – J. W. Webster and E. B. Johnson 14

2.6 Critical Dimensions of Arrays of Aqueous Uranyl Fluoride Solution Containing Uranium Enriched to 5% in ^{235}U – E. B. Johnson 15

2.7 Critical Experiments with SPERT-D Fuel Elements – E. B. Johnson and R. K. Reedy, Jr. 16

2.8 Criticality Safety Tests for a Proposed Irradiation Facility – E. B. Johnson 17

2.9 High Flux Isotope Reactor Critical Experiment No. 3 – J. T. Thomas 17

2.10 Experimental Evaluation of Handling Procedures for High Flux Isotope Reactor Fuel Elements Outside the Reactor – J. T. Thomas and S. J. Raffety 17

2.11 Experiments for the Development of a Reactivity Acceptance Test of High Flux Isotope Reactor Fuel Elements – J. T. Thomas and S. J. Raffety 18

2.12 Potassium Reactivity Coefficient in Small Reflected UO_2 Assemblies – J. T. Mihalczo 19

2.13 Experiments and Calculations on Uranium-Molybdenum Alloy Critical Assemblies – J. T. Mihalczo and W. E. Kinney 19

2.14 Static and Dynamic Transport Calculations for Pulsed-Neutron Experiments with Spheres of Uranyl Nitrate Solution – D. W. Magnuson 19

3. REACTOR SHIELDING 20

3.1 Measurement of the Thermal-Neutron Flux down a Rectangular Concrete Duct – F. J. Muckenthaler, J. J. Manning, J. L. Hull, K. M. Henry, L. B. Holland, and D. R. Ward 20

3.2 Measurement of the Fast-Neutron Dose Rate down a Rectangular Concrete Duct – F. J. Muckenthaler, K. M. Henry, J. J. Manning, J. L. Hull, L. B. Holland, and D. R. Ward 21

3.3 Monte Carlo Calculation of the Fast-Neutron Dose Rate Along the Center Line of a Straight Rectangular Duct Using the Albedo Concept, and Comparison with Experiment – R. E. Maerker 23

3.4 A Monte Carlo Determination of Intermediate-Energy Differential Neutron Albedos for Concrete – W. A. Coleman and R. E. Maerker 24

3.5 Monte Carlo Determination of the Differential Thermal-Neutron Angular Albedos and Capture-Gamma Dose Rates for Concrete Arising from the Slowing Down of Incident Intermediate-Energy Neutrons – R. E. Maerker 24

3.6 Investigation of the Accuracy of the Monte Carlo Method for Calculating Differential Angular Thermal-Neutron Albedos and Thermal-Neutron Captures for a Weakly Absorbing Medium Such as Concrete – R. E. Maerker 27

3.7 Single-Velocity Calculation and Measurement of Differential Angular Thermal-Neutron Albedos for Concrete – R. E. Maerker and F. J. Muckenthaler 29

3.8 Calculation and Measurement of the Fast-Neutron Differential Dose Albedo for Concrete – R. E. Maerker and F. J. Muckenthaler 30

3.9 A Calculation of the Neutron Dose in Ordinary Concrete Due to Air-Scattered Neutrons from a Point Fission Source – D. K. Trubey 31

3.10 Measured Neutron Source Spectra for Angular Scattering Experiments with Small Cylinders – J. C. Courtney and V. V. Verbinski 31

3.11 Fast-Neutron Scattering from Small Cylinders of Steel, Aluminum, Graphite, Concrete, and Lithium Hydride – V. V. Verbinski and J. C. Courtney 31

3.12 Measurement of the Neutron-Source Distribution in a Pool-Type Research Reactor – M. S. Bokhari and V. V. Verbinski 32

3.13 Measurements and Calculations of Spectral and Spatial Details of Fast-Neutron Flux in Water Shields – V. V. Verbinski, M. S. Bokhari, and J. C. Courtney 32

3.14 Propagation of Neutron Waves Through Heterogeneous Multiplying and Non-multiplying Media – V. R. Cain 33

3.15 Differential Dose Albedos for Calculation of Gamma-Ray Reflection from Concrete – M. B. Wells 33

3.16 Neutron and Gamma Radiation Penetration into Concrete-Shielded Underground Structures – R. L. French, M. B. Wells, and N. M. Schaeffer 34

3.17 Structural and Shielding Considerations in the Design of Hardened Facilities – R. H. Karcher and J. H. Wilson 34

3.18 Penetration of Neutron and Gamma Radiation Through the Openings of Underground Structures – R. L. French, M. B. Wells, and N. M. Schaeffer 35

3.19 Gamma-Ray Attenuation Coefficient for Germanium – G. T. Chapman 35

3.20 Gamma-Ray Spectrum Emitted by a Stainless-Steel-Clad Reactor (BSR-II) – G. T. Chapman and W. R. Burrus 35

3.21 SNAP Reactor Installation at the Tower Shielding Facility – C. E. Clifford, F. J. Muckenthaler, and J. Lewin 36

3.22 Calculations for the Scattering of Neutrons by Air, Ground, and Structures for SNAP Shielding Experiments – F. B. K. Kam 39

3.23 Secondary Gamma-Ray Problem in Man-Rated Shields – F. B. K. Kam and E. Whitesides 39

3.24 Monte Carlo Calculations of Neutron Penetration Through Shaped SNAP Shields – F. B. K. Kam 40

3.25 Slowing-Down Spectra of Neutrons in Lithium Hydride – V. V. Verbinski 40

3.26 Angular Distributions of Low-Energy Neutrons Leaking from Various Scattering Materials – V. V. Verbinski 40

4. RADIATION SHIELDING INFORMATION CENTER 42

4.1 Program of the Radiation Shielding Information Center – S. K. Penny, D. K. Trubey, and B. F. Maskewitz 42

4.2 Literature Examined by the Radiation Shielding Information Center – S. K. Penny, D. K. Trubey, and M. B. Emmett 43

4.3 A Survey of Empirical Functions Used to Fit Gamma-Ray Buildup Factors – D. K. Trubey 44

4.4 Comparison of Three Methods Used to Calculate Gamma-Ray Transport in Iron – D. K. Trubey, S. K. Penny, and K. D. Lathrop 44

4.5 Survey of Methods for Calculating Gamma-Ray Heating – H. C. Claiborne 44

4.6 Tabulated Values of Scattered Gamma-Ray Fluxes in Iron Interpolated from Moments-Method Calculations –D. K. Trubey 45

4.7 A Comparison of First- and Last-Flight Expectation Values Used in an O5R Monte Carlo Calculation of Neutron Distributions in Water – D. K. Trubey and M. B. Emmett 45

4.8 Some Calculations of the Fast-Neutron Distribution in Ordinary Concrete from Point and Plane Isotropic Fission Sources – D. K. Trubey and M. B. Emmett 45

4.9 Some Conclusions Regarding the Use of the S_n Method in Shielding Calculations – J. W. Webster 45

4.10 The Exponential Transform as an Importance Sampling Device – A Review – F. H. S. Clark 46

5. MATHEMATICS AND COMPUTER PROGRAMS 47

5.1 JTMS1(O5R:SOURCE), a Neutron Distribution Subroutine for the O5R Monte Carlo Code – J. T. Mihalczo, G. W. Morrison, and D. C. Irving 47

5.2 OGRE-P3, an OGRE System Monte Carlo Code for the Calculation of Gamma-Ray Dose Rate at Arbitrary Points from Point Sources in Laminated Slab Geometry – D. K. Trubey and M. B. Emmett 47

5.3 OGRE-G, an OGRE System Monte Carlo Code for the Calculation of Gamma-Ray Dose Rate at Arbitrary Points in an Arbitrary Geometry – D. K. Trubey and M. B. Emmett 47

5.4 O5R Monte Carlo Analysis Routines of Use in Reactor Problems – J. T. Mihalczo, G. W. Morrison, and D. C. Irving 48

5.5 ACTI-FK(O5R:ANALYSIS), a General-Purpose Code to Analyze O5R Collision Tapes – F. B. K. Kam and K. D. Franz 48

5.6 A Cylindrical Volume Source Routine for the O5R Monte Carlo Code – L. G. Mooney 49

5.7 The FORTRAN Code FANLFR2 to Calculate Nonlocality and Finite Range Effects in Stripping and Pickup Reactions Using the Local-Energy Approximation – J. K. Dickens and F. G. Perey 49

5.8 The FORTRAN Code XBACK3: an Aid in the Analysis and Data Reduction of Pulse-Height Spectra – J. K. Dickens 50

5.9 JTMI1(O5R:INELAS), a FORTRAN Subroutine for Describing Inelastic and $(n,2n)$ Reactions – J. T. Mihalczo, G. W. Morrison, and D. C. Irving 52

5.10 TECHTRAN – A Load-and-Go Compiler for Programs Written in Data-Sheet Format – J. W. Wachter and R. T. Santoro 52

5.11 DWB Deuteron Stripping Computer Program – W. R. Smith 55

5.12 Generalized Hauser-Feshbach Nuclear-Scattering Computer Programs – W. R. Smith 55

5.13 Data-Reduction Programs for the CDC 160-A Computer – W. E. Kinney 55

5.14 Fourier Analysis of Uniform Random-Number Generators – R. R. Coveyou and R. D. MacPherson 55

5.15 Numerical Solution of the Lagrange-Multiplier Formulation with Several Constraints – F. B. K. Kam and F. H. S. Clark 56

5.16 Nonnormal Distributions of the Mean Computed from Sample Characteristics – F. H. S. Clark and N. A. Betz 56

5.17 Significance Arithmetic for FORTRAN – W. R. Burrus and B. W. Rust 56

5.18 The Use of Mathematical Programming for Solving Singular and Poorly Conditioned Systems of Equations – J. Replogle, B. D. Holcomb, and W. R. Burrus 57

5.19 A Simple Algorithm for Computing the Generalized Inverse of a Matrix – B. W. Rust and W. R. Burrus 57

5.20 A FORTRAN Subroutine Package for Linear Programming – C. Schneeberger and W. R. Burrus 57

5.21 Neutron-Cross-Section Library – D. C. Irving, F. H. S. Clark, and J. Gillen 58

6. RADIATION DETECTOR STUDIES (I) 59

6.1 Fast-Neutron Spectrometer Capable of Nanosecond Time Gating – L. E. Beghian, S. Wilenski, and W. R. Burrus 59

6.2 Development of an Epithermal-Neutron Spectrometer – T. V. Blosser and R. M. Freestone, Jr. 59

6.3 Isotropically Responding Fast-Neutron Dosimeter – T. V. Blosser 61

6.4 New Method for the Evaluation of Neutron Emission, Kerma, Kerma Equivalent, Dose Equivalent, and the Spectrum Below 1 Mev for (α,n) Sources, Using Bonner Spheres – S. K. Mehta 62

6.5 Digital Filter for Unfolding Pulse-Height Distributions – H. Young and W. R. Burrus 62

6.6 Fast-Neutron Spectroscopy with Organic Scintillators – V. V. Verbinski, W. R. Burrus, J. C. Courtney, and R. Textor 63

6.7 Use of a Digital Computer in Time-of-Flight Experiments – R. Gwin, L. W. Weston, and R. Ingle 63

6.8 Fast-Neutron Spectrometer for Reactor Environments – V. V. Verbinski and M. S. Bokhari 64

PUBLICATIONS 65

1. Nuclear and Reactor Physics

1.1 NEUTRON SCATTERING CROSS SECTIONS FOR SILICON DETERMINED BY TIME-OF-FLIGHT TECHNIQUE

J. A. Biggerstaff[1] M. V. Harlow, Jr.
J. K. Dickens W. E. Kinney
F. G. Perey

Absolute differential cross sections for elastic scattering and inelastic scattering ($Q = -1.78$ Mev) of 5.03- and 5.6-Mev neutrons from natural silicon have been measured at laboratory angles of 21, 31, 41, 56, 72, 92, 112, and 132°. Bursts of deuterons, 2 nsec wide at half maximum, from the ORNL 3-Mv Van de Graaff accelerator bombarded a double-foil deuterium gas target, thereby producing, by the $D(d,n)^3He$ reaction, bursts of monoenergetic neutrons. Samples of silicon and carbon, the latter used as a standard, were placed at zero degrees and at distances of from 7 to 12 cm from the target. Both samples were right-circular cylinders approximately $\frac{1}{3}$ mean free path thick to 5-Mev neutrons.

Scattered neutrons were detected by a scintillator, which utilized neutron-gamma discrimination, located 3 m from the sample. Figure 1.1.1 shows a schematic diagram of a typical scattering geometry. A long counter, placed at 65°, monitored the neutron intensity from the target. Time-of-flight spectra of the scattered neutrons were taken with a 4096-channel, two-dimensional pulse-height analyzer in which input pulses were sorted according to their height and their time-of-flight amplitude. Output paper tapes from this analyzer were then fed into a CDC 160-A computer, where they were corrected for background effects and for time walk with pulse height.[2] Figure 1.1.2 shows one of these corrected time spectra.

Absolute differential cross sections for silicon were obtained by normalizing relative cross sections of silicon to those measured for the carbon sample at each angle. Although multiple scattering corrections to the data are not yet completed, the uncorrected 5.03-Mev cross sections are in good qualitative agreement with 4.8-Mev data

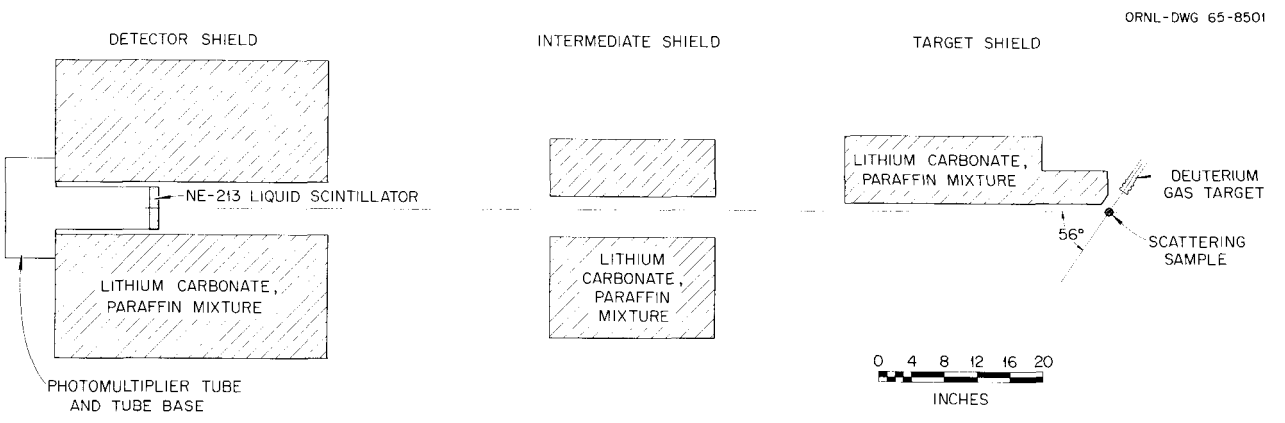

Fig. 1.1.1. Schematic Diagram of Scattering Geometry for Measurement at 56°. Cross-sectional view taken in the horizontal plane.

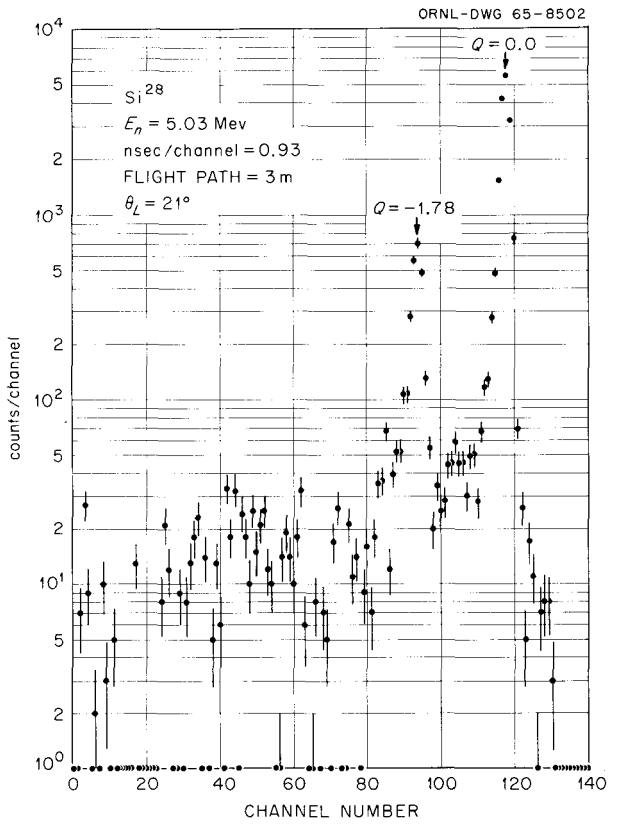

Fig. 1.1.2. Corrected Time Spectrum for ^{28}Si.

taken elsewhere.[3] Final corrected results will partially satisfy a priority 1 request for silicon cross-section data.[4]

References and Notes

[1]Physics Division.

[2]W. E. Kinney, *Data Reduction Programs for the CDC 160-A Computer,* ORNL-TM-1208 (in preparation).

[3]M. D. Goldberg *et al.*, *Angular Distributions in Neutron-Induced Reactions,* BNL-400, 2d ed., vol. I, p. 14-28-1 (October 1962).

[4]A. B. Smith, compiler, *Compilation of Requests for Nuclear Cross Section Measurements,* WASH-1047 (EANDC (US)-53"u"), p. 18 (February 1964).

1.2 LOCAL-ENERGY APPROXIMATION FOR FINITE RANGE IN STRIPPING REACTIONS[1]

J. K. Dickens F. G. Perey
R. M. Drisko[2] G. R. Satchler[3]

Approximate treatments of the finite-range effects in distorted-wave calculations of stripping and pickup reactions are discussed. Preliminary results which compare the local-energy approximation with exact calculations on some typical examples are presented. The ^{40}Ca$(d,p)^{41}$Ca and ^{16}O$(n,d)^{15}$N examples are treated. These results indicate that the local-energy approximation is a good one and should be used when exact calculations are not available.

References and Notes

[1]Abstract of published paper: *Phys. Letters* **15**, 337 (1965).

[2]Electronuclear Division.

[3]Physics Division.

1.3 INELASTIC SCATTERING OF DEUTERONS FROM ^{60}Ni AND ^{114}Cd[1]

J. K. Dickens F. G. Perey
G. R. Satchler[2]

Differential cross sections for inelastic scattering from the first excited states of ^{114}Cd and ^{60}Ni were measured for deuteron bombarding energies between 8 and 15 Mev for ^{114}Cd, and between 9.9 and 13.6 Mev for ^{60}Ni. The data were analyzed by the distorted-wave method using the collective model of excitation. Good agreement with experiment was obtained for all cases, but only by deforming both real and imaginary parts of the optical potential and by including Coulomb excitation. Real coupling alone considerably underestimates the magnitude of the cross sections, even though for nickel it reproduces slightly better the experimental angular distributions. At the lower energies there are large contributions from Coulomb excitation and its interference with the nuclear excitation.

References and Notes

[1]Abstract of paper submitted for publication in *Nuclear Physics* and of ORNL-TM-1242 (to be published).

[2]Physics Division.

1.4 LEVEL STRUCTURE OF ^{64}Zn

J. K. Dickens F. G. Perey
R. J. Silva[1]

During the experiments to measure elastic and inelastic scattering of 11.0- and 12.0-Mev protons from ^{64}Zn it became evident that the available information on the excited states of ^{64}Zn might not be sufficient and that the resulting theoretical analyses of these data would be hindered. Therefore, the experimental program was modified to study the level structure of ^{64}Zn. Specifically, at angles of 45 and 80°, using 12.0-Mev protons, sufficient data were accumulated that uncertainties in peak position due to counting statistics could be reduced to less than 10 kev. The experimental procedure was the same as that used to study the excited states of ^{64}Ni.[2]

Figure 1.4.1 shows the spectrum obtained at 80°. Proton groups resulting from scattering by zinc can definitely be distinguished from those resulting from scattering by the contaminants by utilizing the kinematics of the scattering as well as the expected magnitudes of the inelastic scattering. The proton groups can be distinguished

Table 1.4.1. ^{64}Zn Excited States

Peak Number	E_x(Mev)[a]	Peak Number	E_x(Mev)[a]
1	0.99	22	4.16
2	1.80	23[b]	4.31
3	1.90	24[b]	4.39
4	2.31	25	4.46
5	2.61	26	4.50
6	2.74	27	4.54
7	2.79	28	4.66
8	3.00	29	4.70
9	3.08	30	4.75
10	3.20	31[b]	4.83
11	3.30	32	4.94
12	3.37	33	5.00
13[b]	3.45	34	5.06
14	3.55	35	5.14
15[b]	3.60	36[b]	5.21
16	3.71	37[b]	5.30
17	(3.81)	38[b]	5.41
18	3.86	39	5.50
19	3.93	40	5.63
20	4.03	41	5.73
21	(4.12)		

[a]An error of ±10 kev is assigned to all levels.

[b]The proton group associated with this level has a width larger than expected for a single level and may include scattering by more than one excited state of ^{64}Zn.

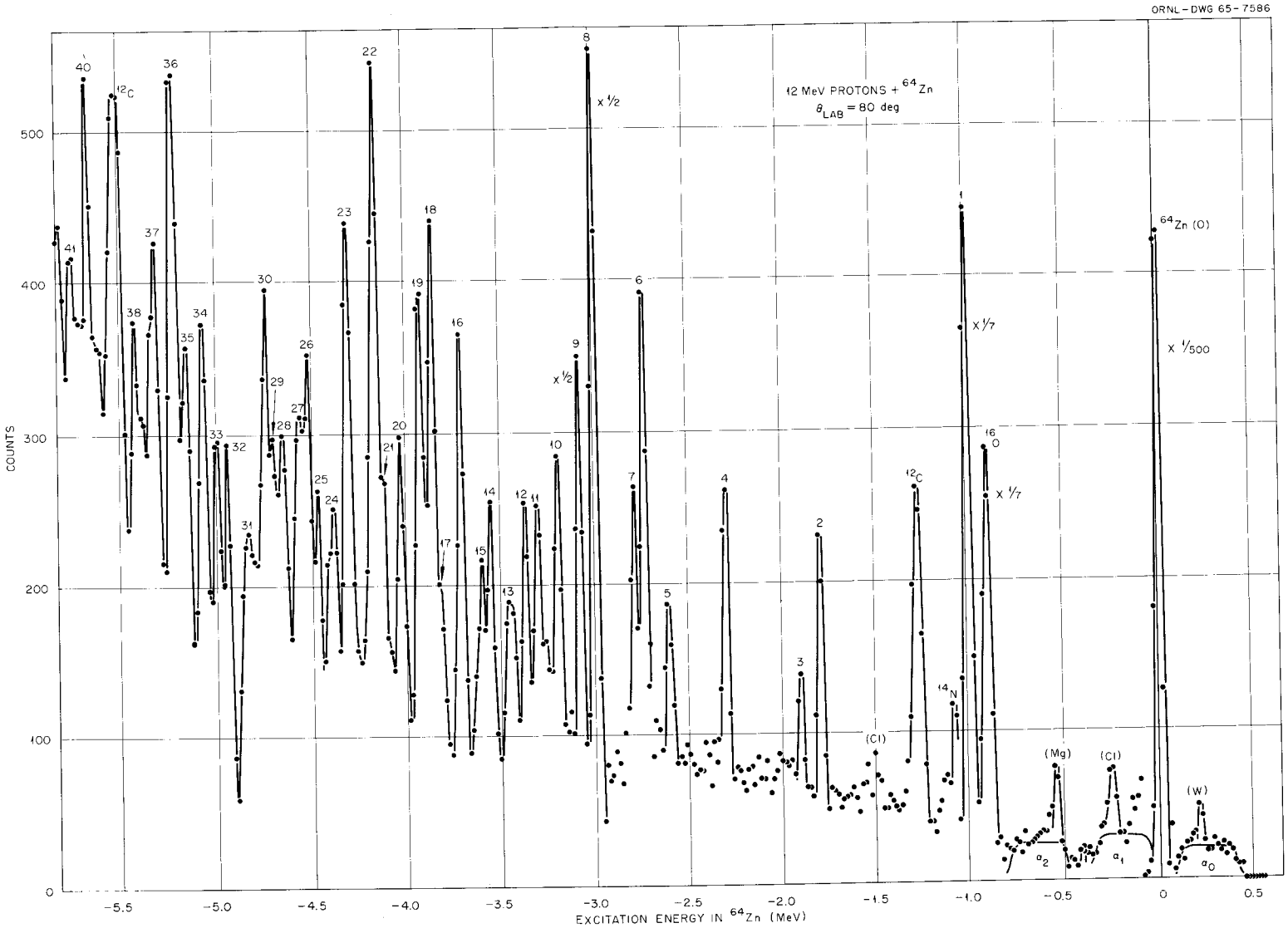

Fig. 1.4.1. Pulse-Height Spectrum of 12.0-Mev Protons Scattered by ^{64}Zn at 80°. Peaks corresponding to Zn excited states are numbered and are identified in Table 1.4.1. Peaks corresponding to protons scattered by a target impurity are marked with the symbol for that nucleus (symbols in parentheses indicate tentative identification). The three broad peaks at the high-energy end of the spectrum are alpha groups from the $^{64}Zn(p,\alpha)^{61}Cu$ reaction.

from the alpha groups by the definitely different pulse-height responses. The isotopic composition of the target was >99% of ^{64}Zn, and it is unlikely that any numbered proton group in Fig. 1.4.1 could result from proton scattering by nuclei other than ^{64}Zn.

Energies of excitation were obtained at several angles for both incident energies. The values were averaged to obtain the excited states presented in Table 1.4.1. In Fig. 1.4.1, the groups from ^{64}Zn are labeled with the peak numbers corresponding to the associated excited states given in Table 1.4.1. In some cases, indicated in the table, the associated proton groups had widths >40 kev, and it is probable that these groups consist of more than one component. In two cases, peaks 18 and 22, smaller bulges on the high-energy side of the larger peak suggested proton scattering from two ^{64}Zn levels with a difference in excitation of ~40 kev. These occurred on all spectra analyzed, but were never clearly resolved. Peak-stripping techniques were applied to the two 12-Mev spectra, and the resulting excitation energies for the less-excited states are shown in parentheses.

Excitation energies for 41 levels between 0.99 and 5.73 Mev are reported, but it is unlikely that all of the levels in this energy region were found. In addition to levels which could not be resolved, levels with large spins are not appreciably excited by proton scattering; the spins of most of these 41 states will be less than 6. Angular distributions for 12.0-Mev proton scattering have been obtained for 21 levels between 0.99 and 4.31 Mev;[3] these data will be analyzed using a deformable optical model to try to obtain spins and parities for several of these levels.

References and Notes

[1]Chemistry Division.

[2]J. K. Dickens, F. G. Perey, and R. J. Silva, *Phys. Rev.* **132**, 1190 (1963).

[3]J. K. Dickens and R. J. Silva, *Elastic and Inelastic Scattering of 12.0-MeV Protons from ^{62}Ni, ^{63}Cu, and ^{64}Zn: Tabulated Differential Cross Sections*, ORNL-3851 (September 1965).

1.5 DEPENDENCE OF PROTON OPTICAL-MODEL PARAMETERS UPON EXPERIMENTAL ERRORS

J. K. Dickens

Optical-model analysis of the elastic scattering of fast nucleons from medium and heavy elements has been used extensively in recent years. Excellent fits to experimental data are usually obtained if most of the parameters of the model are allowed to vary. The fitting procedure consists in varying several of the parameters of the model by an automatic search code until the quantity χ^2, given by

$$\chi^2 = \sum_i \{[\sigma_{exp}(\theta_i) - \sigma_{th}(\theta_i)]/\Delta\sigma_{exp}(\theta_i)\}^2 ,$$

is a minimum.

Recent emphasis has been on the study of the systematics of the model.[1] In these studies many angular distributions of elastic scattering from a variety of targets and over a chosen range of incident energy are analyzed. Very good fits to many angular distributions have been obtained by allowing most of the parameters to vary, but the resulting "best-fit" parameters exhibit considerable variation from one angular distribution to the next. A better understanding can be obtained by fixing the geometrical parameters (e.g., radius, diffuseness parameters) and allowing only the well depths to vary. The data are quite adequately reproduced by this restricted model, and the variation in well-depth parameters is substantially reduced. A qualitative dependence of the well-depth variations upon target parameters has been found, but determining the magnitude of the dependence is difficult. For example, several groups have investigated the magnitude of the isobaric spin dependence [i.e., the $(N - Z)/A$ term]; agreement is only nominal.

Part of this difficulty may be associated with the dependence of the parameters upon various errors inherent in the experimental data being analyzed. Usually, the experimentalist studies these errors and arrives at an overall error that he ascribes to each datum. Each assigned error, then, gives a certain weight to its associated datum during the least-squares search to find the parameters that yield the minimum χ^2. The error does not in any way alter the value of the

datum. Suppose, for example, that there are two angular distributions with exactly the same data but that the errors associated with the data of one distribution are twice those associated with the data of the other. Analyses of these two distributions by minimizing χ^2 will yield identical sets of model parameters; only the value of χ^2 will be different. However, the conclusion that the model parameters have no dependence on experimental error is not demonstrated by the above test. If, instead, two angular distributions – one made up of the experimental data plus the associated errors and the other made up of the experimental data minus the associated errors – are analyzed, the model parameters will usually be different. This has been verified by some of our studies made on 12-Mev deuteron scattering from ^{60}Ni, ^{90}Zr, and ^{114}Cd in which we found that normalizing the data for a particular isotope at one energy changed the model parameters by a factor much larger than the normalization factor.[2]

A study similar to the above has been initiated for the proton optical model. Results indicate that parameter variation with normalization exists for 12-Mev proton scattering from ^{64}Zn (ref. 3) and for 9.8-Mev proton scattering from ^{112}Sn (ref. 4). Also under study are errors associated with the angle measurements and with the incident-energy measurement and errors which alter the shape of the angular distribution.

Figure 1.5.1 shows the results of analysis in which for two different sets of geometry only the real and imaginary well depths were varied. (Errors which alter the shape of the angular distribution are approximated by changing the normalization of the data for $\theta > 110°$.) Even though the results have similar form for the four error types and two sets of geometry, the graphs indicate that the functional dependence of the parameters is not the same for all eight cases. Therefore, a single assigned error does not yield the correct functional dependence of the model parameters on the actual experimental errors. In addition, the variation of V (the real-well depth) is small, certainly smaller than that obtained in a similar six-parameter search. The value of ΔV for ±10% absolute normalization error, ±0.1° error in angle, and ±25 kev error in incident energy is ~500 kev, a small value compared with that of V but fairly large compared with the assumed value for the isobaric spin dependence, ~1.7 Mev.

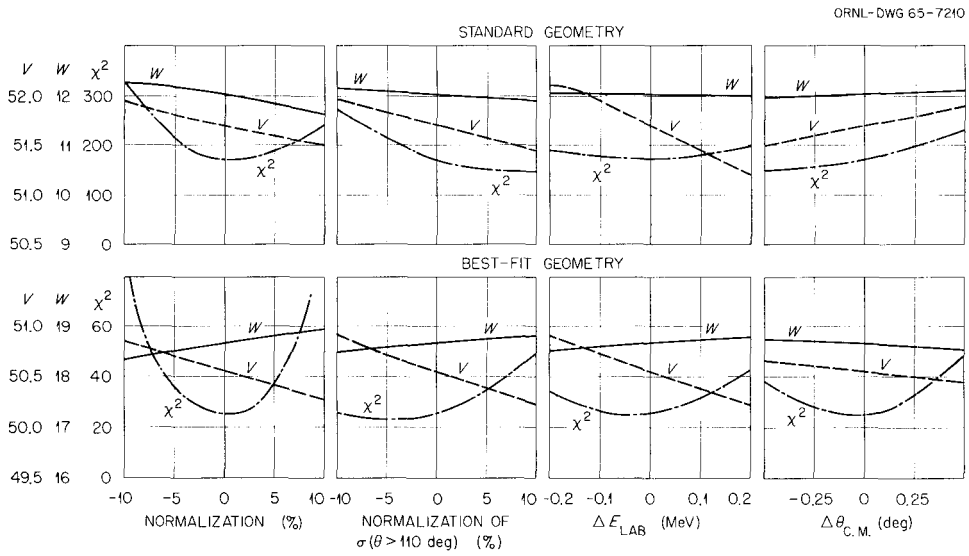

Fig. 1.5.1. Values of the Well-Depth Parameters and Minimum χ^2 as Functions of Errors for 12-Mev Protons Scattering from ^{64}Zn. The standard geometry is given by r_{0_r} = 1.25 fermis, a_r = 0.65 fermi, r_c = 1.2 fermis, r_{0_i} = 1.25 fermis, a_i = 0.47 fermi, and V_{so} = 7.5 Mev. The best-fit geometry is given by r_{0_r} = 1.24 fermis, a_r = 0.774 fermi, r_c = 1.2 fermis, r_{0_i} = 1.386 fermis, a_i = 0.34 fermi, and V_{so} = 4.83 Mev.

These results indicate that while meaningful optical-model analysis may be obtained by using data with the usual quoted errors a study of the fine structure of the model probably requires better data. The normalization of experimental data should be determined without recourse to optical-model calculations since, as shown in Fig. 1.5.1, the value of normalization for minimum χ^2 is dependent on the geometry.

References and Notes

[1]F. G. Perey, *Phys. Rev.* **131**, 745 (1963); C. M. Perey and F. G. Perey, *Phys. Rev.* **132**, 755 (1963); and E. C. Halbert, *Nucl. Phys.* **50**, 353 (1964).

[2]These data are reported in tabular form: J. K. Dickens and R. J. Silva, *Elastic and Inelastic Scattering of 12.0-MeV Protons from ^{62}Ni, ^{63}Cu, and ^{64}Zn: Tabulated Differential Cross Sections*, ORNL-3851 (September 1965).

[3]J. E. Durisch, R. R. Johnson, and N. M. Hintz, *Phys. Rev.* **137**, B904 (1965), and J. E. Durisch and P. Gould, *Phys. Rev.* **137**, B906 (1965).

[4]J. K. Dickens and F. G. Perey, *Phys. Rev.* **138**, B1080 (1965).

1.6 ELASTIC AND INELASTIC SCATTERING OF 12.0-Mev PROTONS FROM ^{62}Ni, ^{63}Cu, AND ^{64}Zn: TABULATED DIFFERENTIAL CROSS SECTIONS[1]

J. K. Dickens R. J. Silva[2]

Numerical values of differential cross sections for elastic and inelastic scattering of 12.0-Mev protons from ^{62}Ni, ^{63}Cu, and ^{64}Zn are reported in tabular form. Cross sections were determined at 5° intervals between laboratory angles of 20 and 165° for ^{62}Ni and ^{64}Zn and between laboratory angles of 20 and 110° for ^{63}Cu. Inelastic-scattering data are reported for two excited states of ^{62}Ni (Q = −1.17 and −2.74 Mev); for seventeen excited states of ^{63}Cu (Q = −0.668, −0.961, −1.327, −1.412, −1.547, −1.862, −2.012, −2.080, −2.210, −2.337, −2.405, −2.50, −2.69, −3.28, −3.45, −3.69, and −4.11 Mev); and for twenty-one excited states of ^{64}Zn (Q = −0.993, −1.804, −1.904, −2.31, −2.61, −2.74, −2.79, −3.00, −3.08, −3.20, −3.30, −3.37, −3.45, −3.55, −3.60, −3.71, −3.86, −3.93, −4.03, −4.16, and −4.31 Mev).

References and Notes

[1]Abstract of ORNL-3851 (September 1965).

[2]Chemistry Division.

1.7 ELASTIC SCATTERING OF 12.0- AND 14.0-Mev DEUTERONS FROM ^{90}Zr AND THE REACTION ^{90}Zr$(d,p)^{91}$Zr: TABULATED DIFFERENTIAL CROSS SECTIONS[1]

J. K. Dickens F. G. Perey
R. J. Silva[2]

Numerical values of differential cross sections for elastic scattering of 12.0- and 14.0-Mev deuterons from ^{90}Zr are reported in tabular form. Cross sections were determined at 5° intervals between laboratory angles of 20 and 165°. Differential cross sections for proton groups from the ^{90}Zr$(d,p)^{91}$Zr reaction are reported. For E_d = 12.0 Mev, data are tabulated for eleven proton groups (Q = 4.981, 3.77, 3.55, 3.09, 2.91, 2.79, 2.42, 1.93, 1.73, 1.53, and 1.33 Mev); and for E_d = 14.0 Mev, data are tabulated for nine proton groups (Q = 4.981, 3.77, 2.91, 2.79, 2.42, 1.93, 1.73, 1.53, and 1.33 Mev).

References and Notes

[1]Abstract of ORNL-3850 (September 1965).

[2]Chemistry Division.

1.8 ANALYSIS OF ELASTIC AND INELASTIC SCATTERING OF NEUTRONS FROM ^{206}Pb, ^{208}Pb, AND ^{209}Bi BELOW 4.5 Mev[1]

W. R. Smith

The Hauser-Feshbach compound-nucleus scattering theory has been applied to neutron elastic and inelastic scattering from ^{206}Pb, ^{208}Pb, and ^{209}Bi in the energy range 0.8 to 4.5 Mev. The theory appears to work quite well for both the compound-elastic scattering and the inelastic scattering,

provided that the imaginary potential W has the correct energy dependence. The results show that for the isotopes considered W should be constant as a function of bombarding-minus-excitation energy and nearly constant as a function of bombarding energy above 4-Mev bombarding energy, but should be made increasingly smaller as the bombarding energy is lowered below this amount.

Reference

[1]Abstract of ORNL-TM-1238 (in preparation).

1.9 USE OF ELASTIC-SCATTERING PARAMETERS IN (d,p) STRIPPING CALCULATIONS[1]

W. R. Smith

The angular distributions of $^{90}Zr(d,p)^{91}Zr$, $^{52}Cr(d,p)^{53}Cr$, $^{206}Pb(d,p)^{207}Pb$, and $Zn(d,p)$ were calculated by means of the distorted-wave Born approximation in which various optical-model parameter sets were obtained by fitting appropriate deuteron and proton elastic-scattering data. In most cases it was found that parameter ambiguities did not greatly affect the relative angular distributions but did cause differences of a factor of more than 2 between the resulting spectroscopic factors. Potential ambiguities of the form VR^n = constant were shown to be of considerably greater importance for the stripping results than were other types of ambiguities.

References

[1]Abstract of ORNL-TM-966 (October 1964); also of *Phys. Rev.* **137**, B913 (1965).

1.10 DWBA ANALYSIS OF THE $^{90}Zr(d,p)^{91}Zr$ REACTION AT ENERGIES BETWEEN 3.5 AND 5.5 Mev[1]

W. R. Smith

The distorted-wave Born approximation (DWBA) theory was applied to $^{90}Zr(d,p)^{91}Zr$ angular distributions corresponding to bombarding energies of 3.5, 4.0, 4.5, 5.0, and 5.5 Mev and to levels in the residual nucleus of 0, 1.21, 2.07, and 2.56 Mev of excitation. A single set of parameters, differing slightly from the predictions of proton and deuteron elastic scattering, was found that reproduced most of the angular distributions satisfactorily. However, the spectroscopic factors obtained thereby were, on the average, 30% smaller than those obtained from analysis of 12-Mev data.

Reference

[1]Abstract of ORNL-TM-1235 (in preparation).

1.11 REGIONS OF VALIDITY OF THE (d,p) COULOMB-STRIPPING APPROXIMATION[1]

W. R. Smith

The validity of the Coulomb-stripping approximation for (d,p) reactions was investigated numerically for six targets, ranging from ^{16}O to ^{238}U. The investigation involved finding the region in (E_d, Q) space where DWBA calculations that include nuclear optical-model potentials yield agreement with calculations that include only the Coulomb potentials. For nuclei between ^{48}Ca and ^{238}U it was found that the boundary between valid and nonvalid Coulomb stripping had an E_d dependence proportional to Z and a Q dependence proportional to $Z/A^{1/3}$ and could be approximated by a straight line which for $^{90}Zr(d,p)^{91}Zr$ has the intercepts E_d = 4.2 Mev and Q = 5.2 Mev.

References

[1]Abstract of ORNL-TM-1240 (in preparation) and of paper to be submitted to *Nuclear Physics*.

1.12 INTEGRAL SPECTRA AND DOSE CONVERSION FACTORS FOR Am-Be, Po-Be, Pu-Be, AND Am-B NEUTRON SOURCES[1]

S. K. Mehta[2] W. R. Burrus

The integral energy spectrum $\Phi(E)$ (that is, the neutron flux below an energy E) and the tissue

dose-conversion factors [the first-collision dose (Kerma) K, the first-collision RBE dose (Kerma equivalent) Keq, and the RBE dose (dose equivalent) DE per unit neutron flux] have been measured for Am-Be, Pu-Be, Po-Be, and Am-B neutron sources with a modified Bonner-sphere neutron spectrometer. Measurements were also made for the Po-Be source at the center of 5.0- and 8.5-in.-diam spheres of water. The spectrometer covered the range 0.01 ev to 15.5 Mev. The dose-vs-flux curves as a function of neutron energy were taken from *NBS Handbooks 63* (Figs. 1 and 13) and *75* (Table A.6). The method used to analyze the data took into account the known smoothness of the spectrum from (α,n) sources and assumed an upper bound for the neutron flux above 5.5 Mev taken from other measurements. The values for the dose conversion factors, K[(ergs/g)/(neutron/cm^2)], Keq[(ergs/g)/(neutron/cm^2)], and DE [rems/(neutron/cm^2)] for the four sources are, respectively:

Am-Be	$(3.72 \pm 0.53)10^{-7}$,	$(2.70 \pm 0.26)10^{-6}$,	$(3.79 \pm 0.23)10^{-8}$
Pu-Be	$(3.61 \pm 0.57)10^{-7}$,	$(2.65 \pm 0.29)10^{-6}$,	$(3.72 \pm 0.28)10^{-8}$
Po-Be	$(3.96 \pm 0.67)10^{-7}$,	$(2.82 \pm 0.31)10^{-6}$,	$(3.84 \pm 0.19)10^{-8}$
Am-B	$(3.51 \pm 0.42)10^{-7}$,	$(2.64 \pm 0.23)10^{-6}$,	$(3.75 \pm 0.21)10^{-8}$.

The values of these conversion factors for the Po-Be source surrounded by water are:

5 in. H_2O	$(2.78 \pm 0.51)10^{-7}$,	$(2.06 \pm 0.27)10^{-6}$,	$(2.85 \pm 0.24)10^{-8}$
8.5 in. H_2O	$(2.60 \pm 0.69)10^{-7}$.	$(1.90 \pm 0.39)10^{-6}$.	$(2.60 \pm 0.38)10^{-8}$.

References and Notes

[1]Abstract of paper to be submitted to *Health Physics*.

[2]Atomic Energy Establishment, Trombay, Bombay, India.

1.13 SIMULTANEOUS MEASUREMENTS OF THE NEUTRON-CAPTURE AND FISSION CROSS SECTIONS OF ^{235}U

L. W. Weston
R. Gwin
R. W. Hockenbury[1]
G. de Saussure
J. E. Russell[1]
R. Ingle[2]

The program for measuring the ratio of the capture and fission cross sections (α) of ^{235}U has been continued with measurements conducted at the Rensselaer Polytechnic Institute Electron Linear Accelerator in the energy range 0.4 to 2 kev. The technique was the same as that used for earlier measurements (see Sect. 1.14 and ref. 3) except that a ^{10}B-NaI detector was used to measure the neutron flux through the ^{235}U fission chamber. The important feature of these measurements is that the capture and fission cross sections were determined simultaneously under identical conditions with the same sample, thus eliminating many relative errors between the capture and fission cross sections such as slight errors in neutron energy, neutron flux, neutron scattering effects, etc.

The analysis of the measurements is incomplete, but a typical, uncorrected time-of-flight spectrum is shown in Fig. 1.13.1, where the scale at the bottom represents a neutron energy from 10 kev at the left to 0.2 ev at the right. The sharp breaks in the spectrum were caused by the computer's changing the effective time-of-flight channel widths.

The measurements will be analyzed to obtain resonance integrals over various neutron energy ranges, as well as the differential cross sections. Resonance integrals are of value in computing

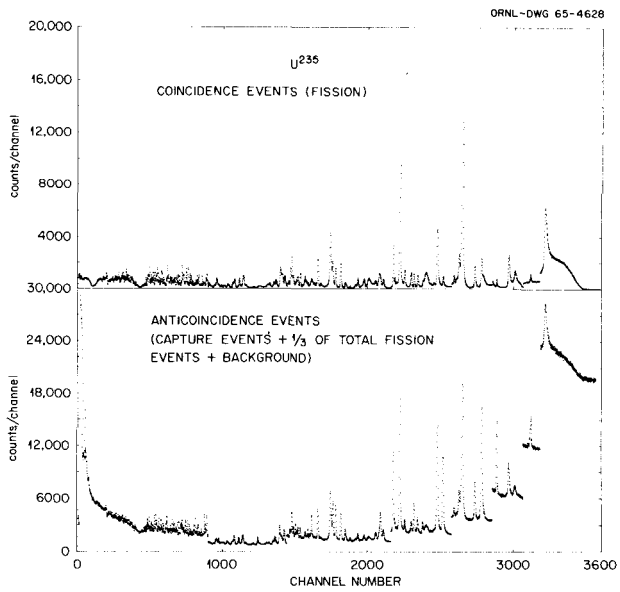

Fig. 1.13.1. Neutron Time-of-Flight Spectra of Capture and Fission Events in the ^{235}U Chamber.

gross characteristics of reactors, whereas differential-cross-section data are used to calculate Doppler coefficients and flux depressions.

A feasibility study on the measurement of the capture and fission cross sections of ^{239}Pu was also performed with the RPI linac. The pulse-height spectrum method of discriminating capture from fission was used.[4] Analysis of this study will be continued.

References and Notes

[1]Rensselaer Polytechnic Institute, Troy, New York.

[2]Instrumentation and Controls Division.

[3]L. W. Weston, G. de Saussure, and R. Gwin, *Nucl. Sci. Eng.* **20**, 80 (1964).

[4]R. Gwin *et al.*, *Neutron Phys. Div. Ann. Progr. Rept. Aug. 1, 1963*, ORNL-3499, vol. I, p. 15.

1.14 MEASUREMENT OF α, THE RATIO OF THE NEUTRON-CAPTURE CROSS SECTION TO THE FISSION CROSS SECTION, FOR ^{235}U IN THE ENERGY REGION 3.25 ev TO 1.8 kev[1]

G. de Saussure J. E. Russell[2]
L. W. Weston R. Gwin
R. W. Hockenbury[2]

The value of α, the ratio of the neutron-capture cross section to the fission cross section, for ^{235}U has been measured over a neutron energy range extending from 3.25 ev to 1.8 kev. In addition, capture and fission cross sections have been measured from 3.25 to 25 ev. The experiment was performed with the neutron time-of-flight facilities at Rensselaer Polytechnic Institute. A multiplate ^{255}U fission chamber, surrounded by a large liquid scintillator, was placed in the neutron beam. Gamma rays emitted when the uranium absorbed a neutron were detected with high efficiency by the scintillator, and, if the absorption resulted in a fission, the fission fragments were detected by the fission chamber itself. The value of α was derived from the ratio of the count rate of the scintillator in anticoincidence with the fission chamber to the count rate of the scintillator in coincidence with the fission chamber. Relative fission and capture cross sections were obtained from these count rates and from an auxiliary measurement of the incident neutron beam spectrum. Results are presented in graphical and tabular form.

References and Notes

[1]Abstract of ORNL-3738 (April 1965).

[2]Rensselaer Polytechnic Institute.

1.15 STUDY OF RESONANCE PARAMETERS OF Pu[1]

J. Blons[2] A. Michaudon[2]
H. Derrien[2] P. Ribon[2]
G. de Saussure

The resonance parameters of ^{239}Pu were determined from total-cross-section measurements up to 200 ev and from previously reported measurements of fission cross sections. The experimental techniques and the method of analysis of the results are briefly described, and the resonance parameters are given. It seems that up to 200 ev few resonances are missed, though there is some ambiguity (asymmetry explicable either by interference or by small resonances). A statistical study is made on level spacings and reduced neutron-, radiation-, and fission-width distributions. Several resonances have very great width ($\Gamma > 1$ ev); the radiation widths Γ_γ fluctuate quite strongly and are not consistent with a constant value; the fluctuations are comparable with the ones observed for ^{235}U.

References and Notes

[1]Abstract of paper submitted by CEN, Saclay, for *EANDC Meeting on Study of Nuclear Structure Using Neutrons, Antwerp, July 1965.*

[2]Centre d'Etudes Nucléaire, Saclay.

1.16 PULSED-NEUTRON MEASUREMENTS OF DIFFUSION PARAMETERS IN ORDINARY ICE AS A FUNCTION OF TEMPERATURE BY THE METHOD OF TIME-DEPENDENT NEUTRON DIFFUSION[1]

E. G. Silver

The parameters λ_a, D, and C in the familiar equation

$$\lambda = \lambda_a + DB^2(1 - CB^2)$$

have been measured for ice over the buckling range 0.039 to 0.738 cm^{-2}. The classical pulsed-neutron method was used with the ice contained in an absorber-lined cryostat at temperatures down to −85°C. Special techniques were developed for producing accurately shaped ice cylinders of uniform density.

A 300-kev deuteron accelerator, both pre- and postacceleration pulsed, was used to produce 20- to 200-μsec bursts of D-D neutrons which impinged on the ice cylinders. [D-T neutrons could not be used, despite intensity advantages, because they caused a high quasi-flat background due to photoneutrons produced by the gamma rays emitted in beta decay of 7.35-sec ^{16}N produced by the $^{16}O(n,p)^{16}N$ reaction.] Each of 65 decays was measured with at least 10^6 counts in an 18-channel time analyzer, after waiting times ranging from 533 μsec (largest cylinder) to 140 μsec (smallest cylinder).

The results were analyzed by a nonlinear least-squares fitting to a two-exponential decay model. A small-amplitude accelerator-derived background of $(6.5 \pm 2.5) \times 10^{-3}$ sec^{-1} was found and corrected for. The corrected data had slopes constant within 1.5% over the time observed.

The results show that the absorption cross section has a $1/v$ dependence over the measured temperature range, making λ_a a constant and yielding an average value of (331.5 ± 3.1) mb for $\sigma_a(H)$. Fitting (vD) to a linear temperature relation yields

$$[3.30 + 0.0123\ T(°C)] \times 10^4\ cm^2/sec\ .$$

The diffusion-cooling coefficient C has large uncertainties but fits a linear temperature dependence of

$$C = [4.55 + 0.025\ T(°C)] \times 10^3\ cm^4/sec\ .$$

References

[1]Abstract of ORNL-TM-1204 (September 1965) and of paper to be published in *Proceedings of International Atomic Energy Agency Symposium on Pulsed-Neutron Research, Karlsruhe, Federal Republic of Germany, 10–14 May 1965* (Paper No. SM-62/72).

1.17 PHOTONEUTRON SPECTRA AND CROSS SECTIONS FOR ^{12}C AND ^{16}O[1]

V. V. Verbinski J. C. Courtney[2]

Partial (γ,n) cross sections have been measured for two self-conjugate nuclei, ^{12}C and ^{16}O, by measuring the spectral intensity of emitted neutrons in conjunction with a determination of the time-integrated absolute photon flux. The maximum-energy photoneutrons which leave the residual nuclei in their ground state were isolated from other transitions, making it possible to study individual excited levels in ^{12}C and ^{16}O. By measuring the neutron spectra at several angles and taking advantage of the use of self-conjugate target nuclei, these isolated levels in ^{12}C and ^{16}O were found to be due to electric-dipole photoabsorption with subsequent emission of d-wave neutrons.

References and Notes

[1]Abstract of ORNL-TM-1158 (June 1965) and of paper to be published in *Nuclear Physics*.

[2]Catholic University, Washington, D.C.; Graduate Fellow, Oak Ridge Institute of Nuclear Studies.

1.18 DIFFERENTIAL NEUTRON CROSS SECTIONS FOR SEVERAL MATERIALS BOMBARDED BY 14-, 18-, AND 56-Mev PROTONS

M. Young[1] W. R. Burrus
V. V. Verbinski J. C. Courtney[2]

Differential "net" (p,n) cross sections have been determined as a function of neutron energy and neutron emission angle for several materials bombarded by 14-, 18-, and 56-Mev proton beams. Targets which removed about 10 Mev from the incident beam of Be, ^{11}B, C, O, and Al were bombarded by 56-Mev protons. Measurements were made at an emission angle of 64° for each element and at 30° for Be alone. Targets which removed about 1 Mev from the incident beam were bombarded by 14- and 18-Mev protons, the measurements covering emission angles of from 0 to 170°. At 18 Mev the targets were Be, N, Al, Fe, In, Ta, and ^{208}Pb; and at 14 Mev they were Be

and ^{208}Pb. The resulting net cross section is defined by

$$\sigma(p,n)_{net} = \sigma(p,n) + \sigma(p,pn) + 2\sigma(p,2n) + \ldots .$$

The final differential (p,n) cross sections will be determined from the thickness of the targets, the integrated proton current, and the absolute neutron spectrum. The absolute spectrum from about 0.5 Mev to the maximum neutron energy is being unfolded by means of the FERDO general-purpose unfolding code from pulse-height distributions measured with a calibrated NE-213 liquid-organic scintillator. The cross-section results will be presented in the laboratory system in terms of barns steradian^{-1} Mev^{-1} as a function of emission angle and neutron energy for each bombarding energy. A transformation to the center-of-mass system cannot be made because the different reaction mechanisms leading to neutrons were not separated.

Notes

[1]Research participant from Louisiana State University.

[2]Catholic University, Washington, D.C.; Graduate Fellow, Oak Ridge Institute of Nuclear Studies.

1.19 DEUTERON POLARIZATION FROM THE ^{9}Be$(p,d)^{8}$Be REACTION AT 3 TO 5 Mev[1]

V. V. Verbinski M. S. Bokhari[2]

The polarization of deuterons produced in the ^{9}Be$(p,d)^{8}$Be ground-state reaction was measured at several angles in the region of the stripping peak and for proton energies of 3, 4, and 5 Mev. Using a carbon analyzer via the ^{12}C$(d,p)^{11}$C ground-state reaction and the relationship ϵ (the asymmetry) = $3\mathbf{P}_p \cdot \mathbf{P}_d$, where $\mathbf{P}$ is the polarization, the sign of the deuteron polarization near the stripping peak was found to be positive at 3 and 4 Mev. This is in agreement with earlier experimental findings and DWBA calculations for which deuteron-wave distortion is assumed to predominate. However, the sign was measured to be negative at 5 Mev, which may be due to a relatively greater proton-wave distortion at this energy.

References and Notes

[1]Abstract of ORNL-TM-1233 (in preparation) and of paper to be submitted to *The Physical Review*.

[2]Now at Lahore Center, Pakistan Atomic Energy Commission, Lahore, Pakistan.

2. Critical Experiments

2.1 DETERMINATION OF NEUTRON FLUX IN NUCLEAR REACTORS BY THE UNCOLLIDED-FLUX ESTIMATOR APPLIED TO MONTE CARLO COLLISIONS[1]

J. W. Webster

An investigation was made of the uncollided-flux estimator, applied to Monte Carlo collisions, as a means of determining the neutron flux at specified spatial points of a reactor. The uncollided-flux estimator is essentially an evaluation of the flux as given by the Boltzmann equation in integral form. The method is applied to two sample reactor problems: the Godiva assembly and an 8-unit interacting array of highly enriched uranium-metal cylinders. The scalar flux in Godiva, calculated by using the collisions from 15,000 neutrons, was found to be in excellent agreement with the flux calculated by the Carlson S_n method. In the second problem, using the collisions from about 10,000 neutrons, the distorting effect on the flux distribution of the nearby interacting cylinder shows up clearly, although more neutrons would be necessary for satisfactory accuracy.

The computer time required on the CDC 1604-A in the first problem was 215 min (36 min per space point), and was 480 min in the second problem (69 min per space point). The uncollided-flux estimator is therefore concluded to be practical only when the flux is needed at a small number of space points or when high accuracy is not desired.

Reference

[1]Abstract of ORNL-TM-1175 (August 1965).

2.2 BOUNDARY CONDITIONS FOR THE CYLINDRICALIZED CELL OF REACTOR-LATTICE CALCULATIONS[1]

J. W. Webster

In the solution for the thermal-flux distribution in a cylindricalized cell using the one-dimensional spherical harmonic method of third order, several different sets of boundary conditions at the outer surface have been proposed in the literature. These are reviewed, and another possible set is derived from a consideration of an analogy between the equations for the moments in cylindrical and plane geometry.

The physical properties existing in actual cells, which are necessarily triangular, square, or hexagonal in cross section, are reflection of neutrons, zero current, and zero normal derivative of scalar flux. None of the possible sets of boundary conditions for the cylindricalized cell satisfy all these physical properties, and it is shown mathematically why they do not.

Reference

[1]Abstract of ORNL-TM-1022 (Dec. 30, 1964).

2.3 ONE-VELOCITY MONTE CARLO CALCULATIONS OF URANIUM-METAL CRITICAL GEOMETRIES[1]

J. T. Mihalczo

A method is described for predicting the multiplication factors of geometrically complicated configurations of bare, unmoderated, enriched

uranium metal from the results of two delayed-critical experiments in simple geometry, one with a nearly minimum surface-to-volume ratio and the other with a large surface-to-volume ratio. The method requires two one-velocity constants, the total collision cross section (Σ_t) and the number of neutrons produced per collision ($\nu\Sigma_f/\Sigma_t$), which are obtained from the two experiments by using S_{12} transport theory calculations with isotropic scattering. These constants, together with the assumption of isotropic scattering, are then used in O5R Monte Carlo neutron-transport calculations to predict the multiplication factors. The method has been tested by predicting the multiplication factors of 21 different delayed-critical configurations to within a standard deviation of 1.5%.

References

[1]Abstract of ORNL-TM-1220 (in preparation) and of paper to be submitted to *Nuclear Science and Engineering*.

2.4 INCREASED YIELD FROM FAST BURST REACTORS: PARTS I AND II[1]

J. T. Mihalczo

The effect on the yield and burst shape of increased fissile mass in superprompt critical-burst reactors consisting of unreflected and of thin stainless-steel-reflected enriched uranium-molybdenum alloy cylinders has been investigated by transport theory calculations employing the S_n method. The alloy was 10 wt % molybdenum and the uranium was enriched to 97% in ^{235}U. Calculations were also performed for critical enriched uranium-metal cylinders, for which experimental data exist. The cylinders range in height-to-diameter ratio (h/d) from 0.1 to 5.7.

Part I

The results show that the peak-to-average power-density ratio, the prompt-neutron decay constant at delayed critical, and the static temperature coefficient of reactivity are essentially independent of h/d. One-velocity space-independent neutron kinetics predict the same burst shape for reactors with equal superprompt critical reactivities and equal prompt-neutron decay constants at delayed critical. In cases where inertial effects become important, a cylinder of greater h/d ratio will produce shorter bursts since a large part (approximately one-half) of the temperature coefficient is associated with vibrations in the small dimension. The temperature coefficient of reactivity of large-diameter cylinders is associated with expansion in the large dimension and will result in wider burst widths. The yield from a 30-in.-diam, 3.23-in.-high unreflected uranium-molybdenum cylinder was calculated to be 7.8×10^{17} fissions; that from a 5.55-in.-diam, 32-in.-high cylinder was 2.9×10^{17}. These yields are greater than the maximum thus far produced by the Health Physics Research Reactor, 1.8×10^{17} fissions, at the same peak temperature, by factors of 4.3 and 1.6 respectively.

Part II

Adding a 1-in.-thick stainless steel reflector to a cylinder of large h/d ratio will result in a decrease of about 25% in the mass required to produce a given yield. Introducing a 2-in.-diam axial hole in this cylinder will increase the yield per unit peak-temperature change by as much as 40%.

Calculations of unreflected 8.47-in.-diam cylinders indicate that the yield, per unit peak-temperature change, from U(97)-Mo can be increased 50% if uranium of 60% ^{235}U content is substituted in the inner 4.5-in.-diam region.

References

[1]Combined abstract of *Increased Yields from Fast Burst Reactors. Part I: Effects of Increased Mass on Uranium and Uranium-Molybdenum Critical Cylinders*, ORNL-TM-1125 (Apr. 30, 1965) and *Part II: Effect of Thin Stainless Steel Reflectors of ^{235}U-Enriched Central Fuel Regions*, ORNL-TM-1215 (in preparation).

2.5 CRITICALITY OF A SINGLE UNIT OF AQUEOUS URANYL FLUORIDE SOLUTION ENRICHED TO 5% IN ^{235}U[1]

J. W. Webster E. B. Johnson

As a part of the continuing criticality program with uranium enriched to 5% in ^{235}U, a comparison

between theory and experiment was made with regard to the criticality of a volume of aqueous $U(4.98)O_2F_2$ solution ($H:^{235}U$ = 496) contained in a thin-walled stainless steel cylinder. The solution had a height-to-diameter ratio of about 2.5, thus making the end leakage reasonably small compared with the radial leakage. Computations indicated that the end leakage from the finite system corresponded to only 1.5% in reactivity. One-dimensional calculations, with an approximate correction for end leakage, are therefore valid.

The Carlson S_n DTF II code with the Hansen-Roach 16-group cross sections was used for the calculation. The computed multiplication factor of 1.002 for the critical system lends further confidence to the method and to the cross-section set.

Reference

[1]Abstract of ORNL-TM-1195 (in press).

2.6 CRITICAL DIMENSIONS OF ARRAYS OF AQUEOUS URANYL FLUORIDE SOLUTION CONTAINING URANIUM ENRICHED TO 5% IN ^{235}U

E. B. Johnson

The program concerned with the determination of critical parameters of aqueous uranyl fluoride solution containing uranium enriched to 4.98% in ^{235}U is being continued. Experiments with cylinders of solution at a concentration of 901 g of uranium per liter ($H:^{235}U$ = 496) contained in aluminum and having no hydrogenous reflector have been reported.[1]

In more recent experiments critical arrays have been assembled in which the $U(4.98)O_2F_2$ solution at the same concentration was contained in 10.75-in.-diam polyethylene bottles having a capacity of about 25 liters. Since these bottles are used for storage and for intraplant transfer of uranium solutions of low enrichment, the results of these experiments form bases for safe and economic handling criteria although the geometry of the units is not amenable to calculation. The bottles were molded polyethylene of varying wall thicknesses (0.25 in. at the bottom and 0.10 in. at the top) with a concave upward bottom and a screw cap. Each bottle contained about 1.1 kg of ^{235}U in 24 liters of solution.

Planar arrays of these units in square and triangular patterns were critical under the conditions indicated in Fig. 2.6.1. It should be emphasized that although the side and bottom reflectors were in contact with the bottle surfaces the top reflector, when present, was about 10 in. from the top of the solution because of the bottle caps. Nine units in a line and in contact were subcritical when completely surrounded with polyethylene. The array of 32 units, surrounded on five sides with 6-in.-thick polyethylene, shown in Fig. 2.6.2, was critical at a surface separation of 8.33 in. between rows. A similar array containing only 16 units, arranged in two rows of eight units each, was critical at a separation of 6.65 in. between rows when surrounded on five sides with 6-in.-thick polyethylene. The effect of Plexiglas centered between the rows of the array with the separation between rows equal to 6 in. was determined; Fig. 2.6.3 indicates that the optimum

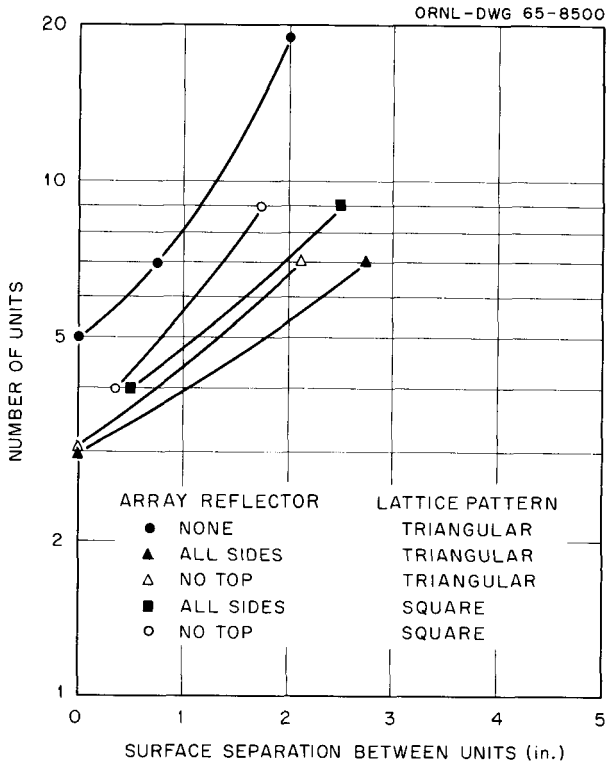

Fig. 2.6.1. The Critical Planar Arrays of Aqueous $U(4.98)O_2F_2$ Solution at a Concentration of 901 g of Uranium per Liter Contained in 10.75-in.-diam Polyethylene Bottles. The reflector was 6-in.-thick polyethylene.

Fig. 2.6.2. An Array of Thirty-Two Units of Aqueous $U(4.98)O_2F_2$ Solution at a Concentration of 901 g of Uranium per Liter Contained in Polyethylene Bottles and Surrounded on Five Sides by 6-in.-Thick Polyethylene.

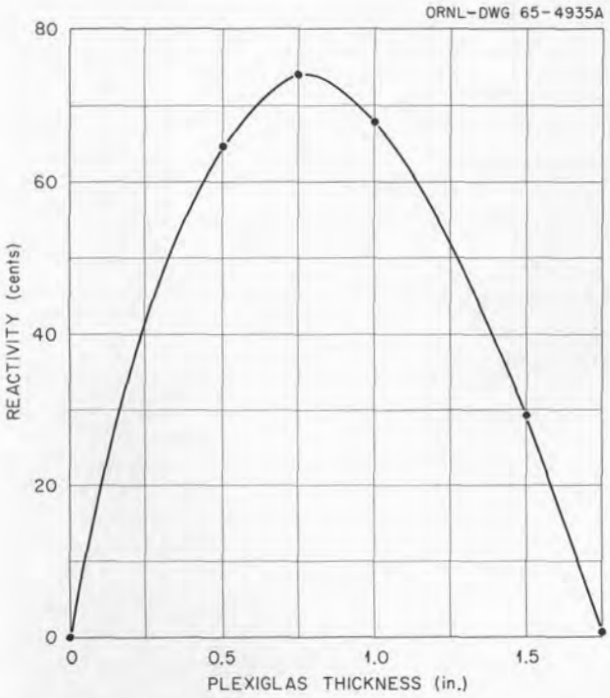

Fig. 2.6.3. Reactivity Introduced by Plexiglas Centered Between the Rows of a Reflected Array of Polyethylene Bottles of Aqueous $U(4.98)O_2F_2$ Solution at a Concentration of 901 g of Uranium per Liter.

thickness of Plexiglas was about 0.75 in. The relative effects of materials such as concrete, wood, Plexiglas, foamed plastic, and Foamglas as reflectors for this enrichment were determined by substitution in one side of the reflector.

Reference

[1]E. B. Johnson and D. F. Cronin, *Neutron Phys. Div. Ann. Progr. Rept. Aug. 1, 1964,* ORNL-3714, vol. I, p. 31.

2.7 CRITICAL EXPERIMENTS WITH SPERT-D FUEL ELEMENTS[1]

E. B. Johnson R. K. Reedy, Jr.

The critical dimensions of lattices of SPERT-D fuel elements in several nonreactor environments were determined in order to establish specifications for use in storage, transportation, and chemical-processing operations. A SPERT-D element consisted of the 3-in.-square aluminum box, typical of pool-type reactor elements, fitted with U-Al fuel plates. The length of the fuel section was 23.9 ± 0.4 in. A complete element contained about 300 g of ^{235}U in 22 aluminum-clad flat plates.

In addition to water as the moderator and reflector of lattices of elements, a dilute aqueous solution of uranyl nitrate was used in some experiments to simulate a dissolver. In still other experiments, varying amounts of boron were added to the uranyl nitrate solution to determine its effect as a soluble neutron absorber in chemical-process materials.

It was shown, for example, that a minimum of about 3.5 kg of ^{235}U is required in a critical lattice moderated and reflected by water. This mass was reduced to 2.8 kg (contained in the elements themselves) when U(92.6) solution having a ^{235}U concentration of 3.99 g/liter was substituted for water. It was increased to 13.6 kg when 1.118 g of natural boron was added to each liter of the uranyl nitrate solution.

Reference

[1]Abstract of ORNL-TM-1207 (in press).

2.8 CRITICALITY SAFETY TESTS FOR A PROPOSED IRRADIATION FACILITY

E. B. Johnson

A 10-in.-long annulus of U(93.4) metal, 3 × 3 in. in inside dimensions, containing 4.32 kg of ^{235}U was found to be subcritical when submerged in either light or heavy water. The metal was used to simulate the fissile material in an irradiation facility proposed for use with the Bulk Shielding Reactor.

2.9 HIGH FLUX ISOTOPE REACTOR CRITICAL EXPERIMENT No. 3

J. T. Thomas

Critical experiments[1] in support of the High Flux Isotope Reactor were completed in April 1965. The HFIRCE-3 element was similar to the HFIRCE-2 element used by Magnuson, and the experiments utilized the same basic equipment as the HFIRCE-2 series.[2] The ^{235}U content of the element was 9.4 kg, an increase of 1.4 kg over the HFIRCE-2 element, and natural boron, containing 2.12 g of ^{10}B, was present in the filler pieces of the fuel plates of the inner annulus.

Relative fission flux measurements were made in the island, throughout the core, and in the water reflector exterior to the beryllium reflector. The shutdown worth as well as the sensitivity of the Ag-Cu-Al control cylinders were determined. Similar measurements were conducted with the Eu_2O_3-Ta-Al control cylinders intended for use in the HFIR.

References

[1]J. T. Thomas, *Neutron Phys. Div. Ann. Progr. Rept. Aug. 1, 1964,* ORNL-3714, vol. I, p. 37.

[2]D. W. Magnuson, *Neutron Phys. Div. Ann. Progr. Rept. Sept. 1, 1961,* ORNL-3193, p. 136.

2.10 EXPERIMENTAL EVALUATION OF HANDLING PROCEDURES FOR HIGH FLUX ISOTOPE REACTOR FUEL ELEMENTS OUTSIDE THE REACTOR

J. T. Thomas S. J. Raffety

A series of experiments have been performed with the High Flux Isotope Reactor Critical Experiment No. 3 (HFIRCE-3) fuel element, which was the same as that described in ref. 1 except that the ^{10}B content was 2.12 g, in order to establish safe conditions for the routine handling, shipping, and storage of HFIR fuel.

The reactivity of the element was −1.15 ± 0.09 dollars, measured by the pulsed-neutron method, when submerged and with an effectively infinite water reflector. However, this fuel element may be made critical when submerged by displacing approximately 15% of the water from the target region; with optimum water displacement, ~69%, the reactivity was maximum, +2.90 ± 0.10 dollars.

When stored in a water-filled pool, the elements will be mounted on a hollow water-filled post, 4.5 in. in outside diameter and consisting of 0.058-in.-thick cadmium sandwiched between 0.109-in.-thick stainless steel cylinders. Under these conditions the element was observed to be approximately 9 dollars subcritical. Displacement of the optimum amount of water from within this post made the element 3 dollars subcritical.

A 0.024-in.-thick sheet of cadmium placed around the element, extending 2 in. above and below the fuel and enclosing a $\frac{1}{8}$-in.-thick water annulus adjacent to the element, was worth about −15.8 dollars when the optimum amount of water was displaced from the target region.

Stainless steel strips, 0.62 × 29 × 0.031 in. and containing 1.66 wt % boron enriched to 92.15% in ^{10}B, were found to be worth −47.93 cents each when inserted between the fuel plates in the inner fuel annulus and to be worth −26.66 cents each when inserted in the outer annulus of the water-moderated and -reflected element. In both cases the strips were separated sufficiently to prevent interaction between them.

To evaluate the feasibility of moving a complete element through the hatch of the massive steel reactor vessel and of shipping an element in a steel-lined lead container, the effects of these materials as reflectors on the reactivity of the submerged element were measured. The results are given in Fig. 2.10.1, in which the observed change in reactivity of the element is plotted as a function of the thickness of the reflector material. The curves show the effects of the metal reflectors extending only half-way around the element. The lead was separated from the element by 0.75-in.-thick steel. A single point on the figure gives the reactivity resulting from the lateral surfaces of the element being completely surrounded with

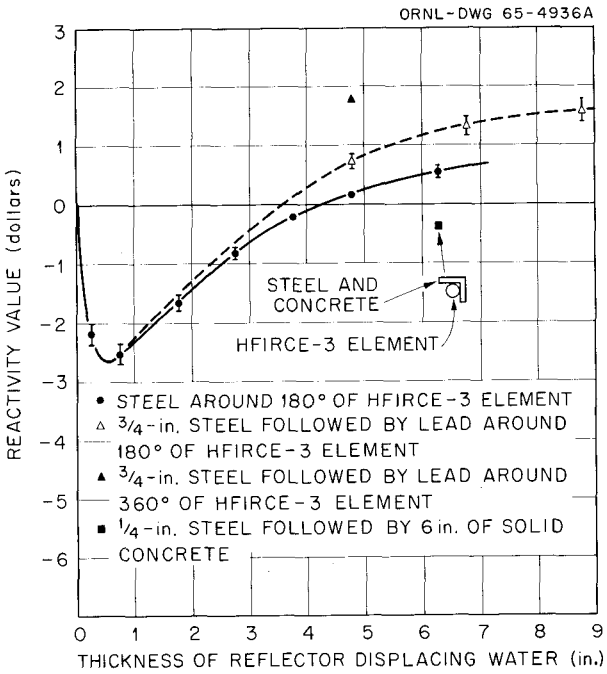

Fig. 2.10.1. Variation of Reactivity of a Critical, Submerged HFIRCE-3 Fuel Element as a Function of Thicknesses of Steel and/or Lead Displacing Water Adjacent to the Element.

0.75-in.-thick steel followed by 4 in. of lead. Shown also is the result of one measurement made with the element reflected as though it were located in a corner of the fuel storage pool. It is to be noted that in every measurement the test material displaced water from the infinitely thick reflector.

In an investigation of the conditions whereby two elements may be adjacent, it was observed that a system composed of two submerged water-reflected elements was subcritical when the surface separation between the elements was greater than 4 in. and that this distance was reduced to 2 in. when one of the steel and cadmium water-filled posts was located in the target region of each element.

Reference

[1]F. T. Binford and E. N. Cramer, *The High Flux Isotope Reactor: A Functional Description,* vol. 1, ORNL-3572, p. 5–3 (May 1964).

2.11 EXPERIMENTS FOR THE DEVELOPMENT OF A REACTIVITY ACCEPTANCE TEST OF HIGH FLUX ISOTOPE REACTOR FUEL ELEMENTS

J. T. Thomas S. J. Raffety

The design requirements for High Flux Isotope Reactor (HFIR) fuel elements, with respect both to burnable poison content and to ^{235}U content and distribution, are expected to change as a result of altered reactivity conditions in the HFIR itself. Therefore the neutron multiplication factor of each new HFIR fuel element will have to be established prior to installation in the reactor. Conformity of the element to its specified reactivity will thereby be established also. A method has been developed for determining the change in reactivity necessary to make an element critical when it is submerged in an infinitely thick water reflector in the absence of beryllium. Experiments to develop the method and to generate the required reference data have been performed with the element fabricated for some of the critical experiments, HFIRCE-3, supporting the reactor design. This element is the same as that described in ref. 1 except that the boron content was 2.12 g of ^{10}B.

Since the HFIRCE-3 element was subcritical when submerged, reactivity was added by placing plates containing ^{235}U or cylinders of Styrofoam in the target region. Each plate was 0.060 × 2.704 × 25.125 in., and contained 14 g of ^{235}U as U(93.2)-Al alloy clad with aluminum. The Styrofoam (expanded polystyrene with noninterconnecting air bubbles and a density of 0.024 g/cm^3) reduced the hydrogen content of the target region. Fine reactivity adjustments were made by placing strips of stainless steel and/or strips of stainless steel containing boron between the fuel plates in the outer annulus of the element. The reactivity contribution of various amounts of fuel in plates, of different voids introduced by the Styrofoam, and of various numbers of steel strips was established in order that the subcritical reactivity of elements could be determined. It was observed, for example, that two plates, separated 2.5 in. and symmetrically mounted about the element axis, added 2.4 dollars of reactivity. The steel strips used for fine adjustment introduced as little as −1.3 cents each.

Since both increases and reductions in reactivity can be evaluated by this method, it can, of course,

be applied to elements which are supercritical when submerged.

Reference

[1]F. T. Binford and E. N. Cramer, *The High Flux Isotope Reactor: A Functional Description,* vol. 1, ORNL-3572, p. 5–3 (May 1964).

2.12 POTASSIUM REACTIVITY COEFFICIENT IN SMALL REFLECTED UO_2 ASSEMBLIES[1]

J. T. Mihalczo

Three small critical assemblies of ^{235}U-enriched UO_2 reflected by beryllium and graphite have provided measurements of the potassium reactivity coefficient to verify methods of calculation.

Reference

[1]Unclassified abstract of ORNL-TM-1222 (classified) (in preparation).

2.13 EXPERIMENTS AND CALCULATIONS ON URANIUM-MOLYBDENUM ALLOY CRITICAL ASSEMBLIES[1]

J. T. Mihalczo W. E. Kinney

A series of clean critical experiments with uranium-molybdenum alloy were performed and compared with reactor physics calculations. The critical heights of three configurations of the alloy were measured: an unreflected solid cylinder 20.32 cm in diameter; an unreflected cylindrical annulus having an inside diameter of 5.08 cm and an outside diameter of 20.32 cm, both filled with stainless steel and left empty; and a Plexiglas-reflected annulus in which the upper 12.7 cm of the hole was enlarged to an 8.89-cm diameter, both with and without cadmium between the core and reflector. In addition, fission density distributions and void coefficients of reactivity were measured for the unreflected assemblies. Transport calculations with Hansen and Roach cross sections successfully predicted the critical heights and fission density distributions for the unreflected assemblies and for assemblies reflected by 2.5 cm of Plexiglas. The calculated void coefficients are from 5 to 20% lower than those measured.

Reference

[1]Abstract of ORNL-TM-1277 (in preparation).

2.14 STATIC AND DYNAMIC TRANSPORT CALCULATIONS FOR PULSED-NEUTRON EXPERIMENTS WITH SPHERES OF URANYL NITRATE SOLUTION[1]

D. W. Magnuson

In static reactor calculations the neutron balance between production by fission and loss by leakage and absorption is artificially maintained by adjusting the value of ν, which is equivalent to adding neutrons at fission energies. In dynamic reactor calculations the neutron balance between production and loss is effectively maintained by the neutrons added by the changing neutron population. These added neutrons are proportional to the fluxes and inversely proportional to the neutron velocity. Since the neutrons added by the two methods have unequal importances, the corresponding static and dynamic reactivities determined by these two methods are unequal. Calculations on some simple systems were made for application to pulsed-neutron experiments on spheres of uranyl nitrate solution.

Reference

[1]Abstract of ORNL-TM-1213 (in preparation).

3. Reactor Shielding

3.1 MEASUREMENT OF THE THERMAL-NEUTRON FLUX DOWN A RECTANGULAR CONCRETE DUCT[1]

F. J. Muckenthaler
J. J. Manning
J. L. Hull
K. M. Henry
L. B. Holland
D. R. Ward

As part of the experimental study of the transmission of neutrons down a rectangular duct with concrete walls, measurements were made of the thermal-neutron flux distribution along the axis of a straight duct and ducts with one and two bends of 90 deg. The detector used for the measurements was a spherically shaped BF_3 proportional counter. For this experiment, the Tower Shielding Reactor II (TSR-II) was placed inside a spherical lead-water shield from which a neutron beam emerged through a 3-in.-diam air-filled collimator. The beam of neutrons impinged on the inside surface of one of the walls (source wall) of the duct, whose axis was placed at an angle of 45° to the incident beam center line. For the background measurements, the source wall was removed and a piece of cadmium was inserted in its place to simulate the attenuation of the source wall to air-scattered thermal neutrons. In order to determine the distribution of the thermal-neutron flux incident on the duct wall, BF_3 counter measurements were made with the source wall of the duct removed (Fig. 3.2.2 of Sect. 3.2). Twenty-two traverses were made horizontally along the plane of the wall, 11 with the counter bare and 11 with the counter cadmium-covered. The integral under these curves gives the total number of thermal neutrons incident on the wall and indicates that the majority strike the wall within 5 ft of the mouth of the duct.

The experiment was designed to determine separately two components of the thermal-neutron flux in the duct, one from slowing down of epithermal neutrons in the duct walls and the other from the incident thermal neutrons on the duct source wall.

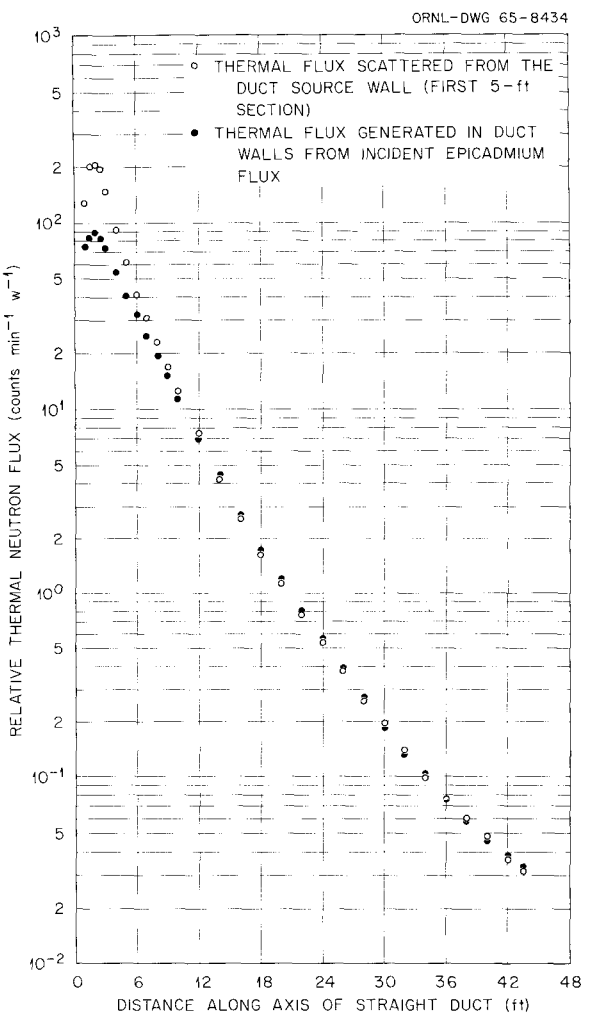

Fig. 3.1.1. Thermal-Neutron Flux as a Function of Distance Along the Axis of a Rectangular Concrete Duct.

Six different measurements along the axis of the duct were necessary to determine these two components. These were

1. bare detector, no source wall,
2. cadmium-covered detector, no source wall,
3. bare detector, no source wall, collimator beam cadmium-covered,
4. bare detector, source wall present,
5. bare detector, source wall present, collimator beam cadmium-covered,
6. cadmium-covered detector, source wall present.

Typical results from these subtractions for the straight duct are given in Fig. 3.1.1.

Note

[1]Work funded by Defense Atomic Support Agency under Order EO-802-65.

3.2 MEASUREMENT OF THE FAST-NEUTRON DOSE RATE DOWN A RECTANGULAR CONCRETE DUCT[1]

F. J. Muckenthaler
K. M. Henry
J. J. Manning
J. L. Hull
L. B. Holland
D. R. Ward

A series of experiments have been initiated at the Tower Shielding Facility to measure the fast-neutron dose rate distribution down a rectangular concrete duct, with a collimated reactor beam used as a source. The duct was placed at an angle of 45° with respect to the beam center line, the mouth of the duct being ~5 ft from the reactor collimator. Measurements have been completed for a 45-ft straight duct, and are being continued for ducts with one and two bends; however, this paper summarizes only the measurements in the straight duct. In conjunction with these measurements, a series of calculations have been made using albedo

Fig. 3.2.1. Experimental Arrangement for Measurement of the Fast Neutrons Transmitted down a Concrete Duct.

results for concrete, obtained analytically and described in Sect. 3.8.

The TSR-II[2] was placed inside a spherical lead-water shield, from which a collimated beam of neutrons emerged. The beam was collimated by placing a 3-in.-diam by 30-in.-long collimator in a beam port of the shield.

The concrete ducts were made of the same steel-reinforced, low silicon content, normal-grade concrete (density = 2.35 g/cm^3) that was used in previous albedo studies with a concrete slab.[3] The experimental setup is shown in Fig. 3.2.1. The ducts were made in various lengths, having an inside cross section 3 ft square with 9-in.-thick walls. A maximum length of ~65 ft could be obtained for the straight duct. Corner sections were built for conversion of the straight duct to a duct containing one or two bends for future experiments.

The fast-neutron dose rate incident on the inside wall of the duct was mapped with a fast-neutron dosimeter, with the wall of the duct removed (Fig. 3.2.2). Measurements were made horizontally along the plane of the wall every 6 in. from the floor of the duct to the ceiling. The data were cross-plotted to give a mapping of the source in the vertical direction; and the area under both the vertical and horizontal curves was found by integration, was converted to number of neutrons, and was multiplied by the cosine of 45° to give the total number of fast neutrons incident on the wall of the duct. The neutron distribution indicates that the source of the scattered neutrons reflected down the duct was contained in the first 5-ft length of the duct wall.

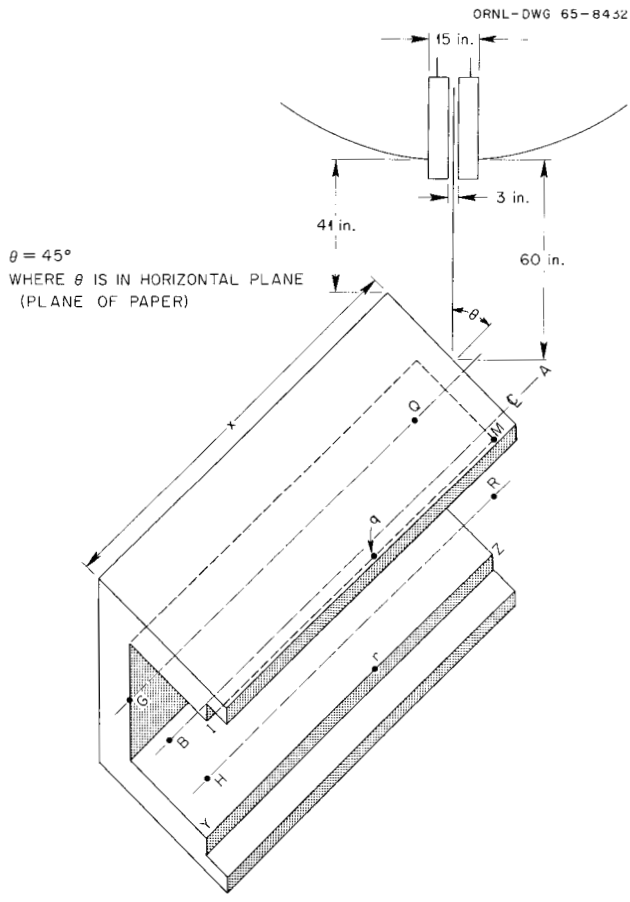

Fig. 3.2.2. Experimental Arrangement of TSR-II and First Section of the Concrete Duct.

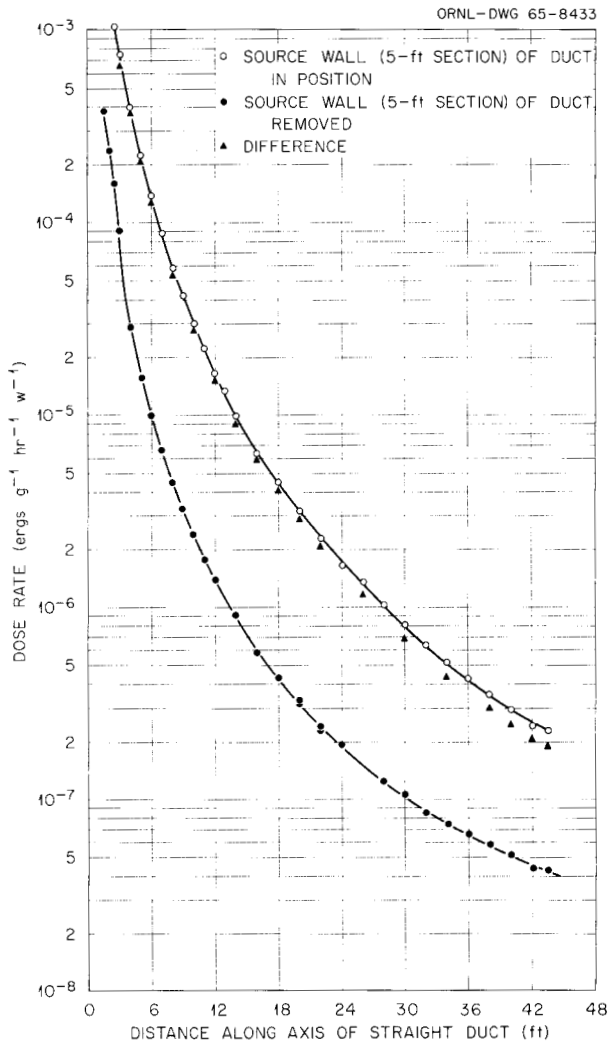

Fig. 3.2.3. Fast-Neutron Dose Rate as a Function of Distance Along the Axis of a Rectangular Concrete Duct.

Measurements were made along the axis of the straight duct with the fast-neutron dosimeter mounted vertically, with and without the duct wall in the reactor beam. The difference between these measurements gives the scattered-fast-neutron dose rate as a function of duct length. A beam catcher was used to reduce the background from air-scattered neutrons which penetrated the duct walls.

Typical results of the measurements are given in Fig. 3.2.3. Measurements down the second leg of a duct with a single 90° bend have been completed.

References and Notes

[1]Work funded by Defense Atomic Support Agency under Order EO-802-65.

[2]L. B. Holland and C. E. Clifford, *Description of the TSR-II and Proposed Preliminary Experiments*, ORNL-2747 (1959).

[3]R. E. Maerker and F. J. Muckenthaler, *Differential Fast-Neutron Albedo for Concrete*, vol. I, ORNL-3822 (in press).

3.3 MONTE CARLO CALCULATION OF THE FAST-NEUTRON DOSE RATE ALONG THE CENTER LINE OF A STRAIGHT RECTANGULAR DUCT USING THE ALBEDO CONCEPT, AND COMPARISON WITH EXPERIMENT[1]

R. E. Maerker

The fast-neutron, doubly differential albedo data for concrete previously reported[2] have been incorporated into the flexible duct code of Cain.[3] Calculations have been made of the fast-neutron dose rate at some 16 locations between the mouth and 40 ft down the center line of a 3- by 3-ft rectangular duct. The incident fast-neutron spectrum was assumed to be the same as that reported previously for a similar TSR-II geometry,[4] and the incident beam was assumed to be monodirectional, striking a side wall of the duct at an angle of 45°. Results of the calculation were normalized to the total neutrons from the TSR-II incident on the wall, the latter being obtained by numerical integration of the measured incident dose rate over the wall surface. From the source

Table 3.3.1 Comparison of Calculated and Measured Center Line Dose Rates

Center Line Distance from Mouth (ft)	$\left(\frac{\text{Singly Scattered Dose Rate}}{\text{Total Dose Rate}}\right)_{\text{Calc.}}$	Dose Rate (ergs g^{-1} hr^{-1} w^{-1}) Measured	Calculated	Error (%)
3	0.73	6.6×10^{-4}	6.23×10^{-4}	−6
4		3.70×10^{-4}	3.24×10^{-4}	−13
5		2.08×10^{-4}	1.84×10^{-4}	−12
6	0.44	1.27×10^{-4}	1.21×10^{-4}	−5
8		5.35×10^{-5}	5.92×10^{-5}	+11
10	0.35	2.75×10^{-5}	2.80×10^{-5}	+3
12	0.38	1.50×10^{-5}	1.42×10^{-5}	−5
15	0.43	7.1×10^{-6}	6.15×10^{-6}	−14
20	0.47	2.85×10^{-6}	2.30×10^{-6}	−20
25		1.30×10^{-6}	1.02×10^{-6}	−22
30	0.61	6.7×10^{-7}	5.37×10^{-7}	−21
35		3.9×10^{-7}	3.19×10^{-7}	−19
40	0.65	2.45×10^{-7}	2.05×10^{-7}	−17

mapping measurements, the plane source for the calculation was determined to be centered at the mouth at a point 1.45 ft from the floor and 1.45 ft from the wall nearest the reactor, and was 0.90 ft in height and 1.34 ft in width measured in the plane of the mouth. Eight thousand histories were run for this problem.

Table 3.3.1 shows a comparison of the calculated and measured dose rates along the duct center line, the measured values being taken from the foreground less the background smoothed curve reported in Sect. 3.1.

References and Notes

[1]Work funded by Defense Atomic Support Agency under Order EO-802-65.

[2]*Neutron Phys. Div. Ann. Progr. Rept. Aug. 1, 1964,* ORNL-3714, vol. 1, p. 57.

[3]V. R. Cain, *Calculations of Thermal-Neutron Flux Distributions in Concrete-Walled Ducts Using an Albedo Model with Monte Carlo Techniques,* ORNL-3507 (January 1964).

[4]*Neutron Phys. Div. Ann. Progr. Rept. Aug. 1, 1963,* ORNL-3499, vol. 1, Fig. 3.3.5, p. 107.

3.4 A MONTE CARLO DETERMINATION OF INTERMEDIATE-ENERGY DIFFERENTIAL NEUTRON ALBEDOS FOR CONCRETE[1]

W. A. Coleman R. E. Maerker

The problem of radiation streaming through multibend air-concrete ducts may be treated by determining the reflected energy-angle spectra for a particular concrete composition and utilizing these data in an albedo random walk for a particular geometry. The authors have calculated differential energy-angle albedo data for a semi-infinite steel-reinforced concrete medium, using a series of incident angle and energy conditions. The energy range from 0.5 ev to 200 kev was divided into ten groups, ΔE_0^i, equally spaced in lethargy. The incident angles were 0, 45, 60, 75, and 85°. A general-purpose Monte Carlo neutron-transport code, O5R, was used to obtain a collision distribution for each incident energy band ΔE_0^i and angle θ_0^j. The distribution of reflected neutrons in energy and angle was determined by computing, at each collision, the probability of escape along each of 54 directions (defined by angles θ_l and ϕ_m). This scheme has been used recently to generate fast-neutron differential dose albedos which agree well with experimental dose measurements.[2]

In addition to the doubly differential energy-angle albedo, the following studies were made for intermediate energies:

1. the radial dispersion of reflected neutrons from the point of incidence,
2. the distribution in depth and energy of intermediate-energy captures,
3. the distribution in polar angle θ_l and depth of those neutrons which were degraded below 0.5 ev before escaping.

The reflected singly scattered spectra calculated analytically agreed (within statistics) with the Monte Carlo estimate of the singly scattered spectra. A comparison study showed the Monte Carlo results to be in good agreement with those obtained in a 30-group S_{16} calculation using DTF, a one-dimensional S_n code developed by General Atomic.[3]

References and Notes

[1]Abstract of ORNL-TM-1205 (to be published); work funded by Defense Atomic Support Agency under Order EO-802-65.

[2]R. E. Maerker and F. J. Muckenthaler, *Nucl. Sci. Eng.* **22**, 4 (1965).

[3]N. M. Green, ORNL, private communication.

3.5 MONTE CARLO DETERMINATION OF THE DIFFERENTIAL THERMAL-NEUTRON ANGULAR ALBEDOS AND CAPTURE-GAMMA DOSE RATES FOR CONCRETE ARISING FROM THE SLOWING DOWN OF INCIDENT INTERMEDIATE-ENERGY NEUTRONS[1]

R. E. Maerker

To complete the determination of the differential neutron albedos of concrete for incident intermediate-energy (200-kev to 0.5-ev) monodirectional neutron beams (Sect. 3.4), one-velocity Monte Carlo calculations were carried out for the diffusion of the neutrons degraded below 0.5 ev.

A series of one-velocity diffusion problems were run to calculate the differential angular reflected

current, the total transmitted current, and the spatial distribution of captures within a semi-infinite 9-in.-thick slab. Each problem was characterized by selecting the location of a point isotropic source of thermal neutrons uniformly within a given depth band inside the slab. Each of the nine depth bands coincided with those used to determine the spatial distribution of neutrons slowing down below 0.5 ev from the intermediate-energy calculations (Sect. 3.4). Six hundred histories were run for each problem, and a doubly correlated sampling technique was used to obtain results as functions of the number of scatterings allowed (50, 100, 200, 400) and the thickness of the slab (9 and 16.75 in.). Isotropic scattering was assumed, and the one-velocity (0.025-ev) parameters Σ_S/Σ_T used were 0.987 and 0.978 for the three concrete and two reinforced-concrete regions respectively. Confidence limits on the differential angular reflected currents average less than ±10%. A technique of estimating the differential angular current through each of nine space-fixed reflected polar angles at each scattering was employed, using the estimation

$$W \frac{\Sigma_S}{\Sigma_T} \frac{e^{-\Sigma_T Z/|\mu_i| t}}{4\pi} ,$$

where the $\mu_i = -(i + 0.5)/9$, $i = 0, 1, \ldots, 8$, are the cosines of the reflected polar angles with respect to an inwardly drawn slab normal and W is the neutron weight before the collision. The captures were calculated by adding

$$W \left[1 - \frac{\Sigma_S}{\Sigma_T}(z) \right]$$

at each collision into the proper depth band. The resulting gamma-ray differential angular current dose rate shape as a function of μ is assumed to be that of the uncollided gamma rays, since the scattered-gamma-ray contribution is less than

Table 3.5.1. Curve-Fitted Values of Thermal-Neutron Albedos Produced by Slowing Down of Incident Intermediate-Energy Neutrons

ΔE_0	$d\alpha_{th}/d\Omega$ [thermal neutrons steradian^{-1} (source neutron)$^{-1}$]	α_{th} (thermal neutrons per source neutron)
55.1–200 kev	$\lvert\mu\rvert (1 + 1.73 \lvert\mu\rvert)(0.0043 + 0.0058\mu_0)$	$0.029 + 0.039\mu_0$
15.2–55.1 kev	$\lvert\mu\rvert (1 + 1.73 \lvert\mu\rvert)(0.0052 + 0.0059\mu_0)$	$0.035 + 0.040\mu_0$
4.2–15.2 kev	$\lvert\mu\rvert (1 + 1.73 \lvert\mu\rvert)(0.0062 + 0.0071\mu_0)$	$0.042 + 0.048\mu_0$
1.15–4.2 kev	$\lvert\mu\rvert (1 + 1.73 \lvert\mu\rvert)(0.0077 + 0.0073\mu_0)$	$0.052 + 0.049\mu_0$
0.32–1.15 kev	$\lvert\mu\rvert (1 + 1.73 \lvert\mu\rvert)(0.0090 + 0.0099\mu_0)$	$0.061 + 0.067\mu_0$
0.087–0.32 kev	$\lvert\mu\rvert (1 + 1.73 \lvert\mu\rvert)(0.011 + 0.012\mu_0)$	$0.074 + 0.081\mu_0$
24–87 ev	$\lvert\mu\rvert [(0.0185 + 0.0150\mu_0) + \lvert\mu\rvert (0.0177 + 0.0235\mu_0)]$	$0.095 + 0.096\mu_0$
6.6–24 ev	$\lvert\mu\rvert [0.0332 + 0.0085\mu_0) + \lvert\mu\rvert (0.0220 + 0.0268\mu_0)]$	$0.150 + 0.084\mu_0$
1.8–6.6 ev	$\lvert\mu\rvert [0.0595 + \lvert\mu\rvert (0.0290 + 0.0305\mu_0)]$	$0.248 + 0.064\mu_0$
0.5–1.8 ev	$\lvert\mu\rvert [(0.124 - 0.035\mu_0) + \lvert\mu\rvert (0.020 + 0.053\mu_0)]$	$0.431 + 0.001\mu_0$

half the total. The uncollided secondary gamma-ray angular current dose rate was thus multiplied by a buildup factor averaged over the capture-gamma-ray spectrum and depth.

The results of all these calculations are summarized in Tables 3.5.1, 2, and 3. Table 3.5.1 gives curve-fitted values of the reflected differential angular current albedo of thermal (i.e., subcadmium) neutrons in neutrons per steradian per incident neutron of energy within ΔE_0, as well as values of the total thermal albedo. The highest six incident-energy groups produce a reflected-thermal-neutron distribution having a shape independent of μ_0, the cosine of the incident polar angle, and identical to the shape calculated by Fermi[2] and Placzek.[3] The curve-fitted values reproduce the Monte Carlo values to within ±15% for the differential thermal albedos and to within ±10% for the total thermal albedos.

Table 3.5.2 gives curve-fitted values of the secondary capture gamma-ray differential angular current dose rate albedo and values of the total current dose rate albedo. The departure of the quantity in parentheses on the extreme right of the first expression from unity represents the dose rate due to epicadmium (0.5 ev to 200 kev) captures; the remainder is due to subcadmium (<0.5 ev) captures. The curve fits reproduce the calculated values to within ±15% for the differential dose rates and to within ±10% for the total dose rates.

Table 3.5.2. Curve-Fitted Values of Secondary-Gamma-Ray Dose Rates Arising from the Slowing Down of Incident Intermediate-Energy Neutrons

ΔE_0	$dD_\gamma/d\Omega$ [rads hr^{-1} steradian^{-1} per incident source neutron sec^{-1}]	D_γ [rads hr^{-1} per incident neutron sec^{-1}]
55.1–200 kev	$10^{-7}\,\lvert\mu\rvert\,(0.43 + 2.17\,\lvert\mu\rvert - 1.67\mu^2)\,(0.40 + 0.60\mu_0)\,(1.10)$	$10^{-7}(1.30 + 1.96\mu_0)$
15.2–55.1 kev	$10^{-7}\,\lvert\mu\rvert\,(0.39 + 1.78\,\lvert\mu\rvert - 1.39\mu^2)\,(0.55 + 0.75\mu_0)\,(1.11)$	$10^{-7}(1.52 + 2.07\mu_0)$
4.2–15.2 kev	$10^{-7}\,\lvert\mu\rvert\,(0.70 + 2.53\,\lvert\mu\rvert - 2.07\mu^2)\,(0.42 + 0.52\mu_0)\,(1.12 - 0.01\mu_0)$	$10^{-7}(1.77 + 2.19\mu_0)$
1.15–4.2 kev	$10^{-7}\,\lvert\mu\rvert\,(0.68 + 2.59\,\lvert\mu\rvert - 2.08\mu^2)\,(0.45 + 0.60\mu_0)\,(1.12 - 0.01\mu_0)$	$10^{-7}(1.93 + 2.57\mu_0)$
0.32–1.15 kev	$10^{-7}\,\lvert\mu\rvert\,(0.66 + 3.18\,\lvert\mu\rvert - 2.60\mu^2)\,(0.48 + 0.57\mu_0)\,(1.14 - 0.02\mu_0)$	$10^{-7}(2.23 + 2.65\mu_0)$
0.087–0.32 kev	$10^{-7}\,\lvert\mu\rvert\,(0.97 + 2.39\,\lvert\mu\rvert - 2.08\mu^2)\,(0.48 + 0.70\mu_0)\,(1.18 - 0.06\mu_0)$	$10^{-7}(2.30 + 3.35\mu_0)$
24–87 ev	$10^{-7}\,\lvert\mu\rvert\,(1.07 + 1.96\,\lvert\mu\rvert - 1.83\mu^2)\,(0.53 + 0.86\mu_0)\,(1.30 - 0.15\mu_0)$	$10^{-7}(2.43 + 3.95\mu_0)$
6.6–24 ev	$10^{-7}\,\lvert\mu\rvert\,(1.75 + 2.25\,\lvert\mu\rvert - 2.32\mu^2)\,(0.50 + 0.54\mu_0)\,(1.11 - 0.04\mu_0)$	$10^{-7}(3.28 + 3.54\mu_0)$
1.8–6.6 ev	$10^{-7}\,\lvert\mu\rvert\,[1.51 + 0.63\mu_0 + \lvert\mu\rvert\,(0.15 + 2.30\mu_0) - \mu^2(0.60 + 2.11\mu_0)]\,(1.09 - 0.03\mu_0)$	$10^{-7}(4.08 + 3.52\mu_0)$
0.5–1.8 ev	$10^{-7}\,\lvert\mu\rvert\,[2.23 + 0.76\mu_0 + \lvert\mu\rvert\,(-1.54 + 3.07\mu_0) + \mu^2(0.42 - 2.82\mu_0)]\,(1.07 - 0.02\mu_0)$	$10^{-7}(4.46 + 4.40\mu_0)$

Table 3.5.3. Curve-Fitted Parameters for the Differential Angular Current Albedos Summed Over All Reflected Energies

ΔE_0	α_1	α_2	β_1	β_2	γ_1	γ_2	a	b	c	δ_1	δ_2
55.1–200 kev	0.190	−0.020	0.020	0.300	0.11	0.91	0.20	0.56	0	0.880	−0.208
15.2–55.1 kev	0.190	−0.025	0.025	0.295	0.11	0.91	0.225	0.69	0	0.865	−0.177
4.2–15.2 kev	0.216	−0.047	−0.004	0.307	0.12	0.91	0.24	0.70	0	0.875	−0.200
1.15–4.2 kev	0.210	−0.046	−0.005	0.310	0.12	0.91	0.24	0.70	0	0.875	−0.232
0.32–1.15 kev	0.208	−0.042	−0.005	0.305	0.12	0.91	0.24	0.70	)	0.860	−0.205
0.087–0.32 kev	0.210	−0.061	−0.003	0.296	0.125	0.865	0.28	0.72	0	0.845	−0.210
24–87 ev	0.205	−0.068	−0.003	0.283	0.13	0.845	0.30	0.73	0	0.830	−0.228
6.6–24 ev	0.202	−0.075	−0.002	0.270	0.13	0.82	0.32	0.74	0	0.815	−0.230
1.8–6.6 ev	0.172	−0.059	0.021	0.218	0.105	0.65	0.40	0.77	0	0.817	−0.244
0.5–1.8 ev	0.105	−0.036	0.115	0.125	0.080	0.48	0.255	−0.072	0.765	0.792	−0.232

Table 3.5.3 presents values of the curve-fitted parameters for the differential angular current albedos summed over all reflected energies from the source energy down to and including thermal and for the total-current albedos. The curve fits reproduce nearly all the Monte Carlo values to within ±15% for the differential albedos and to within ±3% for the total-current albedos. The general curve-fitted expressions are

$$\frac{d\alpha_{\text{total}}}{d\Omega} = \frac{|\mu|\,[(\alpha_1 + \alpha_2\mu_0) + |\mu|(\beta_1 + \beta_2\mu_0)]}{|\mu| + \gamma_1 + \gamma_2\mu_0}$$

$$\times \{1 + (1 - |\mu|)(1 - \mu_0)[a(2\cos^2\phi - 1) + b\cos\phi + c\cos^3\phi]\}$$

and

$$\alpha_{\text{total}} = \delta_1 + \delta_2\mu_0 \,.$$

References and Notes

[1]Work funded by Defense Atomic Support Agency under Order EO-802-65.

[2]E. Fermi, *On the Motion of Neutrons in Hydrogenous Substances,* NP-2385 (1951) [transl. by G. M. Temmer of *Ricerca Sci.* **7**(2), 13 (1936)].

[3]G. Placzek, *Phys. Rev.* **72**, 556 (1947).

3.6 INVESTIGATION OF THE ACCURACY OF THE MONTE CARLO METHOD FOR CALCULATING DIFFERENTIAL ANGULAR THERMAL-NEUTRON ALBEDOS AND THERMAL-NEUTRON CAPTURES FOR A WEAKLY ABSORBING MEDIUM SUCH AS CONCRETE[1]

R. E. Maerker

An investigation was made of the accuracy of the Monte Carlo technique using a single-velocity model for calculating differential angular thermal-neutron albedos from, and thermal-neutron captures within, a medium of relatively small absorption. In particular, the thermal albedos, capture sources, and capture-gamma doses were calculated as a function of both the number of scatterings allowed and the thickness of the medium. The validity of using a single-velocity treatment in representing the true physical situation in the thermal region is discussed in Sect. 3.7.

Table 3.6.1 shows a comparison of the differential angular albedos (i.e., reflected number current per steradian per incident source neutron) for the case of $\Sigma_S/\Sigma_T = 0.975$, an infinite slab, isotropic scattering in the laboratory system, and a normally incident beam of neutrons, with the theoretical

Table 3.6.1 Comparison of Monte Carlo Results with Exact Results of Chandrasekhar

$\lvert\mu\rvert$	$d\alpha/d\Omega$ per Steradian							
	1 Scattering	5 Scatterings	10 Scatterings	20 Scatterings	50 Scatterings	100 Scatterings	200 Scatterings	Exact
1.0	3.92×10^{-2}	1.10×10^{-1}	1.46×10^{-1}	1.73×10^{-1}	1.93×10^{-1}	1.97×10^{-1}	1.98×10^{-1}	2.00×10^{-1}
0.9	3.72×10^{-2}	1.03×10^{-1}	1.35×10^{-1}	1.59×10^{-1}	1.76×10^{-1}	1.79×10^{-1}	1.80×10^{-1}	1.82×10^{-1}
0.8	3.50×10^{-2}	9.47×10^{-2}	1.22×10^{-1}	1.43×10^{-1}	1.58×10^{-1}	1.61×10^{-1}	1.61×10^{-1}	1.63×10^{-1}
0.7	3.24×10^{-2}	8.59×10^{-2}	1.10×10^{-1}	1.27×10^{-1}	1.39×20^{-1}	1.42×10^{-1}	1.42×10^{-1}	1.44×10^{-1}
0.6	2.96×10^{-2}	7.63×10^{-2}	9.63×10^{-2}	1.11×10^{-1}	1.20×10^{-1}	1.22×10^{-1}	1.23×10^{-1}	1.24×10^{-1}
0.4	2.27×10^{-2}	5.46×10^{-2}	6.67×10^{-2}	7.53×10^{-2}	8.09×10^{-2}	8.19×10^{-2}	8.21×10^{-2}	8.26×10^{-2}
0.3	1.85×10^{-2}	4.24×10^{-2}	5.08×10^{-2}	5.67×10^{-2}	6.06×10^{-2}	6.13×10^{-2}	6.14×10^{-2}	6.15×10^{-2}
0.2	1.34×10^{-2}	2.92×10^{-2}	3.43×10^{-2}	3.79×10^{-2}	4.02×10^{-2}	4.06×10^{-2}	4.07×10^{-2}	4.02×10^{-2}
0.1	7.35×10^{-3}	1.51×10^{-2}	1.73×10^{-2}	1.89×10^{-2}	1.99×10^{-2}	2.01×10^{-2}	2.01×10^{-2}	1.94×10^{-2}

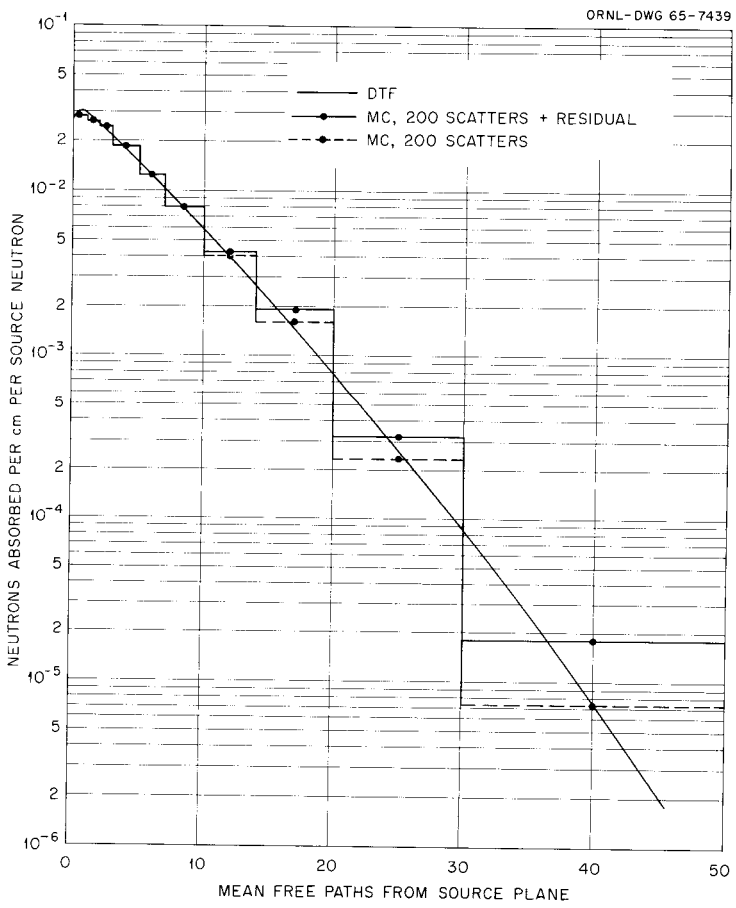

Fig. 3.6.1. Comparison of Capture Sources Calculated by Monte Carlo and DTF for the Case of Normal Incidence and $\Sigma_S/\Sigma_T = 0.987$.

curve of Chandrasekhar,[2] calculated from the expression

$$\frac{d\alpha}{d\Omega} = \frac{0.975}{4\pi} \frac{|\mu|}{|\mu| + 1} \mathscr{H}(0.975, 1) \mathscr{H}(0.975, |\mu|) .$$

A correlated sampling technique on 2000 histories was used to obtain the results as a function of the number of scatterings, and a statistical-estimation technique was used at each scattering.

Figure 3.6.1 shows a comparison of the Monte Carlo results for the capture sources with those of an S_{16}, DTF-II one-group calculation for the case of isotropic scattering, normal incidence, infinite slab, and $\Sigma_S/\Sigma_T = 0.987$. The residual Monte Carlo results presented represent the capture sources due to 200 scatterings or less plus the weight remaining after the 200th scattering. Thus the two Monte Carlo curves should bracket the correct result.

From the above comparisons it is clear that simple Monte Carlo techniques are adequate to treat one-velocity diffusion and can be used in cases where other methods may be inadequate, such as the case of anisotropic scattering in the laboratory system or in heterogeneous media. Azimuthal dependence of the differential angular albedo may also be calculated with these same simple Monte Carlo techniques.

From an analysis of the results of many Monte Carlo problems run for various angles of incidence, it may be concluded that, for weakly absorbing media such as ordinary concrete ($\Sigma_S/\Sigma_T \cong 0.987$), the number of scatterings needed to reach convergence is at least 50 for the thermal albedo, 150 for the capture sources (the number increases as one goes deeper into the slab), and 100 for the capture-gamma dose on the surface. A slab approximately 7 mean free paths thick essentially saturates the differential angular thermal albedo, and one 12 mean free paths thick essentially saturates the capture-gamma dose on the surface.

References and Notes

[1]Paper submitted for presentation at the American Nuclear Society 1965 Winter Meeting, November 15–18, Washington, D.C.; work funded by Defense Atomic Support Agency under Order EO-802-65.

[2]S. Chandrasekhar, *Radiative Transfer*, Oxford University Press, London (1950).

3.7 SINGLE-VELOCITY CALCULATION AND MEASUREMENT OF DIFFERENTIAL ANGULAR THERMAL-NEUTRON ALBEDOS FOR CONCRETE[1]

R. E. Maerker F. J. Muckenthaler

In Sect. 3.6 the Monte Carlo method was concluded to be adequate for describing thermal neutrons diffusing in weakly absorbing media if a sufficient number of scatterings were followed for each neutron. In this section, results from a single-velocity Monte Carlo treatment are compared with experiment for the case of monodirectional neutrons incident on concrete. The extent to which agreement is established indicates the errors involved in representing the properties of subcadmium neutrons by single-velocity parameters.

The statistical-estimation technique used in the calculations is identical to that described for fast neutrons.[2] The composition of the slab assumed for the calculations was identical to that of the low-silicon, steel-reinforced concrete slab employed in the experiment. It was 9 in. thick and was divided into five regions, two of which were 1-in.-thick steel-reinforced regions positioned 1.75 and 7.25 in. from the front face of the slab. These two regions were assumed to be homogeneous and to have a $\Sigma_S/\Sigma_T = 0.978$ for a neutron energy of 0.025 ev. For the three remaining regions (no steel), Σ_S/Σ_T was taken to be 0.987.

Two scattering laws were assumed: (1) isotropic scattering in the laboratory system for all elements; that is, the hydrogen is completely bound to the oxygen in the case of water, and the small anisotropy in the scattering cross sections of the other elements is neglected; (2) anisotropic water scattering, using a scattering law deduced from the results of experiments by Greenspan and Baksys,[3] at an energy of 0.0358 ev, together with isotropic laboratory scattering for nonwater oxygen, calcium, etc. In both cases, the total thermal-neutron cross section (0.025 ev) for water was taken[4] as 105 barns.

Absorptions within 20 depth regions of the slab were also calculated, and the resulting capture-gamma dose on the surface was obtained by integration. The capture spectra of each element were taken from the *Reactor Handbook*.[5] In each of the ten problems run (angles of incidence of 0, 45, 60, 75, and 90° for each of the two assumed scattering laws), 2000 histories were followed,

until a neutron escaped from the front or back face or suffered more than 200 collisions. In the event of the latter occurrence, the residual weight was added into the depth band where the 200th scattering took place; except for depths near the back face, the residual weight contribution is negligible, and amounts at most to 1% of the absorptions.

A series of very careful measurements, utilizing a highly collimated neutron beam and a detector geometry similar to that of the fast-neutron experiment, were performed at the Tower Shielding Facility to determine the thermal differential angular albedos as a function of reflected polar and azimuthal angles for angles of incidence of 0, 45, 60, and 75°. Sixteen different measurements using a BF_3 detector were necessary at each of 72 combinations of the incident angle and the polar and azimuthal reflected angles to effect a single measurement of the angular albedo. Cadmium-covered and bare-detector readings were taken for the cases of cadmium over the slab, cadmium over the reactor collimator, cadmium over both simultaneously, and both slab and collimator bare for both foreground and background geometries. By a series of subtractions, the thermal differential angular albedo was one of the quantities that could be obtained. Measured values were corrected for air attenuation and the inverse square effect, and then divided by the incident subcadmium current integrated over the surface of the slab to determine the thermal differential angular albedos.

A surprising measured azimuthal variation was closely approximated by the anisotropic-water-scattering calculation, which agreed within a root-mean-square deviation of 5.1% for 72 measured differential angular albedos. Therefore, the one-velocity treatment seemed to be quite adequate for concrete.

A simple expression for the thermal differential angular current albedo for this concrete is

$$\frac{d\alpha}{d\Omega} = \frac{0.0875|\mu|}{|\mu| + \mu_0}(1 + 1.28|\mu|)(1 + 1.62\mu_0 - 0.42\mu_0^2) \times [1 + (1 - \mu_0)(1 - |\mu|)(-0.10 + 0.43 \cos\phi + 0.20\cos^2\phi)] ,$$

in which μ and μ_0 are the polar angle cosines, with regard to the inwardly drawn slab normal, of the reflected and incident beams, respectively, and ϕ is the conventional azimuth.

References and Notes

[1]Submitted for presentation at the 1965 Winter Meeting of the American Nuclear Society, November 15–18, Washington, D.C.; work funded by Defense Atomic Support Agency under Order EO-802-65.

[2]R. E. Maerker and F. J. Muckenthaler, *Trans. Am. Nucl. Soc.* **7**(2), 365 (1964).

[3]H. Greenspan and I. G. Baksys, *Differential Scattering Cross Sections for Slow Neutrons in H_2O*, Addenda, Newsletter No. 9, Argonne National Laboratory (March 1963).

[4]D. J. Hughes and R. S. Carter, *Neutron Cross Sections*, BNL-325 (July 1955).

[5]H. Goldstein, "Sources of Neutrons and Gamma Rays," pp. 45–46 in *Reactor Handbook*, 2d ed., vol. III Part B, "Shielding," ed. by E. P. Blizard and L. S. Abbott, Interscience, New York, 1962.

3.8 CALCULATION AND MEASUREMENT OF THE FAST-NEUTRON DIFFERENTIAL DOSE ALBEDO FOR CONCRETE[1]

R. E. Maerker F. J. Muckenthaler

Monte Carlo calculations have been carried out in great detail on the reflection properties of concrete for fast neutrons. This report presents the results for the differential angular dose albedo for various incident-beam conditions and touches upon some of the other distributions calculated. The following formula represents the calculated differential angular dose albedo to better than 10% for about 95% of the values obtained and can be used to extend the results to the entire hemispherical range for both incident- and reflected-neutron velocity vectors:

$$\frac{d\alpha}{d\Omega}(\theta, \phi, \theta_0, \Delta E_0) = \left[\frac{|\cos\theta|}{|\cos\theta| + K_1(\Delta E_0)\cos\theta_0} \sum_{l=0}^{L} A_l(\Delta E_0)\, P_l(\cos\Theta)\right] + \left[\frac{|\cos\theta|}{|\cos\theta| + K_2(\Delta E_0, \theta_0, \theta)} \sum_{k=0}^{K} B_k(\Delta E_0)\, P_k(\cos\Theta)\right],$$

where

θ_0, θ = the incident and reflected polar angles with respect to the inwardly drawn slab normal, respectively,

ϕ = the reflected azimuthal angle,

$\frac{d\alpha}{d\Omega}$ = $|\cos\ \theta| \cdot$(angular flux) in dose units per steradian per incident particle dose,

$\cos\Theta = \cos\theta_0\ \cos\theta + \sin\theta_0\ \sin\theta\ \cos\phi$, $-1 \leq \cos\theta \leq 0$,

and

$$K_2(\Delta E_0, \theta_0, \theta) = \sum_{i=0}^{I} (|\cos\theta|)^i \sum_{j=0}^{J} a_{ij}(\Delta E_0) \cos^j \theta_0.$$

A comparison of the fast-neutron angular dose albedo calculations weighted by an incident spectrum previously measured at the Tower Shielding Facility with the results of a series of dose albedo measurements performed at the TSF shows that from 147 combinations of the incident and reflected angles there is a root-mean-square deviation of 3.1%, with the largest single deviation being 9%. This excellent agreement shows that existing cross sections are adequate to calculate differential albedos to a high precision.

References and Notes

[1]Abstract of *Nucl. Sci. Eng.* **22**, 455 (1965) and of ORNL-3822, vol. 1 (1965); work funded by the Defense Atomic Support Agency under Order EO-802-65.

3.9 A CALCULATION OF THE NEUTRON DOSE IN ORDINARY CONCRETE DUE TO AIR-SCATTERED NEUTRONS FROM A POINT FISSION SOURCE[1]

D. K. Trubey

A calculation of the fast-neutron dose in concrete due to a point fission source located in air at a distance of 100 g/cm^2 has been performed. The moments-method code RENUPAK was used successively to produce the energy spectrum in air from the point source and the energy spectrum in concrete from the air-scattered source. Angular distribution conversion factors and data for conversion to other amounts of air attenuation are given.

Reference

[1]Abstract of ORNL-TM-973 (Mar. 15, 1965).

3.10 MEASURED NEUTRON SOURCE SPECTRA FOR ANGULAR SCATTERING EXPERIMENTS WITH SMALL CYLINDERS[1]

J. C. Courtney[2] V. V. Verbinski

In a series of experiments in which the scattering of fast neutrons from small cylinders of various materials was investigated, a pulsed source of bremsstrahlung-produced neutrons was obtained by irradiating a lead target with 14-nsec bursts of 34-Mev electrons from the General Atomic electron linear accelerator. The differential energy spectra of the source neutrons for the three angles of incidence used are presented.

References and Notes

[1]Abstract of ORNL-TM-1087 (Apr. 9, 1965); work partially funded by the U.S. Army Nuclear Defense Laboratory, Edgewood Arsenal, Maryland, under Order NDL-23-63.

[2]Catholic University, Washington, D.C.; Graduate Fellow, Oak Ridge Institute of Nuclear Studies.

3.11 FAST-NEUTRON SCATTERING FROM SMALL CYLINDERS OF STEEL, ALUMINUM, GRAPHITE, CONCRETE, AND LITHIUM HYDRIDE[1]

V. V. Verbinski J. C. Courtney[2]

Time-of-flight methods were used to measure the spectra of fast neutrons scattered at angles 20, 45, 70, 110, 135, and 160° from an incident beam by small cylinders of steel, aluminum, graphite, concrete, and lithium hydride. The lithium hydride cylinders were 1½ and 3 in. in diameter, the concrete cylinders were 1¾ in. in diameter, and all other samples were 2 in. in diameter. The measurements were made at the General Atomic

electron linear accelerator, where a pulsed source of bremsstrahlung-produced neutrons was obtained by irradiating a lead target with 14-nsec bursts of 34-Mev electrons. The energy spectrum of the neutrons approximated a fission spectrum. Some of the neutrons struck the scattering sample, which was placed 13 in. from the source, and then passed through a system of collimators, down a drift tube, and into a liquid-scintillator fast-neutron detector. Pulse-shape discrimination circuitry was used to eliminate pulses due to any gamma-ray background.

Measured source spectra were used as input for Monte Carlo calculations of the scattered neutrons, and the results were compared with measured scattered spectral intensities. The calculations and experiments, integrated over energy, agreed within 16%. Since the spectral shape was satisfactorily reproduced, it is believed that the uncertainty in the measurement of the integrated fast-neutron flux by foil activation accounts for any discrepancies. These comparisons indicate that the ORNL cross-section library (see Sect. 5.21) for these elements is adequate for neutron-scattering calculations.

References and Notes

[1]Combined abstract of ORNL-TM-1247 (in preparation) and of *Fast-Neutron Scattering from Small Cylinders of Steel, Aluminum, and Graphite* by J. C. Courtney, ORNL-TM-1156 (July 1965); work partially funded by the U.S. Army Nuclear Defense Laboratory, Edgewood, Md., under Order NDL-23-63.

[2]Catholic University, Washington, D.C.; Graduate Fellow, Oak Ridge Institute of Nuclear Studies.

3.12 MEASUREMENT OF THE NEUTRON-SOURCE DISTRIBUTION IN A POOL-TYPE RESEARCH REACTOR[1]

M. S. Bokhari[2] V. V. Verbinski

An absolute-power calibration of a swimming pool type of research reactor was performed in order to obtain the precise source term for some earlier measurements of neutron spectral intensity in the water shield of the reactor (see Sect. 3.13). A straightforward method of flux mapping was used: the relative flux was measured with copper-wire-activation techniques, and the copper wires were calibrated against thin samples of the reactor fuel. The thin uranium foils were activated in both the reactor and the thermal column of the ORNL standard pile, and the activation ratios gave the equivalent thermal-neutron flux for producing fission events in the uranium fuel. The absolute neutron-source density was determined from the flux and the known uranium density. The copper-wire activity was found to be proportional to the fission rate within about 2% over the entire length of the reactor fuel elements. Thus in this type of reactor the copper activation is proportional to power density within 1 to 2% because of averaging over the entire reactor volume.

References and Notes

[1]Abstract of ORNL-3798 (in preparation).

[2]Now at Lahore Center, Pakistan Atomic Energy Commission, Lahore, Pakistan.

3.13 MEASUREMENTS AND CALCULATIONS OF SPECTRAL AND SPATIAL DETAILS OF FAST-NEUTRON FLUX IN WATER SHIELDS[1]

V. V. Verbinski M. S. Bokhari[2]
J. C. Courtney[3]

Measurements have been made of the spectral and spatial details of neutron flux in the water shield surrounding the BSR-1 swimming pool reactor. For these measurements the absolute spectral intensity was obtained for a reactor configuration in which the absolute neutron-source distribution was measured. Using the latter as an input to the NIOBE and DTK neutron-transport codes, both the neutron spectra of angular flux and the absolute intensity were predicted with reasonably good accuracy by the calculations.

Another set of measurements was made for neutrons from a pulsed linac source, using slabs of water and measuring neutron-leakage spectra at 0 and 30° to the slab normal by high-resolution time-of-flight spectroscopy. Sulfur-pellet attenuation ratios were also obtained for each slab thickness. The small, 5-cm-diam, linac source

was surrounded by a 7.5-cm-thick lead housing. A DTK transport calculation that could handle the 5-cm source configuration without divergence difficulties reproduced the main features of both the 0 and 30° experimental spectra fairly well, except that it predicted too low a flux in the 4.5- to 7.5-Mev energy region. Updating the oxygen total cross sections[4] corrected this disagreement. The sulfur-activation ratios, as measured with sulfur pills placed on each side of the water slab, agree with the ratio calculated by the DTK code for a 40-cm slab. All the 0° calculations yielded neutron spectra that were too low in the region of the high, broad transmission peak between 5.5 and 7.5 Mev.

References and Notes

[1]Abstract of paper to be submitted to *Nuclear Science and Engineering*.

[2]Now at Lahore Center, Pakistan Atomic Energy Commission, Lahore, Pakistan.

[3]Catholic University, Washington, D.C.; Graduate Fellow, Oak Ridge Institute of Nuclear Studies.

[4]J. R. Stehn, M. D. Goldberg, B. A. Magurno, and R. Weiner-Chasman, *Neutron Cross Sections*, BNL-325, Suppl. 2, vol. I (May 1964).

3.14 PROPAGATION OF NEUTRON WAVES THROUGH HETEROGENEOUS MULTIPLYING AND NONMULTIPLYING MEDIA[1]

V. R. Cain

The behavior of neutron waves in heterogeneous media was predicted by use of the one-group diffusion theory and the age-diffusion theory. The one-group theory was used in two different finite geometries which allowed reduction to a one-dimensional and a two-dimensional problem. These cases resulted in diffusion kernels, or Green's functions, for the two finite configurations. The theory was then extended to include Fermi-age, or continuous slowing-down, theory for higher-energy neutrons, an approach which is similar to the Feinberg-Galanin heterogeneous-reactor theory except for being applied to a finite geometry and including time dependence. A finite diffusion kernel was obtained which is similar to the results of the simpler calculations, and a finite-medium, Fermi-age kernel which describes the behavior of the slowing-down neutrons in the finite geometry.

Both the one-group and the age-diffusion developments were used to calculate numerically sample configurations which are suitable for experimental verification. These include rectangular assemblies of graphite and heavy water which have poison or fuel rods inserted.

In order to demonstrate better the improvements of this work over the Feinberg-Galanin theory, an extension was made to critical assemblies. This offers the possibility of doing criticality calculations for physically small assemblies which are not amenable to homogenization techniques.

Using the age-diffusion-theory results, it was also shown that data from neutron-wave experiments may be processed in such a way as to give experimental measurements of both the diffusion and the slowing-down kernel.

Reference

[1]Abstract of ORNL-TM-1184 (August 1965).

3.15 DIFFERENTIAL DOSE ALBEDOS FOR CALCULATION OF GAMMA-RAY REFLECTION FROM CONCRETE[1]

M. B. Wells
Radiation Research Associates, Inc.

Differential dose albedos for gamma-ray reflection from concrete were derived from Monte Carlo calculations of gamma-ray scattering in air and concrete for source energies of 0.6, 1, 2, 4, and 7 Mev. Curves showing the albedo for reflection in the plane of incidence are presented for angles of incidence of $\theta_0 = 0$, 30, 45, 60, and 75°. At incident energies greater than 2 Mev, the computed dose albedos are smaller than those reported by Raso[2] (also based on Monte Carlo) and those given by the Chilton-Huddleston[3] formula. However, comparisons with experimental data for ^{137}Cs and ^{60}Co gamma rays reported by Jones *et al.*,[4] Clifford,[5] and Barrett and Waldman[6] indicate that the calculated albedos for these sources agree as well with the experimental data as do calculations based either on the Chilton-Huddleston formula or Raso's Monte Carlo calculations.

References and Notes

[1]Abstract of RRA-T46 (Dec. 30, 1964); work performed by Radiation Research Associates, Inc., for ORNL under subcontract No. 2267; work funded by the Defense Atomic Support Agency under DASA Order EO-800-64.

[2]D. J. Raso, *Monte Carlo Calculations on the Reflection and Transmission of Scattered Gamma Radiations,* TO-B-39 (May 1962).

[3]A. B. Chilton and C. M. Huddleston, *Nucl. Sci. Eng.* **17**, 419 (1963).

[4]T. H. Jones *et al.*, *Experimental Determination of the Gamma-Ray Dose Albedos of Concrete, Aluminum, and Steel,* USNRDL-TR-790 (October 1964).

[5]C. E. Clifford, *Differential Dose Albedo Measurements for 0.66-Mev γ's Incident on Concrete, Iron, and Lead,* Defense Research Chemical Laboratories Report No. 412 (August 1963).

[6]M. J. Barrett and J. Waldman, *Experimental Gamma-Ray Backscattering by Various Materials,* TO-B-64-68 (July 1964).

3.16 NEUTRON AND GAMMA RADIATION PENETRATION INTO CONCRETE-SHIELDED UNDERGROUND STRUCTURES[1]

R. L. French M. B. Wells
N. M. Schaeffer
Radiation Research Associates, Inc.

The fast-neutron and gamma-ray dose rates in concrete-shielded and concrete-lined cylindrical holes and bunkers located 100 to 700 ft from the ORNL Tower Shielding Reactor (TSR-II) were computed and compared with measured dose rates. The calculations, which in most cases agree with the measurements within 25%, show the relative importance of the various radiation components, including direct-beam, shield-scattered, and wall-scattered radiation and secondary gamma rays. Wall-scattered neutrons were found to contribute up to 40% of the fast-neutron dose rate at positions deep inside the structures. Thermal-neutron capture in the concrete shields accounted for as much as 90% of the gamma-ray dose rates for thick shields. Capture gamma rays produced in the walls of the cylindrical holes and bunkers were also important in many cases. Simplified methods were developed for computing most of the radiation components. An appendix gives the application of these methods to a cylindrical hole with laminated iron and concrete shields.

References and Notes

[1]Abstract of RRA-T51 (May 31, 1965); work performed by Radiation Research Associates, Inc., for ORNL under subcontract No. 2267; work funded by the Defense Atomic Support Agency under DASA Order EO-802-65.

3.17 STRUCTURAL AND SHIELDING CONSIDERATIONS IN THE DESIGN OF HARDENED FACILITIES[1]

R. H. Karcher J. H. Wilson
Holmes and Narver, Inc.

Structural requirements and initial radiation shielding requirements have been calculated as a function of weapon yield and separation distance for fully buried domes, arches, and rectangular structures. The two criteria have been superimposed to determine the range and magnitude of the shielding problems attendant to the design of hardened structures. The single-degree-of-freedom spring-mass system was used to describe the response of structures to blast loading. Neutron penetration of structures was calculated by means of removal-diffusion theory, while gamma-ray penetration was calculated by use of point kernel techniques. The interaction of structural and shielding criteria is analyzed in considerable detail, and initial radiation shielding requirements are given as a function of weapon yield for a number of discrete overpressure levels.

References and Notes

[1]Abstract of HN-183 (June 30, 1965); work performed by Holmes and Narver, Inc., for ORNL under subcontract No. 2461; work funded by the Defense Atomic Support Agency under DASA Order EO-802-65.

3.18 PENETRATION OF NEUTRON AND GAMMA RADIATION THROUGH THE OPENINGS OF UNDERGROUND STRUCTURES[1]

R. L. French M. B. Wells
N. M. Schaeffer
Radiation Research Associates, Inc.

Calculations were performed of the radiation intensities in open concrete-lined cylindrical holes and in open concrete bunkers due to a fission source suspended in air at distances of 100 to 700 ft away. The calculations are part of an analysis of experiments performed with the Tower Shielding Reactor II (TSR-II) at ORNL; included were numerous radiation measurements in the underground structures with and without shields over the openings. The approach followed in the calculations was to determine, from geometric considerations, the portion of the incident radiation intensities which could enter the structures. Methods were developed to account for effects of the air-ground interface, and albedo models were devised to simplify calculation of wall-scattered radiation and production of secondary gamma radiation in the walls. In general, the calculated and measured data agree within approximately 25%.

References and Notes

[1]Abstract of RRA-T41 (Nov. 30, 1965); work performed by Radiation Research Associates, Inc., for ORNL under subcontract No. 2267; work funded by the Defense Atomic Support Agency under DASA Order EO-800-64.

3.19 GAMMA-RAY ATTENUATION COEFFICIENT FOR GERMANIUM[1]

G. T. Chapman

The increasing use of lithium-drifted germanium diodes for the detection of gamma rays necessitates knowing the attenuation coefficients as a function of gamma-ray energy to make even approximate calculations of the efficiency for a given diode. Since these coefficients could not be found in the literature, an interpretative method was used to derive them. The method is explained in detail, and the resulting coefficients are given for gamma-ray energies from 0.05 to 15 Mev.

Reference

[1]Abstract of ORNL-TM-1237 (in preparation).

3.20 GAMMA-RAY SPECTRUM EMITTED BY A STAINLESS-STEEL-CLAD REACTOR (BSR-II)[1]

G. T. Chapman W. R. Burrus

The data taken to determine the spectrum of gamma rays emitted by the BSR-II reactor operating at a 2-w power level were reported elsewhere[2] as pulse-height distributions. The pulse-height distributions were not a satisfactory approximation to the desired gamma-ray spectrum because of the "tails" introduced by the spectrometer and because of the changing efficiency due to the detector crystal and the changing acceptance angle of the collimator. Therefore, a program was written to remove the tails and to correct for the changing effects as a function of energy. The final gamma-ray spectrum still retains the inherent energy resolution of the spectrometer.

The final results show the gamma-ray differential spectrum and the integral spectrum as a function of distance from the reactor surface (1 to 60 cm), and as a function of angle about two points 10 and 25 cm from the surface. The integral spectrum (which is the integral of the differential spectrum from E to ∞) may prove useful in shielding calculations in which it is desired to know how much gamma flux there is between two energy limits. Confidence intervals for the differential and integral spectra are included which consider the counting statistics and the power-measurement uncertainty.

This report includes a FORTRAN analysis code which. with minor changes, is also applicable to other types of spectrometers.

References and Notes

[1]Abstract of ORNL-TM-1284 (in preparation).

[2]G. T. Chapman, K. M. Henry, and J. D. Jarrard, *Pulse-Height Spectra of Gamma Rays Emitted by the Stainless-Steel-Clad Bulk Shielding Reactor Reactor (BSR-II)*, ORNL-3609 (November 1964).

3.21 SNAP REACTOR INSTALLATION AT THE TOWER SHIELDING FACILITY

C. E. Clifford F. J. Muckenthaler
J. Lewin

It is proposed to install a SNAP 2/10A (Space Nuclear Auxiliary Power) reactor at the Tower Shielding Facility in 1966 for the purpose of providing experimental results for comparison with Monte Carlo calculations of the radiation intensities transmitted through shadow shields. The reactor and the detector collimator configurations that will be used to make the measurements are shown in Fig. 3.21.1.

The reactor is to be a modification of SNAP-10A (described in ref. 1) and will be designed and fabricated by Atomics International, Division of North American Aviation, Inc. The principal modifications required are the following: a decrease in the reactivity of the core, replacement of two of the four control drives by pneumatically actuated drives which can be scrammed by the action of springs, and installation of a NaK-to-air heat exchanger above the reactor. The heat exchanger is designed to be wholly within the conical shadow cone of the shield. Existing reflector assemblies and fuel elements will be utilized to minimize the cost of the new installation. The 5- to 10-kw power level is established by the maximum allowable temperature of components near the heat-rejection system.

The Tower Shielding Facility will be modified to receive the new reactor. A shelter consisting of three thick concrete walls for shielding and a roof will be constructed adjacent to the existing reactor storage pool. A shielding window and manipulators will be located in one wall of the shelter. The pool itself will be converted to a dry chamber for containing the detectors and their shields. The reactor will be suspended rigidly at the end of a lead screw, which will in turn be part of a rotating and elevating mechanism suspended at the end of a 10-ft boom extending from a vertical column. Thus the reactor can be swung out over the chamber or into the shelter. Both positions will be used for measurements. A collimated detector within the shelter will be used for mapping

ORNL-DWG 65-7616

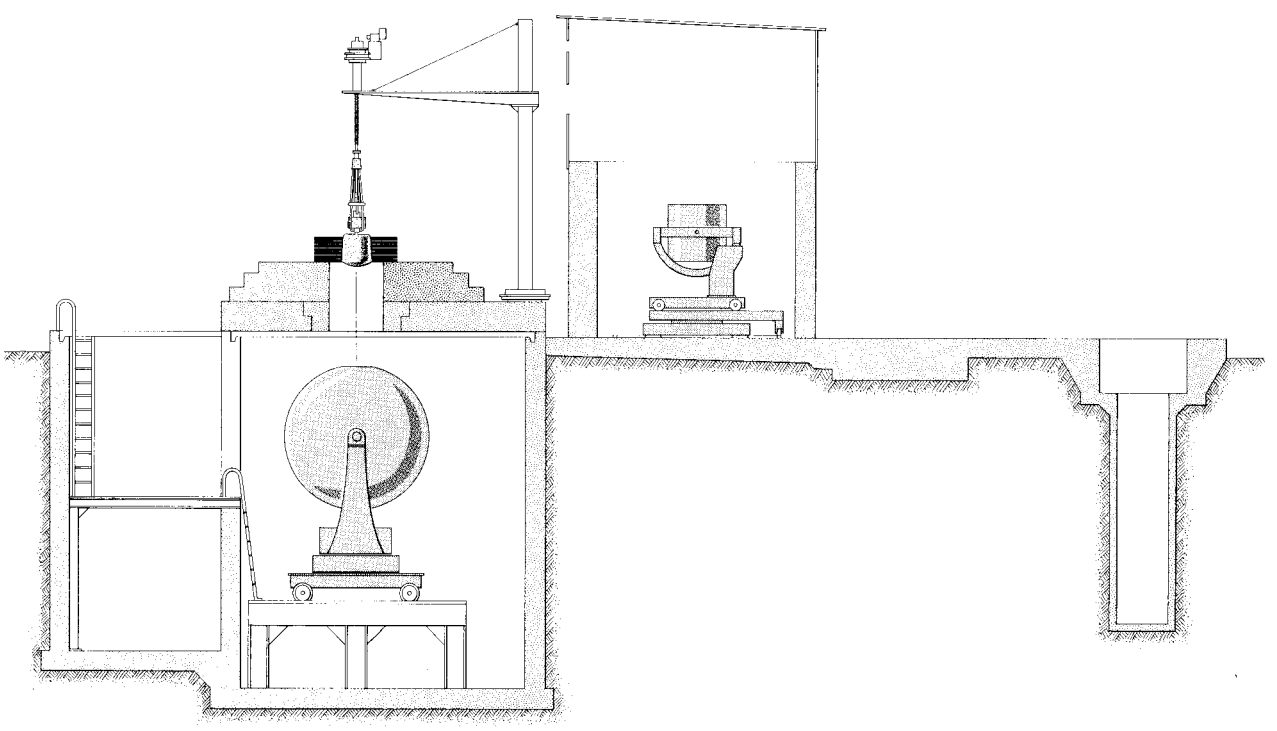

Fig. 3.21.1. Arrangement for SNAP Shielding Experiments.

ORNL-DWG 65-723C

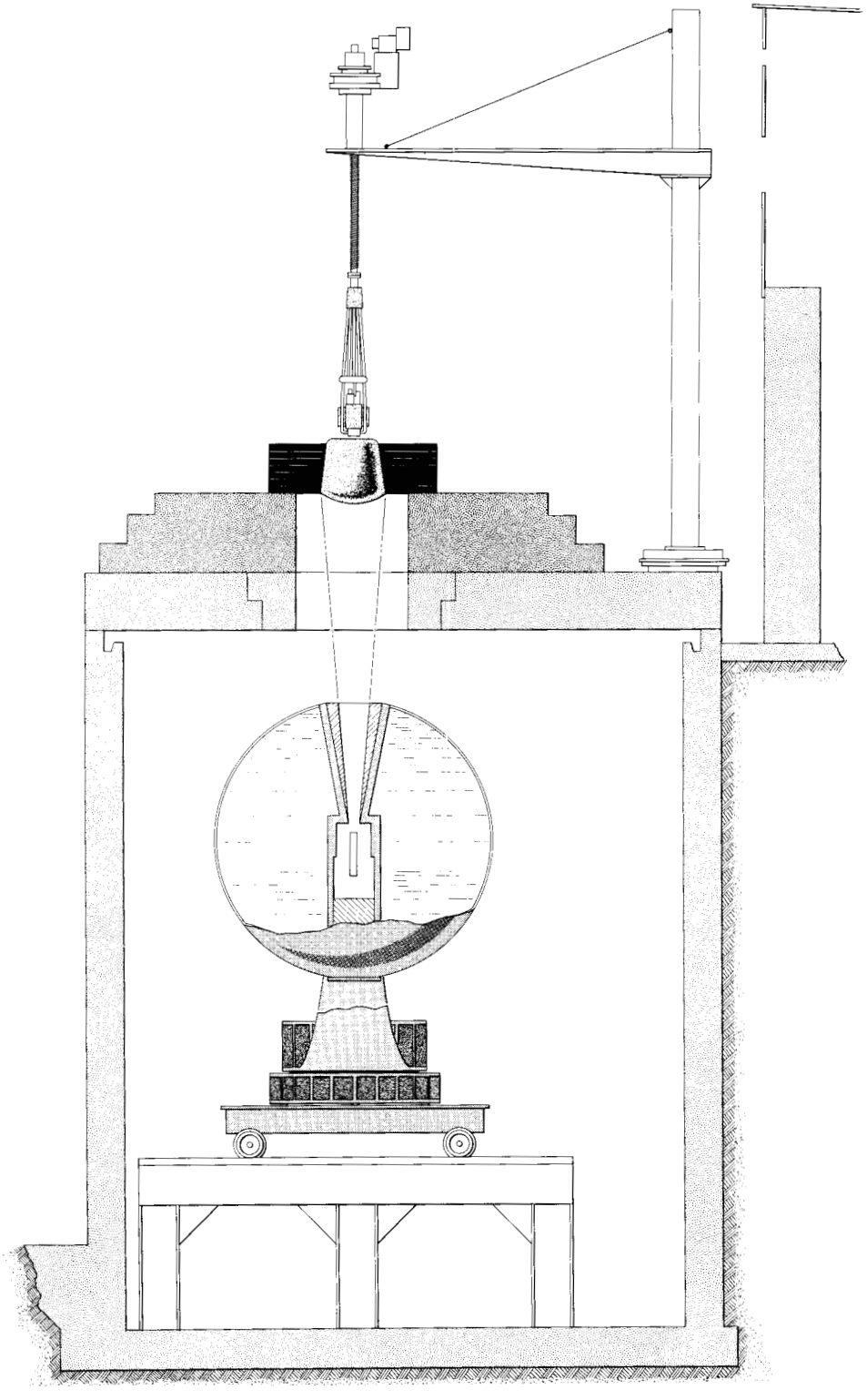

Fig. 3.21.2. Arrangement for Transmitted-Dose Mapping.

ORNL-DWG 65-7231

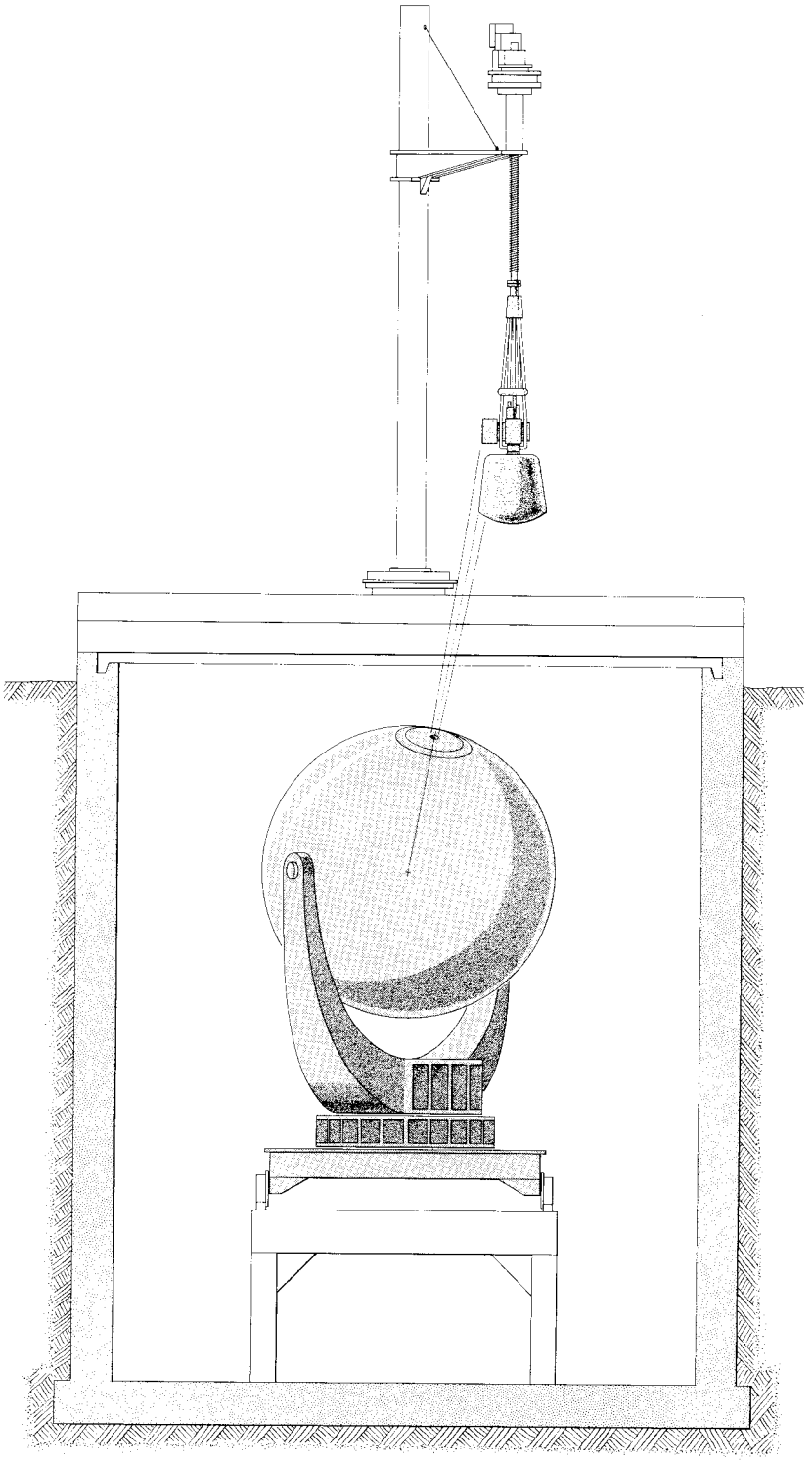

Fig. 3.21.3. Arrangement for Evaluation of Neutron Scattering from Structural Components.

the core leakage spectrum, while the converted 10-ft-diam collimator[2] located in the chamber will be used for mapping the dose transmitted through a LiH shield. The arrangement for the latter measurement is shown in Fig. 3.21.2.

The role of structural components in scattering neutrons will be assessed in an arrangement of equipment as shown in Fig. 3.21.3.

References and Notes

[1]J. Susnir and T. Harmon, *SNAP-10A Reactor Design Summary*, NAA-SR-Memo 8679 (S-RD) (classified).

[2]Figure 12.3 in ORNL-2942 (classified).

3.22 CALCULATIONS FOR THE SCATTERING OF NEUTRONS BY AIR, GROUND, AND STRUCTURES FOR SNAP SHIELDING EXPERIMENTS[1]

F. B. K. Kam

Tables of neutron air-, ground-, and structure-scattering calculations have been compiled for use of the experimenter who wishes some quantitative estimates of these effects in designing his experiment. In all calculations the source was assumed to be a point isotropic fission source. The tables containing calculations of the flux and dose scattering effects in air as a function of the solid angle subtended at the detector and the source-detector separation distance were computed by using single-scattering theory in which material attenuation was neglected and the scattering cross section was assumed to be isotropic in the laboratory system. The air-scattering results obtained by this method were in good agreement with those obtained by the Monte Carlo method. Tables of the dose ground-scattering effect (assumed to be concrete) as a function of the distance of the source above the ground and the solid angle of the ground seen from the source and of the structure-scattering effects (dose units) from different sections of the wall and ceiling for the Plumbrook Facility were calculated by using differential angular dose albedos computed by the Monte Carlo method.[2] The equations for the structure-scattering effect can be applied to any building having cylindrical walls and capped by a hemispherical dome.

References and Notes

[1]Abstract of ORNL-TM-1269 (in preparation).

[2]R. E. Maerker *et al.*, *Differential Fast-Neutron Albedos for Concrete*, vol. I, ORNL-3822 (in press).

3.23 SECONDARY GAMMA-RAY PROBLEM IN MAN-RATED SHIELDS

F. B. K. Kam E. Whitesides[1]

Shielding calculations for manned vehicles containing reactor power sources are much more difficult than those for instrumented vehicles in that much larger neutron attenuations must be considered; also, the doses from secondary (n, γ) gamma rays must be predicted for the man-rated shields. In order to calculate the source strength of secondary gamma rays produced within the shield, the low-energy neutron flux distribution must be determined.

The basic approach which is being investigated uses the Carlson S_n technique. Considerable attention is being given to developing an operational two-dimensional S_n transport code which will allow a higher-order polynomial expansion of the cross sections than do the existing P_1 approximations. A STRETCH, FORTRAN IV program, 2 DF, has been chosen as the code to which modifications will be made to obtain a code compatible with the IBM 360-75 and having such features as angular-flux printout and options to use the step-function S_n equations whenever a negative flux is produced. Many of the changes have been completed, but considerable testing remains to be done.

In addition, two-dimensional coupling of the O5R Neutron Monte Carlo code to S_n codes is being investigated for use with cases which require a three-dimensional geometrical representation in some spatial regions. Coupling of O5R to DTF-ANISO, a one-dimensional S_n code, has been completed and a test problem run. Checks against experimental results have not yet been made.

If the coupling of Monte Carlo codes to S_n codes is successful, attention will be directed to running the codes separately and/or in combination with each other to determine an efficient procedure of getting the secondary gammas in a realistic configuration.

Note

[1]Central Data Processing Facility, Oak Ridge Gaseous Diffusion Plant.

3.24 MONTE CARLO CALCULATIONS OF NEUTRON PENETRATION THROUGH SHAPED SNAP SHIELDS[1]

F. B. K. Kam

The Monte Carlo method was used to investigate neutron penetration through a realistic SNAP shield (LiH) from a bare cylindrical homogeneous reactor source. Although the reactor is not typical of SNAP reactor designs, it was felt that such a model for the reactor was the most practical source which could be used at the time the calculations were done. Results were obtained with several parabolic outer surfaces (the shield surface nearest the detector) in order to determine the surface that produces the desired shielding with minimum weight.

Using this model with the SNAP-10A shield, the calculations indicated that the 10-A design is close to optimum for the neutron dose on the center line of the system.

Later calculations will include a better reactor description and will give parametric data, for several points on the dose plane, to be used in determining optimum shield shapes.

Note

[1]The technical memorandums covering this study will also include more basic LiH neutron penetration calculations. The calculations will consist of the dose rate from a point isotropic fission source in an infinite medium and of the dose rate at a collimated detector from a collimated source through slab shields. Comparisons will be made with experimental data taken at the Tower Shielding Facility.

3.25 SLOWING-DOWN SPECTRA OF NEUTRONS IN LITHIUM HYDRIDE[1]

V. V. Verbinski

The spectra of neutrons moderated in lithium hydride were measured over the energy range from about 0.01 to 1000 ev, and the results were compared with calculated spectra obtained with the NIOBE, O5R, and SPECTRUM codes and with the moments method. The measurements were performed at the General Atomic linear accelerator facility, where a source with a near-fission neutron spectrum was obtained by placing a lead target in the electron beam. Spectra of the leakage flux, forward-directed flux, and scalar flux were obtained at depths from 2.5 to 10 cm. In each case the spectrum attained an asymptotic shape at <5 cm. The shapes of the calculated spectra agree with the shapes of the measured spectra for all energy regions in which each calculation is valid. A large discrepancy between the NIOBE results and the measurements below 0.08 ev is caused by upscattering and molecular-binding effects, which are neglected by NIOBE. These effects were included in a SPECTRUM calculation for an infinite medium with a constant source density; however, agreement with measurement was obtained only for the case in which the measurement had been made in a nearly gradient-free region. The scalar-flux spectrum and the forward-directed-flux spectrum at several depths in LiH were found to be properly related by the energy-dependent transformation of Purohit.[2]

References

[1]Abstract of ORNL-TM-1077 (May 1965) and of paper submitted to *Nuclear Science and Engineering*.

[2]S. N. Purohit, *Milne Problem with Capture*, ORNL-3005 (Sept. 28, 1960).

3.26 ANGULAR DISTRIBUTIONS OF LOW-ENERGY NEUTRONS LEAKING FROM VARIOUS SCATTERING MATERIALS[1]

V. V. Verbinski

Experiments in which a wide range of scattering materials in the form of slabs were bombarded by reactor neutrons showed that the angular distribution of low-energy (<5-ev) neutrons leaking from the side of each slab opposite to the source is independent of the source term and of the slab thickness for thicknesses greater than some minimum thickness z_{min}. In the cases of pure lead, pure water, and mildly poisoned water, the resulting

distributions are in agreement with the Fermi expression $\Phi(\mu) = 1 + \sqrt{3}\mu$. The results for pure lead are also in excellent agreement with one-velocity calculations. An imperfect experiment with poisoned lead is in qualitative agreement with one-velocity calculations. The angular distribution for lithium hydride is described by $\Phi(\mu) = 1 + A\mu$, where A is less than $\sqrt{3}$ at 1.5 and 5 ev.

Numerical calculations describing the angular distributions for water and LiH were only partially successful. The DTK code was nearly correct for water, while the NIOBE code predicted a value for A that was much too high everywhere. Neither of these two codes appears to be correct for LiH at all energies, but a Monte Carlo calculation seems to give reasonable values of A above 5 ev, its low-energy cutoff.

Reference

[1]Abstract of ORNL-TM-1078 (May 13, 1965) and of paper submitted to *Nuclear Science and Engineering*.

4. Radiation Shielding Information Center

4.1 PROGRAM OF THE RADIATION SHIELDING INFORMATION CENTER

S. K. Penny D. K. Trubey
B. F. Maskewitz

The program of the Radiation Shielding Information Center (RSIC) has been expanded to include information on shielding of manned space vehicles and high-energy accelerators.[1,2] No major changes have been made in the library functions of the Center, but the technical functions have increased to the point of now comprising the most important part of the Center's work. Since January 1965 the international shielding community has been informed through monthly newsletters of the activities of RSIC and other organizations oriented toward shielding and of the literature and computer codes acquired by the Center.

Library Functions

Through the Center's information retrieval system,[3,4] bibliographic information continues to be stored, retrieved, and printed; as the system is updated,[5] the information is automatically and selectively disseminated to the individual scientist. The third cumulative bibliography of reactor and weapons shielding literature was published, and a loose-leaf volume of abstracts (ORNL-RSIC-6, Vol. I) of the references contained in the bibliography was included with those bibliographies issued to the scientists on the Center's mailing list. The abstracts will be updated and issued with the fourth bibliography, which is now in preparation (to be published as ORNL-RSIC-15).

A bibliography (ORNL-RSIC-11) and a loose-leaf volume of abstracts (ORNL-RSIC-12) containing references on the shielding of manned space vehicles and high-energy accelerators are being prepared by techniques similar to those used for the bibliographies and abstracts on reactor and weapons shielding.[6] In general, only work on space-vehicle shielding done after 1962 is included, but, because of its much less voluminous nature, all pertinent work on accelerator shielding is included. Shielding per se will be emphasized, and in the important areas of space radiation sources and particle-particle interactions only review articles will be included.

Also in preparation is a loose-leaf notebook (ORNL-RSIC-13) of abstracts of the complete code packages assembled by RSIC. A collection of the literature on shielding codes, which is now disseminated only through the monthly newsletters, is continuing and will probably be published within the next year. Upon request, the computer code packages which have been assembled by RSIC are now distributed by the Center's staff. Cooperation along the lines of standardization and exchange of codes has been established with the Argonne Code Center and the European Nuclear Energy Agency (ENEA) Computer Programme Library. An example of such cooperation is the joint paper that was recently presented at an international meeting.[7]

The Center has taken on the responsibility of distributing spectral data from the Monte Carlo intranuclear cascade calculations for nucleon-nucleus collisions in the energy range 50 to 400 Mev. These data are distributed on microfilm, on reels of magnetic tape, and, more rarely, as printed listings.

Technical Functions

The technical work of RSIC has increased considerably in the past year. Three reports have been written which review or survey certain topics in shielding (see Sects. 4.3, 4.5, and 4.10). An additional report is being prepared which surveys

the methods used to calculate neutron heating in shields. Three reports have been written in which calculational methods are compared with each other, as well as with some experimental results (see Sects. 4.4, 4.7, and 4.9). In addition, two reports have been published which tabulate data in scattered gamma-ray fluxes in iron and on the fast-neutron distribution in ordinary concrete (see Sects. 4.6 and 4.8).

The Center continues to fill requests for specific advice and information, either by letter or telephone; this constitutes one of the most important services provided. In this area, the information retrieval system was used to produce many special literature searches, and advice was given on the implementation of computer codes.

The computer code section has assembled 36 complete code packages.[8] These packages contain all the computer-oriented media necessary (punched cards, magnetic tapes, etc.); the auxiliary codes for data preparation, etc.; sample input and output; and all relevant documentation. Some 30 other codes have been collected which will be complete code packages when they contain the one or more items now lacking.

References and Notes

[1]Work partially funded by National Aeronautics and Space Administration under NASA Order R-104.

[2]The selection and categorization of material on manned-space-vehicle and high-energy accelerator shielding were carried out by R. G. Alsmiller, Jr., and F. S. Alsmiller.

[3]S. K. Penny, D. K. Trubey, and M. B. Emmett, *Neutron Phys. Div. Ann. Progr. Rept. Aug. 1, 1963,* ORNL-3499, vol. I, p. 166.

[4]Jane Gurney, a member of the Central Data Processing Facility Staff, is responsible for the data-handling and computer-code operations involved in the RSIC information retrieval system.

[5]S. K. Penny *et al., Neutron Phys. Div. Ann. Progr. Rept. Aug. 1, 1964,* ORNL-3714, vol. I, p. 68.

[6]Work partially funded by Defense Atomic Support Agency under DASA Order EO-800-64.

[7]M. Butler, B. Maskewitz, and J. Rosen, "Activities of the ANL-ENEA Computer-Program Libraries and the ORNL Radiation Shielding Information Center," session 2, paper 1 of *The International Conference on the Application of Computing Methods to Reactor Problems, May 17–19, 1965,* Argonne National Laboratory.

[8]Hemma Francis, Henrietta Hendrickson, and Juanita Brown, members of the Central Data Processing Facility staff, assist in all phases of the RSIC computer code operations, as well as handle production codes for the Neutron Physics Division research staff. Nan Watts, ORNL Mathematics Division, gives assistance as needed on CDC 1604-A computer codes.

4.2 LITERATURE EXAMINED BY THE RADIATION SHIELDING INFORMATION CENTER

S. K. Penny D. K. Trubey
M. B. Emmett[1]

The third cumulative bibliography of the literature examined by the Radiation Shielding Information Center was published[2] along with a collection of abstracts of the literature.[3] This bibliography supersedes the second one and differs from it in several important ways. Documents of a definitely preliminary nature have been replaced, and subject categories have been revised. The latter change was primarily made to include literature relating to the shielding of radiation from nuclear weapons, which RSIC is now providing.[4] Also, the List of Subject Categories has been arranged in outline form so that differences between related categories would be immediately obvious. In addition, a Key Word Index has been included which should serve as an aid in locating bibliographic references to a given subject. The pages associated with a word in the index will contain a list of documents that might be relevant to the word. The accompanying abstracts are in a loose-leaf binder so that, as new bibliographies are issued, abstracts corresponding to additions or replacements in the system can be included in the binder.

References and Notes

[1]Mathematics Division.

[2]S. K. Penny, D. K. Trubey, and M. B. Emmett, *Bibliography, Subject Index, and Author Index of the Literature Examined by the Radiation Shielding Information Center (December 1964),* ORNL-RSIC-5.

[3]*Abstracts of the Literature Examined by the Radiation Shielding Information Center,* ORNL-RSIC-6 (vol. I).

[4]The work related to weapons is funded by the Defense Atomic Support Agency under DASA Order EO-801-65.

4.3 A SURVEY OF EMPIRICAL FUNCTIONS USED TO FIT GAMMA-RAY BUILDUP FACTORS[1]

D. K. Trubey

The use of simple functions for estimating gamma-ray buildup factors is reviewed on the basis of simplicity and accuracy. Analysis shows that the most accurate form is four-term-polynomial fit with coefficients published by Capo.[2] For most purposes, however, a function proposed by Berger[3] is recommended since it is as simple to use as the linear form and is essentially as accurate as the more complicated forms.

Tables of the coefficients are given for the linear, quadratic, Berger, and Taylor fitting functions. Some typical graphs of the functions are also given.

Use of the Berger and quadratic functions is demonstrated for the case of exponential source distributions in slab geometry.

References

[1]Abstract of ORNL-RSIC-10 (in preparation).

[2]M. A. Capo, *Polynomial Approximation of Gamma-Ray Buildup Factor for a Point Isotropic Source,* APEX-510 (1958).

[3]M. J. Berger, p. 47 in *Proceedings of Shielding Symposium Held at the Naval Radiological Defense Laboratory,* USNRDL Reviews and Lectures No. 29 (1956).

4.4 COMPARISON OF THREE METHODS USED TO CALCULATE GAMMA-RAY TRANSPORT IN IRON[1]

D. K. Trubey S. K. Penny
K. D. Lathrop[2]

Three methods for determining the gamma-ray energy spectra, dose rate, and heating in a sphere of iron were compared: the Monte Carlo method, the S_n method, and integration of moments-method data (Goldstein-Wilkins). The source was taken to be isotropic and to be distributed uniformly within a sphere with an energy distribution proportional to $e^{-1.1E}$, where E is the energy in Mev. The results of all calculations were in very good agreement.

References and Notes

[1]Abstract of ORNL-RSIC-9 (in preparation).

[2]Los Alamos Scientific Laboratory.

4.5 SURVEY OF METHODS FOR CALCULATING GAMMA-RAY HEATING[1]

H. C. Claiborne[2]

The engineering design of nuclear reactors is largely governed by the heat liberated in the fission process and the subsequent absorption of the associated radiation. External to the fuel region, the main contribution to the heat generation rate usually results from energy degradation and absorption of gamma photons escaping from the fuel region. For some design conditions, gamma radiation arising from neutron capture can contribute significantly to the heat generation rate.

This survey is concerned only with heat generation due to gamma rays, regardless of the source, interacting with the usual reactor materials. The purpose is to examine the various methods used in calculating gamma-ray heating for reactor design purposes. Comparisons of experiments with calculations are made where possible, and recommendations are made as to the applicability of each method to reactor design.

The methods discussed that are adaptable to hand calculations include the buildup-factor method and the straightahead-scattering method. Other methods require a high-speed digital computer. These include the differential-energy-spectrum method and the same methods used in neutron attenuation: Monte Carlo, direct integration of the Boltzmann equation, moments method, S_n and P_n approximations to the Boltzmann equation, and diffusion theory. A listing of the available machine codes is made for each method.

References and Notes

[1]Abstract of ORNL-RSIC-8 (June 1965).
[2]Reactor Division.

4.6 TABULATED VALUES OF SCATTERED GAMMA-RAY FLUXES IN IRON INTERPOLATED FROM MOMENTS-METHOD CALCULATIONS[1]

D. K. Trubey

Tables of scattered gamma-ray fluxes in iron that are suitable for integration over source spectra have been generated on the IBM 7090 computer by Lagrangian interpolation of Goldstein-Wilkins moments-method results for point isotropic gamma-ray sources. Values of the fluxes were obtained for a consistent set of scattered gamma-ray energies taken in steps of 0.1 Mev from 0.2 to 1.0 Mev and in steps of 0.25 Mev from 0.25 to 10 Mev. One table was obtained for each scattered energy for various values of the source energy and of the distance from the source in mean free paths. Tables were then generated in which the distance from the source was converted from mean free paths to centimeters. The latter set may be integrated over any source spectrum to obtain the flux of scattered gamma rays in iron and, with small error, in any material for which the cross section is similar.

Reference

[1]Abstract of ORNL-RSIC-7 (May 1965).

4.7 A COMPARISON OF FIRST- AND LAST-FLIGHT EXPECTATION VALUES USED IN AN O5R MONTE CARLO CALCULATION OF NEUTRON DISTRIBUTIONS IN WATER[1]

D. K. Trubey M. B. Emmett[2]

The distributions in water of fast neutrons from isotropic fission and 14-Mev point sources have been calculated with the O5R Code. Two methods of scoring the same case histories were used to estimate the energy distribution and the dose rate. The estimators employed were the first- and last-flight expectation, or statistical estimation, values. The first-flight estimator was found to be somewhat better, due to the importance of the first flight in the total transport of the neutrons. The results are in good agreement with RENUPAK moments-method results and with experimental results.

References and Notes

[1]Abstract of ORNL-RSIC-3 (May 1965).
[2]Mathematics Division.

4.8 SOME CALCULATIONS OF THE FAST-NEUTRON DISTRIBUTION IN ORDINARY CONCRETE FROM POINT AND PLANE ISOTROPIC FISSION SOURCES[1]

D. K. Trubey M. B. Emmett[2]

Fast-neutron dose rates and energy distributions due to point and plane isotropic fission sources in an infinite medium of ordinary concrete have been calculated by the moments-method code RENUPAK. As a check on the method, one Monte Carlo calculation was performed which yielded results that are in good agreement with those for the corresponding RENUPAK case. The effects of varying the concrete composition, especially the hydrogen content, and the lower energy cutoff were examined for several cases and found to be significant. Detailed tables of the energy spectra are given at lethargy steps of 0.1 from 0.001 to 18 Mev.

References and Notes

[1]Abstract of ORNL-RSIC-4 (June 1965).
[2]Mathematics Division.

4.9 SOME CONCLUSIONS REGARDING THE USE OF THE S_n METHOD IN SHIELDING CALCULATIONS[1]

J. W. Webster

In order to gain further numerical experience with the S_n method as a tool for shielding analysis,

a study was made of the fundamental problems of neutron penetration from a point fission source into hydrogen and water.

Some of the results and conclusions are as follows:

The S_n method, as applied by means of the DTF-II code, gives excellent agreement with the moments method for fast-neutron penetration over the distances from the point source studied here up to 90 cm in hydrogen and 120 cm in water. It seems reasonable to conclude that satisfactory agreement would be obtained at even greater penetration.

An angular segmentation of flux of at least $n = 12$ should be used for fast-neutron penetration, and even greater segmentation is necessary for accurate computation of the spatial distribution of slow neutrons.

Taking into account the terms of the Legendre expansion of the scattering cross section up to order 2 gives good results. However, the effect of including higher terms was not quantitatively evaluated.

A spatial mesh (Δr) of 5 cm or less is necessary for fast-neutron penetration problems and of 2 cm or less if the distribution of slow neutrons is of interest.

A 28-group structure, with a lethargy width per group of 0.2 for $E > 1$ Mev, was used in all the calculations, and it is concluded that this is a quite satisfactory energy mesh.

Reference

[1]Abstract of ORNL-TM-1196 (to be published).

4.10 THE EXPONENTIAL TRANSFORM AS AN IMPORTANCE SAMPLING DEVICE – A REVIEW[1]

F. H. S. Clark

The exponential transform is reviewed with emphasis on its use as a guide to effective importance sampling in the solution of the Boltzmann equation by Monte Carlo methods. Contributions of various workers are assembled, along with numerical results. Special consideration is given to approximate forms and to effective practical methods. Problems related to negative effective cross sections, tracking across discontinuities, directional biasing in inhomogeneous media, and high variance in back-scattered components are specifically treated.

Reference

[1]Abstract of ORNL-RSIC-14 (in preparation).

5. Mathematics and Computer Programs

5.1 JTMS1(O5R:SOURCE), A NEUTRON DISTRIBUTION SUBROUTINE FOR THE O5R MONTE CARLO CODE[1]

J. T. Mihalczo G. W. Morrison[2]
D. C. Irving

The FORTRAN subroutine JTMS1(O5R:SOURCE) has been written for determining the energy, the speed, and the initial spatial distribution of neutrons arising from fission. The energy distribution within the batch of neutrons is obtained by sampling a Maxwellian fission spectrum which depends upon the energy of the neutrons producing fission. The program locates the neutrons at a point or distributes them spatially, either uniformly or according to a cosine function. Two isotopes producing fission neutrons having slightly different energy distributions can be treated in this program by an approximation (using an average temperature) giving the correct first moment of the resulting overall energy distribution.

References and Notes

[1]Abstract of ORNL-TM-1192 (Aug. 12, 1965).
[2]Central Data Processing Facility, Oak Ridge Gaseous Diffusion Plant.

5.2 OGRE-P3, AN OGRE SYSTEM MONTE CARLO CODE FOR THE CALCULATION OF GAMMA-RAY DOSE RATE AT ARBITRARY POINTS FROM POINT SOURCES IN LAMINATED SLAB GEOMETRY[1]

D. K. Trubey M. B. Emmett[2]

An OGRE system gamma-ray Monte Carlo code has been written for the calculation of dose rate by statistical estimation at arbitrary points outside a laminated slab. The monoenergetic point source is also located outside the slab. It may be monodirectional (gun barrel) or have an isotropic or cosine angular distribution. Options also allow the simultaneous calculation of one-dimensional reflection and/or transmission.

References and Notes

[1]Abstract of ORNL-TM-1211 (in preparation).
[2]Mathematics Division.

5.3 OGRE-G, AN OGRE SYSTEM MONTE CARLO CODE FOR THE CALCULATION OF GAMMA-RAY DOSE RATE AT ARBITRARY POINTS IN AN ARBITRARY GEOMETRY[1]

D. K. Trubey M. B. Emmett[2]

An OGRE system gamma-ray Monte Carlo code has been written for the calculation of dose rate at arbitrary points by statistical estimation. The general geometry routine GEOM of D. C. Irving has been utilized to provide almost completely arbitrary material and statistical weight geometries. Input source parameters may be read to specify point source configurations, or binary tapes may be read to provide the initial particle parameters for arbitrary source configurations.

References and Notes

[1]Abstract of ORNL-TM-1212 (in preparation).
[2]Mathematics Division.

5.4 O5R MONTE CARLO ANALYSIS ROUTINES OF USE IN REACTOR PROBLEMS

J. T. Mihalczo G. W. Morrison[1]
D. C. Irving

Various FORTRAN programs which analyze the neutron-history tapes produced by the O5R Monte Carlo neutron-transport code and calculate quantities of interest to reactor problems have been developed.

SPCTRM[2] is a program which obtains the energy spectra of neutrons crossing a boundary, of neutrons in the medium, or of source neutrons. Up to 100 equal energy intervals or equal logarithmic energy intervals can be used. It also computes the total fraction of neutrons leaking from the system and the average number of collisions before loss by absorption, leakage, or reduction in energy to a value below which the neutrons are not followed. The standard deviation of a neutron leakage spectrum is also computed.

TIMDIE, TIMBTH, TIMDIELK, and VOIDTIME are programs[3] which calculate, respectively, the mean time from fission birth to loss, from birth to fission production, and from birth to loss minus the time since the last real collision and the mean time spent in internal voids. The standard deviations for these quantities are also calculated.

REACT is a program for calculating the probability that a neutron born in one region will produce a neutron in another region.

CONVRG is a program for forming a matrix of the probabilities calculated by REACT and for iterating on the initial source distribution with this matrix until convergence is obtained. The number of iterations required for convergence is the average number of batches that must be calculated before spatial convergence. CONVRG also calculates the largest eigenvalue of this matrix, which is the neutron multiplication factor.

FISRATE is a program which calculates the number of neutron reactions of a particular type in a specified region. These reactions may be with the nuclei used in the O5R Monte Carlo calculation or with nuclei introduced only for the purpose of analysis.

References and Notes

[1]Central Data Processing Facility, Oak Ridge Gaseous Diffusion Plant.

[2]J. T. Mihalczo, G. W. Morrison, and D. C. Irving, *SPCTRM, An O5R Monte Carlo Analysis Routine for Calculating the Neutron Energy Spectrum*, ORNL-TM-1245 (in preparation).

[3]J. T. Mihalczo, G. W. Morrison, and D. C. Irving, *O5R Monte Carlo Analysis Routines for Calculating Various Mean Times in Reactor Problems*, ORNL-TM-1246 (in preparation).

5.5 ACTI-FK(O5R:ANALYSIS), A GENERAL-PURPOSE CODE TO ANALYZE O5R COLLISION TAPES[1]

F. B. K. Kam K. D. Franz[2]

ACTI-FK(O5R:ANALYSIS) has been written to facilitate the analysis of the collision tapes generated by the O5R code.[3] The code has been successfully applied to a wide range of problems and has reduced considerably the time required to achieve an operational program. ACTI-FK requires that subroutines be written before it can be used. However, this disadvantage is minor when the user considers the following advantages: (1) one of the methods of analysis already written can be used, or the user can devise his own method; (2) any nonelastic event can be treated through the use of a nonelastic scattering package incorporated in the code; (3) most of the bookkeeping tasks, such as tape reading and writing, initialization of parameters, finding the proper cross sections, checking for any overlapping of data and programs, etc., have been built into the code; (4) an optional statistical analysis code is included which the authors have found important in determining the significance of the Monte Carlo results; and (5) very little coding effort is required, as has been evidenced by all the problems solved to date, many of which have been complicated.

References and Notes

[1]Abstract of ORNL-3856 (in preparation).

[2]Central Data Processing Facility, Oak Ridge Gaseous Diffusion Plant.

[3]R. R. Coveyou, D. C. Irving, *et al.*, *O5R, A General-Purpose Monte Carlo Neutron Transport Code*, ORNL-3622 (February 1965).

5.6 A CYLINDRICAL VOLUME SOURCE ROUTINE FOR THE O5R MONTE CARLO CODE[1]

L. G. Mooney
Radiation Research Associates, Inc.

A computer subroutine entitled SOURCE[2] has been coded in FORTRAN-63 to generate the initial neutron starting parameters required to perform reactor shielding calculations with the ORNL O5R Monte Carlo code. These parameters include the neutron energy, weight, direction, and spatial location within the reactor core. While coded primarily for calculations involving the SNAP-10A reactor, subroutine SOURCE is applicable to all cylindrical source geometries in which the radial distribution of the source strength is symmetrical. Reactor information required by SOURCE includes the axial and radial power distributions and the reactor core dimensions. The sampling schemes included in subroutine SOURCE permit biased sampling to emphasize those core regions and energy and angular groups which make particularly important contributions to the leakage from the reactor surface. Included with the description of subroutine SOURCE is a program utilization. Test problems and a listing of the FORTRAN statements are given in appendices to the report.

References and Notes

[1]Abstract of RRA-T53 (June 30, 1965); work performed by Radiation Research Associates, Inc., for ORNL under subcontract No. 2478.

[2]Editor's note: The name SOURCE is generic for all O5R neutron generator subroutines, but at the time this report was published the authors had not been informed of the convention for naming of O5R-related subroutines. This convention, which applies also to O5R routines such as GEOM, ANALYSIS, etc., requires an additional identification, by the user, plus the O5R generic name in parentheses. For example, "LGMCV(O5R:SOURCE)" could have been used here to properly identify the code.

5.7 THE FORTRAN CODE FANLFR2 TO CALCULATE NONLOCALITY AND FINITE RANGE EFFECTS IN STRIPPING AND PICKUP REACTIONS USING THE LOCAL-ENERGY APPROXIMATION

J. K. Dickens F. G. Perey

All distorted-wave theories of direct reactions have the same structure. In the usual formulation the transition amplitude for, say, $A(d,p)B$ stripping has the form

$$T = \iint d\mathbf{r}_p \, d\mathbf{r}_d \; \chi_p^{(-)*}(\mathbf{k}_p, \mathbf{r}_p) \; \Psi_n^*(\mathbf{r}_n) \times D(r_{np}) \; \chi_d^{(+)}(\mathbf{k}_d, \mathbf{r}_d) \; , \quad (1)$$

where Ψ_n^* is the wave function for the captured neutron, the scalar function $D = V_{np}\Psi_d$ is the product of the (n,p) interaction and the internal state of the deuteron, and the χ's are the incoming and outgoing distorted waves. Considerable success in reproducing experimental data has been obtained by generating the distorted waves using local optical potentials which reproduce the elastic scattering for the input and output channels and by using the "zero-range" approximation, which consists of replacing D by a delta function in r_{np}. Although exact calculations can be performed to obtain nonlocal wave functions[1] and to incorporate finite range exactly[2] in Eq. (1), very good approximations for both effects have been obtained which reduce considerably the complexity of these calculations.

The approximated nonlocal wave function is obtained by multiplying the local wave function [i.e., that obtained using the appropriate local optical-model potential, $U(\mathbf{r})$] by the factor F:

$$F = C \left[1 - \frac{\beta^2 U(r)}{4(\hbar^2/2m)} \right]^{-1/2} , \quad (2)$$

where β is the range of the nonlocality;[3] $C = 1$ for scattering, or $C \geqq 1$ for the bound state and is chosen to give the correct wave-function normalization.

The approximation to the exact finite-range calculation consists of multiplying the bound-state wave function in Eq. (1) by the factor Λ:[4]

$$\Lambda(r) = 1 - y(r) \; ,$$
$$y(r) = [\, U_d(r) - U_n(r) - U_p(rM_A/M_B) - B_d]/2(\hbar^2/mR^2)(M_d/M_pM_n) \; . \quad (3)$$

Here n is the captured particle, $U_i(r)$ is the (complex) optical potential for particle i, M_i is the mass of particle i, m is an atomic mass unit, B_d is the separation energy of n from d leaving p, and the "range" is R.

The program FANLFR2 computes the local bound-state wave function,[5] multiplies this wave function

by the appropriate form of F, and renormalizes the resulting wave function. This nonlocal bound-state wave function is then multiplied by suitable forms of F to simulate the nonlocal effects in the input and output distorted waves. Lastly, the wave function is multiplied by the finite-range approximation factor Λ. The resulting radial wave function is punched on cards suitable for input for the distorted-wave code JULIE.[6]

FANLFR2 is programmed in the FORTRAN-63 language to make use of the complex-arithmetic routines, simplifying the coding of the factors F and Λ.

References and Notes

[1]F. G. Perey and B. Buck, *Nucl. Phys.* **32**, 353 (1962).

[2]N. Austern *et al.*, *Phys. Rev.* **133**, B3 (1964).

[3]F. G. Perey, p. 125 in *Proceedings of the Conference on Direct Interactions and Nuclear Reaction Mechanisms, University of Padua, September 3–8, 1962*, ed. by E. Clementel and C. Villi, Gordon & Breach, New York, 1963.

[4]P. J. A. Buttle and L. J. B. Goldfarb, *Proc. Phys. Soc. (London)* **83**, 701 (1964); G. Bencze and J. Zimanyi, *Phys. Letters* **9**, 246 (1964); E. Ivash, *Phys. Letters* **12**, 327 (1964); and F. G. Perey and D. Saxon, *Phys. Letters* **10**, 107 (1964).

[5]This part of the calculation is performed using the code BINDE, written by B. Buck.

[6]R. H. Bassel, R. M. Drisko, and G. R. Satchler, *The Distorted-Wave Theory of Direct Nuclear Reactions*, ORNL-3240 (1962).

5.8 THE FORTRAN CODE XBACK3: AN AID IN THE ANALYSIS AND DATA REDUCTION OF PULSE-HEIGHT SPECTRA

J. K. Dickens

To experimentally measure the elastic and inelastic scattering of protons from some target for every 5° between laboratory angles of 20 and 165° requires obtaining ~35 pulse-height spectra. In our case these 35 spectra will be stored on a magnetic tape. The ideal data-reduction computer routine will digest each spectrum, locate and classify peaks, ascertain background if necessary, determine a detector response for the particles being studied, and apply this response function (or use some other technique) to the peaks of interest to obtain the numbers of counts in each of these peaks. Any further input to aid in these calculations should be applicable to all the spectra and should not require more than a cursory inspection of all the spectra nor entail a detailed study of more than one spectrum.

At present, XBACK3 reads in a spectrum; obtains and subtracts an exponential background from valley to valley; finds and classifies peaks according to position, maximum counts, and number of channels peak to valley; finds a standard peak, usually the one corresponding to elastic scattering; determines trial parameters and then fits this peak by least squares using a skewed-Gaussian response function;[1] determines which of the remaining peaks satisfy minimum requirements of peak height and peak to valley; uses the elastic response-function parameters as trial parameters in order to obtain the areas of the peaks chosen for further analysis; and finally, prints out all this information plus diagnostic messages which aid in judging the validity of the calculations. This routine is repeated for all spectra of interest. Input data include two background parameters, two parameters to reduce the search for the elastic peak, one peak-choosing criterion, two least-squares fitting criteria, the four skew parameters of the seven-parameter skewed-Gaussian response function, several control integers, and the identification numbers of the spectra to be reduced.

The routine has several drawbacks: The criteria for choosing peaks to be analyzed depend upon the relative size and isolation of the peak and are not related to the Q value or to the type of reaction. Peaks corresponding to two or more unresolved groups are not correctly reduced; however, a diagnostic message indicates this difficulty. The full width at half maximum (FWHM) of the standard peak is limited to be between 2 and 5 channels for optimum operation. The quality of calculation decreases for FWHM <2 or >5 channels.

Another flaw is the inability to satisfactorily fit the standard peak while searching on any of the skew parameters. The response function is given by

$$y(x) = \sum y_i(x)$$

and

$$y_i(x) = \frac{A_i}{\sqrt{2\pi}\,\sigma} e^{-(1/2)(x-\bar{x}_i/\sigma)^2}\left[1 - \frac{\alpha}{2}\left(\frac{x-\bar{x}_i}{\sigma}\right)\right]$$

$$+ \begin{cases} A_i P_4\, e^{P_5(x-\bar{x}_i)}\left[1 - e^{-(1/2)(x-\bar{x}_i/\sigma P_6)}\right] & \text{for } x < \bar{x}_i \\ 0 & \text{for } x \geq \bar{x}_i \end{cases},$$

where $\bar{x}_i$, σ, and A_i are the usual Gaussian parameters and P_4, P_5, P_6, and α are the skew parameters. For the time being only $\bar{x}_i$, σ, and A_i are allowed to vary. Good trial parameters for $\bar{x}_i$, σ, and A_i are determined by the routine, reducing the time used in the search for a best fit. The code satisfactorily analyzes two or more closely spaced but resolved groups, handling up to an eleven-parameter search made up of five values of x and of A and one value of σ.

Although the code is continually being modified, it is being used, and reduces the amount of drudgery associated with data reduction by a factor of at least 3. Recently obtained data for the scattering of 11-Mev protons from ^{52}Cr have been reduced using XBACK3; an example is shown in Fig. 5.8.1. The time required to obtain the results shown in this figure was ~1 min on the CDC 1604-A computer.

Note

[1]Grateful appreciation is extended to A. G. Blair and W. S. Hall of Los Alamos Scientific Laboratory for providing their data-reduction routine SKEWED and several very useful references.

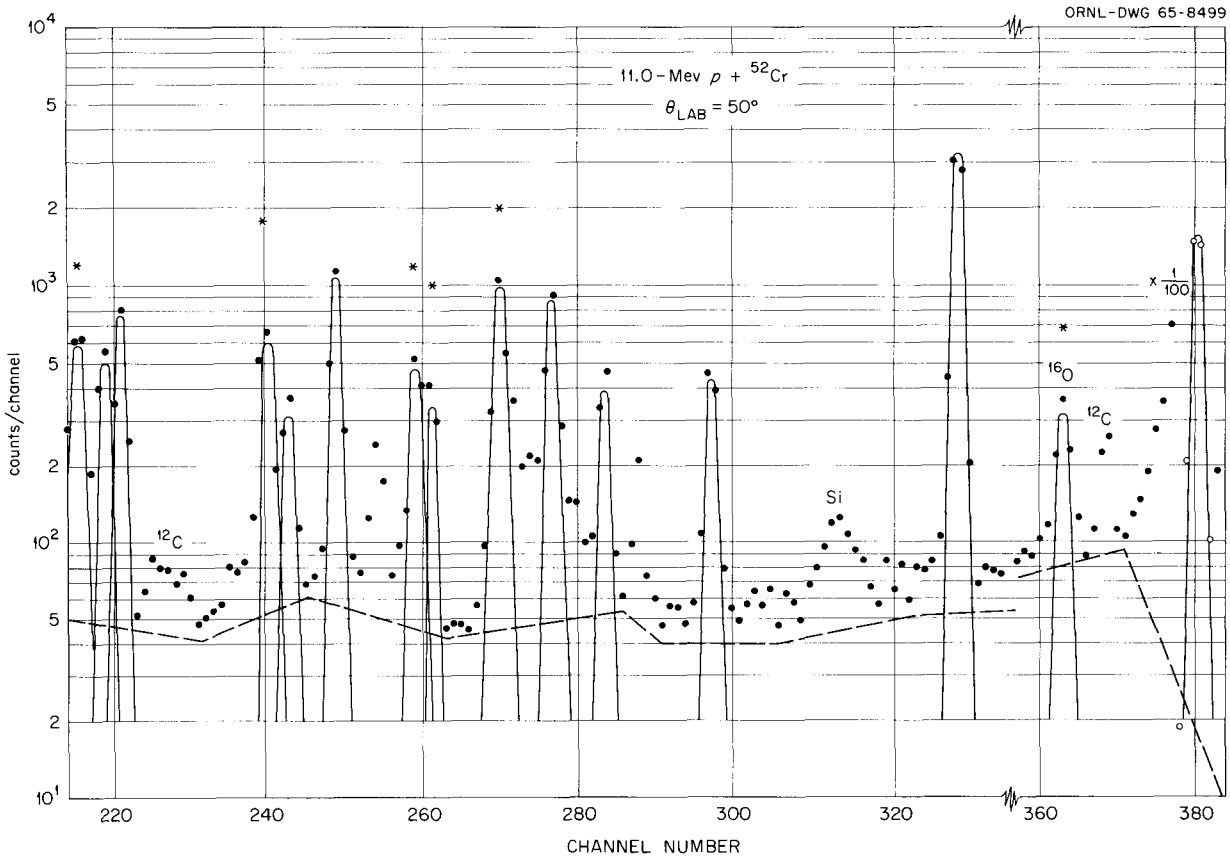

Fig. 5.8.1. Pulse-Height Spectrum of 11-Mev Protons Scattered from ^{52}Cr at 50°. The portion between channels 336 and 356 has no interesting features and was deleted. Peaks corresponding to protons scattered by a target impurity are marked with the symbol for that nucleus. The asterisks indicate peaks for which diagnostic messages accompanied the standard output. The dashed curve indicates the background subtraction computed by the routine.

5.9 JTMI1(O5R:INELAS), A FORTRAN SUBROUTINE FOR DESCRIBING INELASTIC AND (*n*,2*n*) REACTIONS[1]

J. T. Mihalczo G. W. Morrison[2]
D. C. Irving

JTMI1(O5R:INELAS) is a FORTRAN subroutine which determines for the O5R Monte Carlo neutron-transport code the energy and scattering angle of neutrons inelastically scattered or produced in (*n*,2*n*) reactions. Both evaporation and level-excitation theory are used for inelastic scattering. In evaporation theory the scattering is isotropic in the center-of-mass system, and in level excitation theory the scattering from each level can be anisotropic or isotropic. The subroutine uses evaporation theory to describe both the neutrons emitted isotropically in (*n*,2*n*) reactions.

References and Notes

[1]Abstract of ORNL-TM-1221 (in preparation).
[2]Central Data Processing Facility, Oak Ridge Gaseous Diffusion Plant.

5.10 TECHTRAN – A LOAD-AND-GO COMPILER FOR PROGRAMS WRITTEN IN DATA-SHEET FORMAT

J. W. Wachter R. T. Santoro

The TECHTRAN program provides a method of computation in which the numerical data and the mathematical steps to be performed are presented to a computer in a data-sheet form nearly identical to that used when a desk calculator or slide rule is employed. TECHTRAN input can be prepared by persons without computer experience after they have been briefly instructed in the conversion of conventional data-sheet notation to a form suitable for punched-card input to the computer. TECHTRAN, moreover, introduces considerable time saving into routine calculations normally performed on the desk calculator and has the added advantage of rapid evaluation of such functions as sin, cos, log, exp, square root, etc. Also gained are the inherent accuracy of the computer, options for plotting the results, production of data cards for input to other computer programs, and an orderly display of results.

TECHTRAN input is designed to utilize existing conventions of data-sheet layout. Figures 5.10.1*a* and *b* show the similarities in appearance of a data sheet prepared for desk-calculator computation and for TECHTRAN. Each TECHTRAN column is ten characters wide. The first data-sheet column identifies the line as containing column designators (*COLS), constant designators (*CONSTANTS), column headings (*HEAD), etc. The conventional data-sheet forms have been changed somewhat to comform to existing computer symbols: Thus, column designators 1, 2, and 3 become C1, C2, C3, etc., and 1 × 2 becomes C1 * C2, 3 ÷ 2 becomes C3/C2, etc. Program steps may utilize most standard FORTRAN library functions (EXP, ABS, LOG, SIN, COS, etc.) as well as certain special functions which perform such operations as summing a column, squaring and summing sequential row elements, generating a column of evenly spaced values, and the like. The designation "*XEQ" indicates the end of the program and data and the point at which computation of the missing elements of the data sheet can be performed.

Each line of TECHTRAN is transferred to a single punch card, and the resultant card deck forms the data of a program written in FORTRAN II. The program operates as a load-and-go compiler in reducing columnar program steps to equivalent arrays of address indices and numerical operation codes. All program steps are compiled, and improperly written steps are flagged. All columns of the data sheet are executed up to the last column entered or to the first erroneous program step. Following execution, all original and derived data columns are published in data-sheet form (Fig. 5.10.1*c*).

Since TECHTRAN is intended for programs which may be executed only once, attention has been focused on simplification of data entry to prevent errors and on maximum retrieval of information when errors occur. For example, within a data-sheet column, all blanks are ignored and characters may be left-adjusted, including exponents of numerical constants. A key-punching error in a numeric data field does not prevent compilation or execution of preceding and following data, but affects only the number in which it appears, which is set to zero. Many computational types of error (e.g., the square root of a negative number) are guarded against and are flagged. Execution, however, continues at the start of the next

ORNL-DWG 65-10475

DAMPED OSCILLATION FOR RCL NETWORK $I = A_1 e^{A_2 t} \sin A_3 t$

$A_1 = I_M = 100$ amps
$A_2 = R/2L = -3$
$A_3 = 2\pi f = 2000$ rad

① IN STEPS OF 0.005 sec	② ① x A_2	③ ① x A_3	④ sin③	⑤ $e^{+②}$	⑥ ⑤ x ④	⑦ ⑥ x A_1
t(sec)						I(amps)
0.005	-0.015	10	0.174	0.985	0.171	*17.10*
0.010	-0.030	20	0.342	0.970	0.331	*33.19*
0.015	-0.045	30	0.500	0.956	0.478	*47.80*
0.020	-0.060	40	0.643	0.941	0.605	*60.54*
0.025	-0.075	50	0.766	0.927	0.710	*71.07*
0.030	-0.090	60	0.866	0.913	0.791	*79.15*
0.035	-0.105	70	0.939	0.900	0.846	*84.61*
0.040	-0.120	80	0.984	0.886	0.813	*87.34*
0.045	-0.135	90	1.000	0.873	0.873	*87.37*

(*a*) CONVENTIONAL HAND WRITTEN DATA SHEET. (ITALICS DENOTE RESULTS OBTAINED FROM A DESK CALCULATOR)

TECHTRAN CODING SHEET

80 COLUMN ENTRY

PROGRAMMER PROBLEM DATE PAGE OF

*TITLE	DAMPED OSCILLATION FOR R-C-L NETWORK					
*CONSTANTS	A1	A2	A3			
*VALUES	100	-3	2000			
*COLS	C1	C2	C3	C4	C5	C6	C7
*PROGRAM	ACC(0.005)	C1*A2	EXP (C2)	C1*A3	sin (C4)	C5*C3	C6*A1
*HEAD	TIME (sec)						I (amps)
*WIDTH	7						
*ROWS	199						
*XEQ							
*CALL PGPLOT (1,7)							

(*b*) TECHTRAN CODING SHEET 80 COLUMN ENTRY

DAMPED OSCILLATION FOR R-C-L NETWORK 09/23/65

ROW	C 1 ACC(.005) TIME(SECS)	C 2 C1*A2	C 3 EXP(C2)	C 4 C1*A3	C 5 SIN(C4)	C 6 C5*C3	C 7 C6*A1 I(AMPS)
1	0.50000E-02	-0.15000E-01	0.98511	10.0000	0.17365	0.17106	17.1063
2	1.00000E-02	-0.30000E-01	0.97045	20.0000	0.34202	0.33191	33.1912
3	0.15000E-01	-0.45000E-01	0.95600	30.0000	0.50000	0.47800	47.7999
4	0.20000E-01	-0.60000E-01	0.94176	40.0000	0.64279	0.60535	60.5355
5	0.25000E-01	-0.75000E-01	0.92774	50.0000	0.76604	0.71069	71.0693
6	0.30000E-01	-0.90000E-01	0.91393	60.0000	0.86603	0.79149	79.1488
7	0.35000E-01	-0.10500	0.90032	70.0000	0.93969	0.84603	84.6028
8	0.40000E-01	-0.12000	0.88692	80.0000	0.98481	0.87345	87.3446
9	0.45000E-01	-0.13500	0.87372	90.0000	1.00000	0.87372	87.3716
10	0.50000E-01	-0.15000	0.86071	100.0000	0.98481	0.84763	84.7632
11	0.55000E-01	-0.16500	0.84789	110.000	0.93969	0.79676	79.6760
12	0.60000E-01	-0.18000	0.83527	120.000	0.86603	0.72337	72.3365
13	0.65000E-01	-0.19500	0.82283	130.000	0.76604	0.63033	63.0328
14	0.70000E-01	-0.21000	0.81058	140.000	0.64279	0.52103	52.1034
15	0.75000E-01	-0.22500	0.79852	150.000	0.50000	0.39926	39.9258
16	0.80000E-01	-0.24000	0.78663	160.000	0.34202	0.26904	26.9043
17	0.85000E-01	-0.25500	0.77492	170.000	0.17365	0.13456	13.4563
18	0.90000E-01	-0.27000	0.76338	180.000	0.41723E-06	0.31851E-06	0.31851E-04
19	0.95000E-01	-0.28500	0.75201	190.000	-0.17365	-0.13059	-13.0586
20	1.00000E-01	-0.30000	0.74082	200.000	-0.34202	-0.25337	-25.3374
21	0.10500	-0.31500	0.72979	210.000	-0.50000	-0.36489	-36.4894
22	0.11000	-0.33000	0.71892	220.000	-0.64279	-0.46211	-46.2115
23	0.11500	-0.34500	0.70822	230.000	-0.76604	-0.54253	-54.2528
24	0.12000	-0.36000	0.69768	240.000	-0.86603	-0.60421	-60.4205
25	0.12500	-0.37500	0.68729	250.000	-0.93969	-0.64584	-64.5841
26	0.13000	-0.39000	0.67706	260.000	-0.98481	-0.66677	-66.6771

(*c*) TECHTRAN COMPUTER OUTPUT SHEET

Fig. 5.10.1. (*a*) **Conventional Handwritten Data Sheet;** (*b*) **TECHTRAN Coding Sheet;** (*c*) **TECHTRAN Computer Sheet.**

data-sheet row. More subtle computational errors cause termination of execution, a printout (in the usual data-sheet form) of the results obtained up to that point, and a skip to the next TECHTRAN job.

In its simplest and most easily learned form, TECHTRAN involves one operation per column, using constant or column designators; however, more sophisticated forms are possible and additional flexibility can be obtained by special control cards. For example, the statement *CALL PGPLOT (1,7) causes a print-plot of the values of column 7 vs those of column 1, as shown in Fig. 5.10.2, where column headings serve as axis labels. Additional statements produce internal tables of the columnar data so that succeeding program steps may use values obtained by a forward or backward interpolation of the table. Derivatives or integrals of the tabulated values are also made available. Other options cause generation of tape input to a Benson-Lehner plotter, punching of data in standard formats, and read-in of data cards using routines common to other computer programs.

In order to simplify the use of TECHTRAN, special data sheets are in preparation which can be submitted directly to the Central Data Processing Facility at the Oak Ridge Gaseous Diffusion Plant for processing. Also, a manual describing TECHTRAN programming and its capabilities and options will be published.

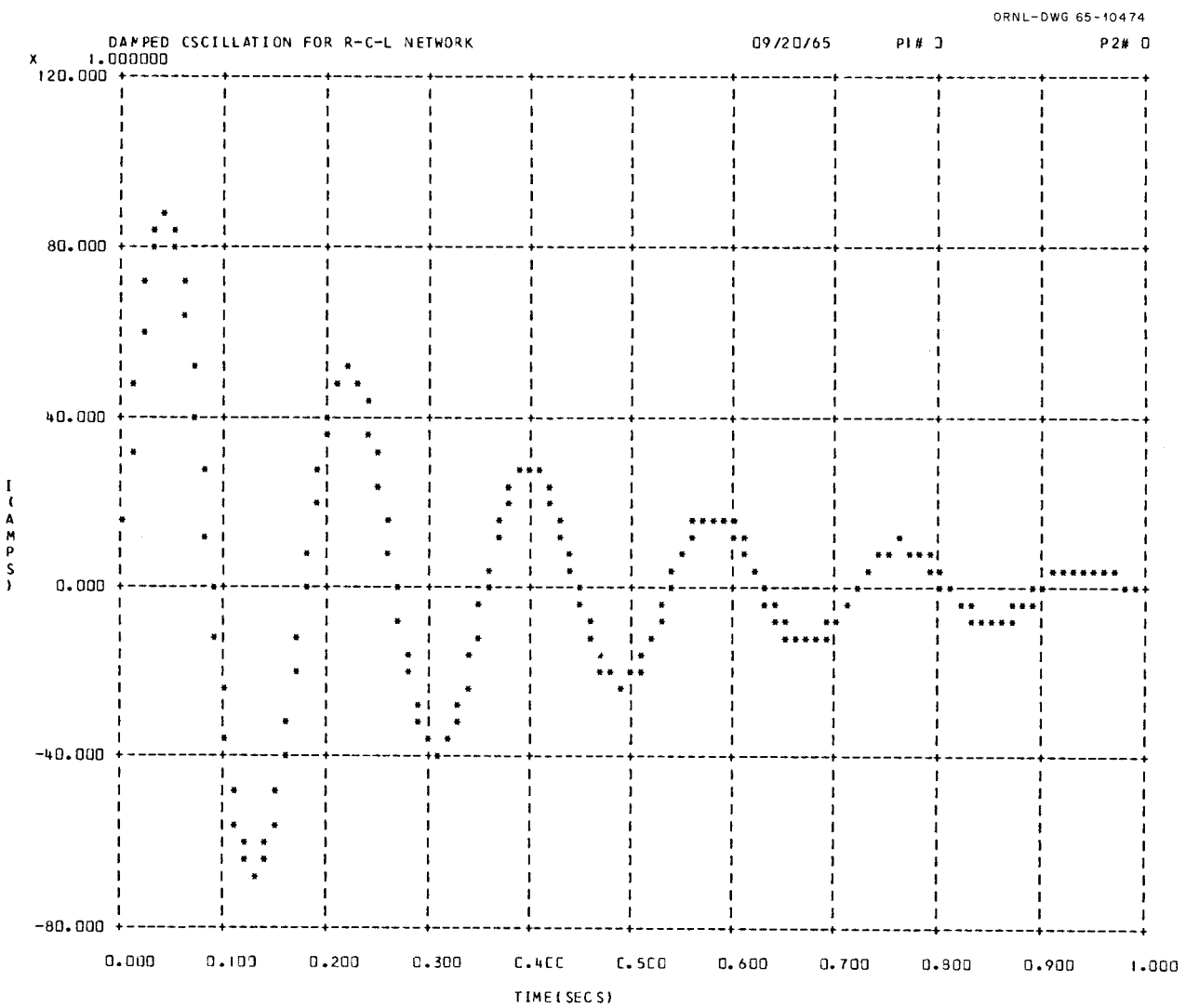

Fig. 5.10.2. Print-Plot Damped-Oscillation Problem.

5.11 DWB DEUTERON STRIPPING COMPUTER PROGRAM[1]

W. R. Smith

The DWB program described here calculates (d,p) and (d,n) stripping angular cross sections with the inclusion of nuclear optical-model potentials and Coulomb interactions. The Q value is restricted to values greater than -2.226 Mev. Provision is also made for approximating the finite-range n-p interaction, the deuteron polarizability, and the nonlocality of the nuclear forces. The program is set up to run on a CDC 1604-A computer, but should be easily adaptable to other computers using FORTRAN.

Reference

[1]Abstract of ORNL-TM-1151 (June 10, 1965).

5.12 GENERALIZED HAUSER-FESHBACH NUCLEAR-SCATTERING COMPUTER PROGRAMS[1]

W. R. Smith

Two programs, one (ORNL-TM-1117) written in CDC 1604 symbolic machine language and the other (ORNL-TM-1234) written in FORTRAN, are available which compute the scattering angular distribution and integrated cross section for any two-particle nuclear reaction by making use of the Hauser-Feshbach theory modified to include spin-orbit coupling. The first code is limited by the mathematical methods employed to a maximum of 16 partial waves in any one channel. The second code is presently set up to include a maximum spin of 5 and up to 31 partial waves, but the methods employed are general and these restrictions can be relaxed by allotting larger storage blocks to certain variables in the program. This latter program also contains as options a Porter-Thomas width-fluctuation correction and an approximate nonlocal potential. The input required by the programs is the charge, mass, spins, parity, and optical-model parameters for all channels through which the compound nucleus can decay.

References

[1]Combined abstract of ORNL-TM-1117 (May 1965) and ORNL-TM-1234 (in preparation).

5.13 DATA-REDUCTION PROGRAMS FOR THE CDC 160-A COMPUTER[1]

W. E. Kinney

A series of programs have been written for processing the data from the neutron-scattering cross-section experiment (Sect. 1.1), which are accumulated in an ND-160 4096-channel analyzer and punched on paper tape. The programs are written in FORTRAN for the CDC 160-A computer to correct for walk and to report the corrected data, and are linked by a simple chain routine written for this problem. The first link reads the ND-160 paper tapes and normalizes and subtracts background. The second link selects the case to be walk-corrected from a library of cases and also allows the insertion of comments for identification. Link 3 computes the amount by which each channel is to be shifted in correcting for walk, while link 4 performs the correction itself and prints the resulting spectrum. The fifth link condenses the channel shifts and corrected spectrum, prints it, and then computes and prints the position, the maximum count, and the full width at half maximum of selected peaks. Link 6 punches on paper tape the corrected spectrum, if desired.

A typical running time to correct and report a sample-in less background, a standard-in less background, and the background alone is 30 min.

Reference

[1]Abstract of ORNL-TM-1208 (in preparation).

5.14 FOURIER ANALYSIS OF UNIFORM RANDOM-NUMBER GENERATORS[1]

R. R. Coveyou R. D. MacPherson[2]

A requisite for the success of Monte Carlo calculations is a quick method for the generation of a sequence of numbers which are essentially uniformly and independently distributed on the unit interval. Many methods are known for producing these sequences of requisite uniformity. Whether output sequences produced by such methods have satisfactory independence properties has not been known. This question can be reduced to that of determining the degree of uniformity of the distribution of n-triples of successive members

of the output sequences within its n-dimensional unit cube. We have developed a measure of independence for such sequences. The tool used is the theory of finite Fourier series, the form of the Fourier transform appropriate to the discrete range and finite cycle length imposed by digital computation.

Number theoretic methods are used for a priori calculation of figures of merit for specific generators taken from widely used classes of such generators.

In many instances, unsatisfactory statistical performance had been observed for certain methods of generation. In each case, the method used here has predicted (or explained) such abnormal performance. The random-number generators currently used in ORNL Monte Carlo codes are found to be reasonably satisfactory, although improvement is possible.

References and Notes

[1]Abstract of ORNL-3866 (in preparation).
[2]Summer employee.

5.15 NUMERICAL SOLUTION OF THE LAGRANGE-MULTIPLIER FORMULATION WITH SEVERAL CONSTRAINTS[1]

F. B. K. Kam F. H. S. Clark

A program has been written in FORTRAN for the CDC 1604-A computer for numerical solution of the Lagrange-multiplier method with several constraints. The program, XTREME, is an extension of MAX (ref. 2) and can deal with up to 25 independent variables. It finds an extreme value for an object function subject to a number of equality constraints, at most one less than the number of independent variables. All second derivatives of the object function and the constraining functions must exist everywhere in the domain of computation.

References

[1]Abstract of ORNL-3846 (in preparation).
[2]F. H. S. Clark and F. B. K. Kam, *A Generalized One-Constraint Lagrange Multiplier Numerical Formulation,* ORNL-3742 (June 1965).

5.16 NONNORMAL DISTRIBUTIONS OF THE MEAN COMPUTED FROM SAMPLE CHARACTERISTICS[1]

F. H. S. Clark N. A. Betz[2]

It is assumed, for distributions of the mean only, that two distributions are equivalent provided that their first moments and the absolute values of their second, third, and fourth central moments are equal. (This assumption makes no distinction between distributions which are mirror images of each other about the mean.) Subject to this assumption, a method is given for computing the distribution of the mean in units of the estimated standard deviation when the coefficients of skewness and kurtosis of the population are known. The coefficients of skewness and kurtosis of the sample are taken as estimates of these quantities for the population. References are given to assess the confidence limits associated with such estimates.

Computed distributions of the mean, in estimated standard-deviation units, are given for a representative set of sample characteristics.

References and Notes

[1]Abstract of a paper to be submitted to *Nuclear Science and Engineering.*
[2]Mathematics Division.

5.17 SIGNIFICANCE ARITHMETIC FOR FORTRAN[1]

W. R. Burrus B. W. Rust[2]

The FORTRAN statement X # 193./71. – 272./1001. has a true value of 0.0000284093.. , but a single-precision FORTRAN computation (27 bit fraction) yields 0.2813339-04 (using an E13.7 output FORMAT) due to loss of significance when subtracting. When the number of significant digits is questionable, the same problem may be run in both single and double precision. This is inconvenient because programs must be modified and because double precision requires twice as much storage space. We have implemented a simple alternative due to Goldstein[3] for keeping track of the amount of significance in floating-point numbers by representing them in unnormalized form.

Programs may be written in ordinary FORTRAN IV, and the significance operations implemented by use of the ALTER feature of the loader. Some problems and applications of significance arithmetic are discussed.

References and Notes

[1]Abstract of ORNL-TM-1249 (in preparation).
[2]Central Data Processing Facility, Oak Ridge Gaseous Diffusion Plant.
[3]M. Goldstein, *Significance Arithmetic on the IBM 7090*, NYO-9190 (May 1, 1962).

5.18 THE USE OF MATHEMATICAL PROGRAMMING FOR SOLVING SINGULAR AND POORLY CONDITIONED SYSTEMS OF EQUATIONS[1]

J. Replogle[2] B. D. Holcomb[2]
W. R. Burrus

It is well known that Fredholm integral equations of the first kind frequently lead to systems of singular or poorly conditioned equations. Then there are many solutions which satisfy the system of equations $Ax = b$ within a specified nonzero error. Many ad hoc techniques have been used to obtain useful solutions. In this paper, we obtain rigorous upper and lower bounds for the solutions (or linear functions of the solutions) by making use of additional information which may be available about the solution. The effect of this information is to reduce the size of the possible solution space. We show how the use of monotonicity, smoothness, or nonnegativity restricts the solution of a problem introduced by R. Bellman.[3]

References and Notes

[1]Abstract of paper to be submitted to the *Journal of Mathematical Analysis and Applications*.
[2]Central Data Processing Facility, Oak Ridge Gaseous Diffusion Plant.
[3]R. Bellman, R. Kalaba, and J. Lochett, *Dynamic Programming and Ill-Conditioned Linear Systems*, Memorandum RM3815PR (December 1963).

5.19 A SIMPLE ALGORITHM FOR COMPUTING THE GENERALIZED INVERSE OF A MATRIX[1]

B. W. Rust[2] W. R. Burrus

The generalized inverse of a matrix is important in analysis because it provides an extension of the concept of an inverse which applies to all matrices. It also has many applications in numerical analysis, but is not widely used because the existing algorithms are fairly complicated and require considerable storage space. We have found a simple extension of the conventional orthogonalization method for inverting nonsingular matrices which gives the generalized inverse with little extra effort and with no additional storage requirements. The algorithm gives the generalized inverse for any m by n matrix A, including the special case when $m = n$ and A is nonsingular as well as the case when $m > n$ and rank $(A) = n$. In the first case the algorithm gives the ordinary inverse of A. In the second case the algorithm yields the ordinary least-squares transformation matrix $(A^TA)^{-1}A^T$ and has the advantage of avoiding the loss of significance which results in forming the product A^TA explicitly.

References and Notes

[1]Abstract of paper submitted to the *Journal of the Association for Computing Machinery*.
[2]Central Data Processing Facility, Oak Ridge Gaseous Diffusion Plant.

5.20 A FORTRAN SUBROUTINE PACKAGE FOR LINEAR PROGRAMMING[1]

C. Schneeberger W. R. Burrus

A FORTRAN program has been written for linear programming using the symmetric algorithm of Talacko.[2] It is compatible with FORTRAN II, IV, or FORTRAN-63 without any changes. The main regime consists of two subroutines, TALAKO and DIFF. TALAKO performs the major linear programming computation, and DIFF is a subroutine used to carry out the elimination step efficiently, yet independently of the language. Included are several auxiliary routines which make it easy to unscramble the transformation matrix, the solution, and the slacks.

References

[1]Abstract of ORNL-TM-1250 (in preparation).
[2]J. V. Talacko, *Tabaios de Estadistica* **24**, 17, 159 (1963).

5.21 NEUTRON-CROSS-SECTION LIBRARY

D. C. Irving F. H. S. Clark
J. Gillen[1]

In view of the frequent use of the O5R Monte Carlo code[2] for neutron calculations, it is desirable to have a library of neutron-cross-section data available for use with O5R. A single, central library would avoid the duplication of effort inherent in the maintenance of separate libraries by the various users of O5R. A continuing effort will be necessary to keep the library up to date.

A library has been compiled consisting of published neutron cross sections for the following elements: H, Li, Be, B, C, N, O, F, Na, Mg, Al, Si, S, K, Ca, Cr, Fe, Ni, Cu, Zr, U, and Pu. A small amount of evaluation work has been done when published evaluations did not adequately cover the region of interest. The library consists of point cross-section data in the format used by O5R. It is maintained on magnetic tape at both the CDC 1604-A and the IBM 7090 computer installations. The O5R cross-section-handling subroutines have been modified to make use of a library cross-section tape. Memorandums concerning the contents of the library and any revisions or updating are sent to all users of O5R at Oak Ridge.

References and Notes

[1]Central Data Processing Facility, Oak Ridge Gaseous Diffusion Plant.

[2]R. R. Coveyou, D. C. Irving *et al.*, *O5R, A General-Purpose Monte Carlo Neutron Transport Code*, ORNL-3622 (1965).

6. Radiation Detector Studies (I)

6.1 FAST-NEUTRON SPECTROMETER CAPABLE OF NANOSECOND TIME GATING[1]

L. E. Beghian[2] S. Wilenski[2]
W. R. Burrus

A fast-neutron spectrometer has been constructed which is capable of 200-kev energy resolution at 1 Mev and can be time-gated to several nanoseconds. The spectrometer is a proton-recoil scintillation detector. The neutron spectrum is obtained from the detector pulse-height response by a modified least-squares unfolding technique. The response of the detector to monoenergetic neutrons has been measured and is used in conjunction with a computer code, SLOP, for unfolding the neutron spectrum. Results are presented to indicate the capabilities of the detector. Unfolded neutron spectra containing 1.0- and 1.3-Mev lines are presented. The neutron spectra leaking out of a carbon assembly at two different time delays after the injection of a monoenergetic neutron pulse are also presented.

References and Notes

[1]Abstract of *Nucl. Instr. Methods* **35**, 34 (1965); work supported by National Science Foundation.
[2]Massachusetts Institute of Technology.

6.2 DEVELOPMENT OF AN EPITHERMAL-NEUTRON SPECTROMETER[1]

T. V. Blosser R. M. Freestone, Jr.

In a previous report[2] a design for a neutron spectrometer intended for use in the neutron energy range from thermal to approximately 10 kev was outlined. Fabrication of this instrument, shown in Fig. 6.2.1, has now been completed.[3]

The spectrometer essentially consists of an isotropically responding spherical BF_3 proportional counter enclosed in a concentric spherical boron (92.27% ^{10}B) shield, plus a conical boron collimator with a 1-in.-diam opening. Principal dimensions are shown in Fig. 6.2.2. A rotatable aluminum disk is placed so that each of the twelve ^{10}B filters which it carries can successively be positioned in front of and closely adjacent to the collimator. With the use of two such disks, one of which has an open hole, 24 filters, each of a different thickness, are available. Remotely controlled drives

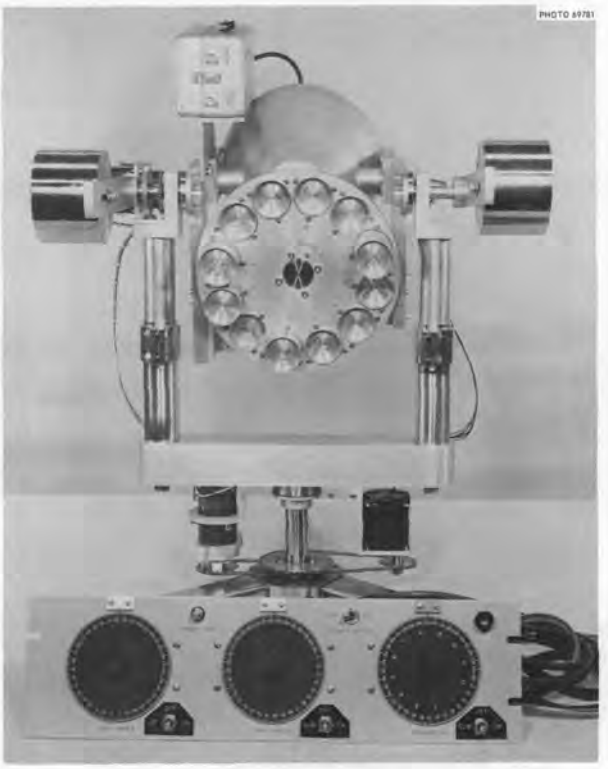

Fig. 6.2.1. The Epithermal-Neutron Spectrometer.

ORNL-DWG 65-8498

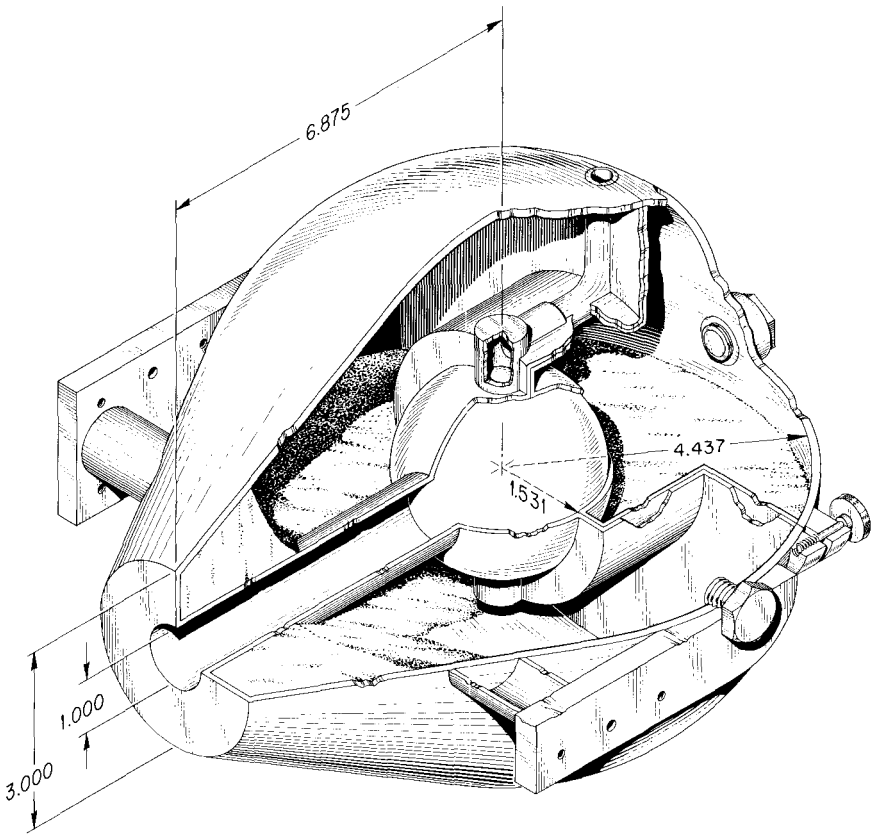

NOTE: DIMENSIONS IN INCHES

Fig. 6.2.2. Cutaway Diagram of the Spectrometer.

and mechanical linkages permit scanning through large polar and azimuthal angles.

The basic principle of the design is that, as the thickness of the filter is increased, various increments of a neutron energy spectrum are attenuated at different rates. Analysis of the counting rates obtained at all 24 positions should then result in a description of the incident neutron spectrum.

Probably the most unique feature of the spectrometer is its isotropic BF_3 proportional counter. As presently constituted,[4] the counter consists of a 3-in.-OD thin-walled copper sphere filled to a pressure of $\frac{1}{2}$ atm with enriched (96% ^{10}B) BF_3. (Copper spheres were used simply because they were readily available at the time of construction.) Ion collection within the sphere is by a double $\frac{1}{2}$-in.-diam loop of 2-mil-diam tungsten wire, with the two loops at right angles to each other. By using a double-loop collector, so-called "end effects" common to straight-wire collectors are effectively eliminated.

The counter has a calculated efficiency of 0.233 for thermal neutrons, a high-voltage plateau with a slope of not more than 2 to 3% over 200 v, and, based upon tests with an Am-Be source embedded in polyethylene, a response that is isotropic to within 5%.

The twenty-three ^{10}B filters were calibrated by transmission measurements made at the ORNL Fast Chopper Facility.[5] The transmission data were fitted by the method of least squares to functions of the form

$$\text{transmission} = \exp\{-[\Sigma(E)t + k]\},$$

where

$\Sigma(E)$ = macroscopic ^{10}B total cross section,

t = filter thickness (obtained from the curve fit as the effective thickness of the filter and therefore taking into account all errors in the experimental determination of ^{10}B thickness and density),

k = a constant lumping together the effects of the aluminum cladding of each filter, the ^{11}B content, and any contamination not identified.

The fit was excellent over the entire energy range, and encourages confidence in the accuracy of the calibrations.

In connection with the development of the spectrometer a series of Monte Carlo calculations utilizing the O5R neutron transport code[6] were carried out. These calculations were principally directed toward estimating the effect upon the detector of neutrons that are scattered back into the detector from the ^{10}B shield at the rear of the instrument, but several other quantities were also estimated. The most recent results of these calculations indicate that for monoenergetic neutrons of 10-ev energy approximately 4% of the counts from the detector will come from backscattered neutrons, but for 100-ev neutrons this value increases to 5%; for 1000-ev neutrons, however, the value does not increase further. From these results it may be concluded that in most applications the effect of backscattering will be effectively lost within the counting statistics. This conclusion is in agreement with experiments conducted with the spectrometer viewing an approximately $1/E$ spectrum emanating from a temporary beam tube at the Bulk Shielding Facility. In these experiments counts taken with the back shield alternately in place and removed showed no differences greater than counting errors.

The transmission predicted for the ^{10}B filters by the calculations was in excellent agreement with the experimental calibrations described earlier.

The epithermal-neutron spectrometer is now at the stage of final adjustment and checkout and is expected to shortly be put to practical test in connection with neutron-scattering experiments at the Tower Shielding Facility.

References and Notes

[1]Work funded by Defense Atomic Support Agency under DASA Order EO-851-64.

[2]T. V. Blosser, *Neutron Phys. Div. Ann. Progr. Rept. Aug. 1, 1964,* ORNL-3714, vol. 1, p. 84.

[3]Expansion of the basic concepts into the design and fabrication of the final instrument have been principally the work of T. F. Sliski, Instrumentation and Controls Division.

[4]The counters were designed and constructed by R. K. Abele and W. T. Clay of the Instrumentation and Controls Division.

[5]Made available through the cooperation of J. A. Harvey, R. C. Block, and G. G. Slaughter, all of the Physics Division.

[6]R. R. Coveyou *et al., O5R, A General-Purpose Monte Carlo Neutron Transport Code,* ORNL-3622 (February 1965).

6.3 ISOTROPICALLY RESPONDING FAST-NEUTRON DOSIMETER[1]

T. V. Blosser

The development of a highly sensitive, isotropically responding fast-neutron dosimeter was outlined in a previous report.[2] Briefly, the goal of this development is the production of an instrument which will have a lower limit of sensitivity of the order of 0.02 millirad/hr, which will have an isotropic response proportional to the Snyder-Neufeld multicollision dose curve,[3] and which will be usable over an energy range from the epithermal region to ~15 Mev.

The basic scheme of the dosimeter is that of a relatively small, sensitive thermal-neutron detector (a BF_3 proportional counter) centrally embedded in a sphere of moderating material. Experiments to date have used moderating spheres of 8-, 10-, and 12-in. diameters, consisting either of pure polyethylene or, in a few experiments, of polyethylene with a thin boron-loaded plastic shell around the detector.

The detector used within the spheres consists of a 2-in.-diam spherical BF_3 proportional counter containing a double-loop ion collector and filled to a pressure of ½ atm with BF_3, enriched to 96% in the ^{10}B isotope. In arriving at this choice, 1-, 1½-, and 2-in.-diam counters, single- and double-loop ion collectors, and pressures of ½ and 1 atm were studied. The preferred ion collector is formed as a double circular loop, ⅜ or ½ in. in diameter, of 2-mil-diam tungsten, with the loops perpendicular

to each other and concentric with the thin-walled copper sphere which forms the body of the counter.

Thus far the simple configuration of counter and polyethylene sphere have been studied with ~3- and ~14-Mev accelerator-produced neutrons, and some tests and calibrations have been made using an approximately $1/E$ neutron beam from the Bulk Shielding Reactor. In the latter tests the beam was attenuated by a series of the ^{10}B filters which are part of the epithermal-neutron spectrometer described in Sect. 6.2.

The optimum diameter for the moderating sphere appears to be about 10 in. The use of boron shells around the detector did not seem to have any effect other than a straightforward lowering of all counting rates. However, it is more or less expected that some addition to the material of the moderating sphere will eventually be desirable in order to improve (increase) the response of the dosimeter in the energy region between 10 and 15 Mev. Materials undergoing (n,n') or $(n,2n)$ reactions will be investigated for this purpose.

References and Notes

[1]Work funded by Defense Atomic Support Agency under DASA Order EO-850-65.

[2]T. V. Blosser, *Neutron Phys. Div. Ann. Progr. Rept. Aug. 1, 1964,* ORNL-3714, vol. 1, p. 84.

[3]W. S. Snyder and C. Neufeld, *Radiation Res.* **6**(1), 67 (1957).

6.4 NEW METHOD FOR THE EVALUATION OF NEUTRON EMISSION, KERMA, KERMA EQUIVALENT, DOSE EQUIVALENT, AND THE SPECTRUM BELOW 1 Mev FOR (α,n) SOURCES, USING BONNER SPHERES[1]

S. K. Mehta[2]

Neutron emission (F), kerma (K), kerma equivalent (Keq), dose equivalent (DE), the ratios K/F, Keq$/F$, and DE$/F$, and an upper bound to the neutron spectrum below 1 Mev have been obtained for Am-Be, Pu-Be, Po-Be, and Am-B neutron sources by using a modified Bonner-sphere neutron spectrometer. The spectrometer consisted of 0- to 12-in.-diam Bonner spheres and 0- to 3-in.-diam spheres modified by the addition of boron and cadmium covers. The results were computed by the OPTIMO linear programming code, which synthesizes optimal combinations of the response of the various spheres. The known smoothness of the neutron spectrum from each source was utilized, and an upper bound to the spectrum above 5.5 Mev was taken from other measurements, since the response of the Bonner spheres does not have enough variation above 5.5 Mev. The response of the modified spheres to monoenergetic neutrons was calculated by assuming exponential absorption below 1 kev and by S_n transport calculations above 1 kev. The values of DE$/F$ in units of rems neutron^{-1} cm^{-2} for the Am-Be, Pu-Be, Po-Be, and Am-B sources are $(3.79 \pm 0.23)10^{-8}$, $(3.72 \pm 0.28)10^{-8}$, $(3.84 \pm 0.19)10^{-8}$, and $(3.75 \pm 0.21)10^{-8}$ respectively. The errors given refer to the 68% confidence intervals and include all known sources of error.

References and Notes

[1]Abstract of ORNL-TM-1171 (July 1965).

[2]Atomic Energy Establishment Trombay, Bombay, India.

6.5 DIGITAL FILTER FOR UNFOLDING PULSE-HEIGHT DISTRIBUTIONS[1]

H. Young[2] W. R. Burrus

A digital "filter" computer program has been developed which removes undesired spurious features (such as Compton tails, escape peaks, etc.) from the response of a scintillation spectrometer. The input to the filter is the digital representation of the pulse-height distribution, and the output consists of a digital representation of the desired unfolded spectrum. A relatively clean Gaussian line is obtained from the filter. The filtering procedure is simple enough that small computers or built-in circuitry can be used on-line to give rapid unscrambled results. Thus far we have simulated the filter off-line and, by using the respective pulse-height data of R. Heath and of G. Chapman, have demonstrated its capabilities with a 3- by 3-in. NaI(Tl) gamma spectrometer and an 8- by 12-in. NaI(Tl) total-absorption gamma spectrometer. A QUIKTRAN[3] version of the filter is given which includes nonlinearity corrections and rigorous error estimates. The execution time of the QUIKTRAN program off-line is about 1 sec on the IBM 7090 computer.

References and Notes

[1]Abstract of paper to be submitted to *The Review of Scientific Instruments*.

[2]ORINS Research Participant at ORNL during summer of 1965.

[3]A remote terminal computing system which can be leased to be used via a data phone to an IBM computer center.

6.6 FAST-NEUTRON SPECTROSCOPY WITH ORGANIC SCINTILLATORS[1]

V. V. Verbinski J. C. Courtney[2]
W. R. Burrus R. Textor[3]

Part I

The proton-recoil scintillator technique for measuring neutron spectra has been extended to larger scintillators than those used previously; this was made possible by taking into account multiple scattering, charged-particle reactions, and carbon recoils. The main features are high efficiency, moderately good resolution, simple circuitry, and gamma-ray pulse rejection. The code used to analyze the data was the recently developed FERDO code, which is based on quadratic programming and utilizes the known nonnegativity of the neutron spectrum. This code requires accurate responses to monoenergetic neutrons for the scintillator. These responses were obtained by a combination of calculations and experimental measurements as described in Part II of this series. The code forms combinations of the counting efficiency functions for each channel of the analyzer, so that the resulting combinations approximate an idealized spectrometer with the desired response function.

Part II

The response of a 2- by 2-in. and a 5- by 5-in. cylindrical organic scintillator has been obtained with Monte Carlo calculations that utilized measured light-response functions of the scintillator material to recoil protons, alpha particles, and recoil carbon nuclei. Several precision experiments utilizing the associated-particle technique were employed to check the absolute pulse-height distribution for a unit flux and also to provide data on the response of the scintillators to carbon recoils and alpha particles. The 2- by 2-in. scintillator is especially suitable for neutron spectroscopy by the method of unfolding pulse-height distributions described in Part I of this series, but either scintillator can be used in time-of-flight spectroscopy. For the latter application, the scintillators can be used directly or as standards of calibration for scintillators of arbitrary size and shape.

References and Notes

[1]Combined abstracts of ORNL-TM-1272 (Part I, *Instrumentation and Data Reduction*) (in preparation) and ORNL-TM-1273 (Part II, *Response of Some Organic Scintillators to 0.2–20 Mev Neutrons*) (in preparation).

[2]Catholic University, Washington, D.C.; Graduate Fellow, Oak Ridge Institute of Nuclear Studies.

[3]Central Data Processing Facility, Oak Ridge Gaseous Diffusion Plant.

6.7 USE OF A DIGITAL COMPUTER IN TIME-OF-FLIGHT EXPERIMENTS[1]

R. Gwin L. W. Weston R. Ingle[2]

A general-purpose digital computer has been incorporated as an integral part of a data acquisition and processing system for use in neutron time-of-flight experiments. The experiments are designed to measure the neutron-capture and fission cross sections of ^{235}U, ^{233}U, and ^{239}Pu as a function of neutron energy.

A digital computer[3] was chosen for the time-of-flight experiments because its data-handling capacity was greater than that of a conventional analyzer. In the application of conventional analyzer systems to time-of-flight spectroscopy, the channel width, Δt, is chosen to meet the energy resolution required by the experiment. The computer was programmed to simulate a series of analyzers, each having a channel width appropriate for the energy region covered. Eight regions were used, with the channel width changing by a factor of 2 in successive regions.[4] The recording of data in this manner greatly increases the time range which can be covered without sacrificing energy resolution.

Other advantages of the digital computer are the increased flexibility in the control of the experi-

ments and the scope display, which permits a detailed visual inspection of the data during the experiment and programmed operations on memory regions displayed by the scope.

References and Notes

[1]Abstract of paper submitted for presentation at 12th Nuclear Science Symposium, San Francisco, Calif., October 1965.

[2]Instrumentation and Controls Division.

[3]The computer was a PDP-4 manufactured by the Digital Equipment Company.

[4]J. E. Russell and R. Hockenbury of Rensselaer Polytechnic Institute, Troy, New York, participated with the ORNL group in this set of experiments.

6.8 FAST-NEUTRON SPECTROMETER FOR REACTOR ENVIRONMENTS[1]

V. V. Verbinski M. S. Bokhari[2]

A ^{6}Li diode sandwich fast-neutron spectrometer has been designed and applied to spectral measurements in the water shield of a pool-type research reactor where the gamma flux was as high as 10^6 r/hr. By using the ^{6}Li(n,α)T reaction having a Q value of 4.78 Mev, demanding a coincidence count between the alpha particle and the triton, and selectively shielding the diodes, backgrounds from gammas and fast neutrons striking the diodes are reduced. In addition, these reduced backgrounds are accurately determined by substituting a ^{7}Li foil for the ^{6}Li sensitive element. The spectral intensity of angular flux, $\Phi(\mu, r, E)$, was mapped at points near the reactor and compared with the results of a neutron transport calculation, with both measurement and calculation normalized to the same absolute neutron source intensity.

References and Notes

[1]Abstract of paper to be submitted to *Nuclear Instruments & Methods*.

[2]Now at Lahore Center, Pakistan Atomic Energy Commission, Lahore, Pakistan.

Publications

(Through October 1, 1965)

ALSMILLER, R. G., JR.

"Statistical Model Calculations of Nucleon-Nucleon and Pion-Nucleon Collisions: Center-of-Mass Spectra," ORNL-3713 (November 1964).

"Statistical Model Calculations of Nucleon-Nucleon and Pion-Nucleon Collisions: Laboratory-Angle Distributions Assuming Isotropy in the Center-of-Mass System," ORNL-3716 (November 1964).

ALSMILLER, R. G., JR., AND J. BARISH*

"Calculation of the Nuclear Cascade in Steel Initiated by 10- and 19.2-GeV/c Protons and Comparison with Experiment," ORNL-TM-1072 (May 1965).

"The Nucleon-Meson Cascade Initiated by 200-GeV Protons," ORNL-TM-1121 (May 3, 1965).

ALSMILLER, R.G., JR., F. S. ALSMILLER, AND J. BARISH*

"Nucleon-Meson Calculations: Transverse Shielding for a 45-GeV Electron Accelerator. Part IV," ORNL-3734 (March 1965).

ALSMILLER, R. G., JR., D. C. IRVING, W. E. KINNEY, AND H. S. MORAN

"The Validity of the Straightahead Approximation in Space Vehicle Shielding Studies," in *Second Symposium on Protection Against Radiation Hazards in Space, Gatlinburg, Tennessee, Oct. 12–14, 1964,* NASASP-71 (in press).

BEGHIAN,* L. E., S. WILENSKY,* AND W. R. BURRUS

"A Fast Neutron Spectrometer Capable of Nanosecond Time Gating," *Nucl. Instr. Methods* **35**, 34 (1965).

BRIENT, C. E.,* E. L. HUDSPETH,* E. M. BERNSTEIN,* AND W. R. SMITH

"The $^{90}Zr(d,p)^{91}Zr$ Reaction at Energies Below 4 MeV," ORNL-TM-1102 (April 1965).

BERTINI, H. W.

"Angular Momentum Calculation from Intranuclear Cascades," ORNL-TM-1033 (Feb. 19, 1965).

"Particles Emitted in the Forward Direction from High-Energy Nucleon-Nucleus Knock-on Reactions," in *Second Symposium on Protection Against Radiation Hazards in Space, Gatlinburg, Tennessee, Oct. 12–14, 1964,* NASASP-71 (in press).

BLIZARD, E. P., A. D. CALLIHAN, AND F. C. MAIENSCHEIN

"Neutron Physics Division Annual Progress Report for Period Ending August 1, 1964," ORNL-3714, Vols. 1 and 2.

BOKHARI, M. S., AND V. V. VERBINSKI

"Fast Neutron Transport in Water," *Trans. Am. Nucl. Soc.* **7**(2), 370 (1964).

*Non-Division personnel.

BURRUS, W. R.
"The Utilization of *a Priori* Information by Means of Mathematical Programming in the Statistical Interpretation of Measured Distributions," ORNL-3743 (June 1965).

BURRUS, W. R., AND V. V. VERBINSKI
"Recent Developments in the Proton-Recoil Scintillation Neutron Spectrometer," *Trans. Am. Nucl. Soc.* **7**(2), 373 (1964).

CAIN, V. R.
"Propagation of Neutron Waves Through Heterogeneous Multiplying and Nonmultiplying Media," ORNL-TM-1184 (August 1965).

CALLIHAN, DIXON, AND E. B. JOHNSON
"A Standard for Operations with Fissionable Materials Outside Reactors," *Mag. Std.* **36**, 81 (1965).

CHAPMAN, G. T.
"Determination of Thermal-Neutron Flux Distributions in the Bulk Shielding Reactor II by Copper Wire Activation Techniques," ORNL-3759 (March 1965) (formerly referred to as ORNL-TM-846).

CHAPMAN, G. T., K. M. HENRY, AND J. D. JARRARD
"Pulse-Height Spectra of Gamma Rays Emitted by Stainless-Steel-Clad Bulk Shielding Reactor II (BSR-II)," ORNL-3609 (November 1964).

CHILDERS, R. L., C. D. ZERBY, C. M. FISHER,* AND R. H. THOMAS*
"Shielding Experiments with Iron for 10 and 20 GeV/c Protons. Part III. Measurement of the Nuclear Cascade at 10 GeV/c with Emulsion," *Nucl. Instr. Methods* **32**, 53 (1965).

CLAIBORNE, H. C.*
"Survey of Methods for Calculating Gamma-Ray Heating," ORNL-RSIC-8 (June 1965).

CLARK, F. H. S., AND F. B. K. KAM
"A Generalized One-Constraint Lagrange Multiplier Numerical Formulation," ORNL-3742 (March 1965).

CLARK, F. H. S., F. B. K. KAM, AND F. J. MUCKENTHALER
"Measurements and Calculations of Neutron Transmission Through Lithium Hydride," *Trans. Am. Nucl. Soc.* **7**(2), 354 (1964).

COLEMAN, W. A.
"A Determination of Intermediate-Energy Neutron Albedo Data for Concrete Using Monte Carlo," ORNL-TM-1205 (September 1965).

COLLINS,* D. G., R. L. FRENCH,* L. G. MOONEY,* K. W. TOMPKINS,* AND M. B. WELLS*
"Simplified Methods for Calculating the Penetration of Neutron and Gamma Radiation into Underground Concrete Structures," Radiation Research Associates Report RRA-M45 (Nov. 25, 1964).

COURTNEY, J. C.
"Fast-Neutron Scattering from Small Cylinders of Steel, Aluminum, and Graphite," ORNL-TM-1146 (July 1965).

COURTNEY, J. C., AND V. V. VERBINSKI
"Measured Neutron Source Spectra for Angular Scattering Experiments with Small Cylinders," ORNL-TM-1087 (Apr. 9, 1965).

COVEYOU, R. R.
"A Monte Carlo Technique for Selecting Scattering Angles from Anisotropic Distribution," *Nucl. Sci. Eng.* **21**, 257 (1965).

COVEYOU, R. R., D. C. IRVING, R. M. FREESTONE, JR., F. B. K. KAM, J. G. SULLIVAN,* AND H. P. CARTER*
"O5R, A General-Purpose Monte Carlo Neutron Transport Code," ORNL-3622 (February 1965).

*Non-Division personnel.

de SAUSSURE, G., L. W. WESTON, R. GWIN, J. E. RUSSELL,** AND R. W. HOCKENBURY*
"Measurement of the ^{235}U Neutron Capture-to-Fission Ratio, α, for Incident Neutron Energies from 3.25 eV to 1.8 keV," ORNL-TM-1041 (Jan. 26, 1965); also *Nucl. Sci. Eng.* **23**, 45 (1965).

"Measurement of α, the Ratio of the Neutron Capture Cross Section to the Fission Cross Section, for ^{235}U in the Energy Region 3.25 eV to 1.8 keV," ORNL-3738 (April 1965).

DICKENS, J. K., R. M. DRISCO,* F. G. PEREY, AND G. R. SATCHLER*
"Local Energy Approximation for Finite-Range in Stripping Reactions," *Phys. Letters* **15**(4), 337 (1965).

DICKENS, J. K., AND F. G. PEREY
"Effect of Data Normalization upon Deuteron Optical-Model Parameters," ORNL-TM-970 (October 1964); also *Phys. Rev.* **138**, B1080 (1965).

"Elastic Scattering of Low-Energy Deuterons from ^{60}Ni and ^{114}Cd and the Effect of the Deuteron Electric Polarizability in the Optical-Model Potential," ORNL-TM-962 (October 1964); also *Phys. Rev.* **138**, B1083 (1965).

DICKENS, J. K., F. G. PEREY, AND R. J. SILVA*
"Elastic Scattering of 12.0- and 14.0-MeV Deuterons from ^{90}Zr and the Reaction ^{90}Zr$(d,p)^{91}$Zr: Tabulated Differential Cross Sections," ORNL-3850 (September 1965).

DICKENS, J. K., AND R. J. SILVA*
"Elastic and Inelastic Scattering of 12.0-MeV Protons from ^{62}Ni, ^{63}Cu, and ^{64}Zn: Tabulated Differential Cross Sections," ORNL-3851 (September 1965).

DRESNER, L.
"The Exclusion of Ions from Charged Microporous Solids," *J. Phys. Chem.* **69**, 2230 (1965).

"Neutron Physics," translated by L. Dresner, ed. by K. H. Beckurts and K. Wirtz, Springer, New York, 1964.

FRENCH, R. L.,* M. B. WELLS,* AND N. M. SCHAEFFER*
"Penetration of Neutron and Gamma Radiation Through the Openings of Underground Structures," Radiation Research Associates Report RRA-T41 (Nov. 30, 1964).

"Neutron and Gamma Radiation Penetration into Concrete-Shielded Underground Structures," Radiation Research Associates Report RRA-T51 (May 31, 1965).

GIBSON, W. A., W. R. BURRUS, W. E. KINNEY, J. WACHTER, AND C. F. JOHNSON*
"Comparison of Measured Neutron and Proton Spectra with Calculated Spectra in the Energy Region Between 50 and 160 MeV," in *Second Symposium on Protection Against Radiation Hazards in Space, Gatlinburg, Tennessee, Oct. 12–14, 1964,* NASASP-71 (in press).

GWIN, R., G. de SAUSSURE, L. W. WESTON, E. HADDAD,* AND W. M. LOPEZ*
"An Investigation of a Technique for Measuring the Fission and Capture Cross Sections of ^{233}U and ^{239}Pu," *Trans. Am. Nucl. Soc.* **7**(2), 269 (1964).

HILL, N. W.*
"A Sensitive Tunnel-Diode Discriminator," ORNL-TM-998 (Jan. 12, 1965).

HILL, N. W.,* AND C. O. McNEW*
"The Choice of Capacitors for Nanosecond Circuits," ORNL-TM-999 (Apr. 26, 1965).

IRVING, D. C., R. G. ALSMILLER, JR., W. E. KINNEY, AND H. S. MORAN
"The Secondary-Particle Contribution to the Dose from Monoenergetic Proton Beams and the Validity of Flux-to-Dose Conversion Factors," in *Second Symposium on Protection Against Radiation Hazards in Space, Gatlinburg, Tennessee, Oct. 12–14, 1964,* NASASP-71 (in press).

*Non-Division personnel.

**Deceased.

IRVING, D. C., AND J. T. MIHALCZO
"Monte Carlo Calculations for Enriched Uranium Metal," *Trans. Am. Nucl. Soc.* **7**(2), 287 (1964).

JOHNSON, E. B., AND D. F. CRONIN*
"Critical Dimensions of Aqueous UO_2F_2 Solutions Containing 4.9% Uranium-235-Enriched Uranium," *Trans. Am. Nucl. Soc.* **7**(2), 301 (1964).

KINNEY, W. E.
"Some Tests of Coveyou's Anisotropic Selection Technique," *Nucl. Sci. Eng.* **21**, 257 (1965).

"NTC: A Transport Code for Protons and Neutrons of Energy up to 400 MeV," *Trans. Am. Nucl. Soc.* **7**(2), 324 (1964).

KINNEY, W. E., AND C. D. ZERBY*
"Calculated Tissue Current-to-Dose Conversion Factors for Nucleons Below 400 MeV," in *Second Symposium on Protection Against Radiation Hazards in Space, Gatlinburg, Tennessee, Oct. 12–14, 1964,* NASASP-71 (in press); also ORNL-TM-1038 (May 1965).

McCONNELL, J. W.*
"Nanosecond Light Sources for Gain Stabilization," ORNL-TM-985 (June 1965).

MAERKER, R. E., AND F. J. MUCKENTHALER
"Calculation and Measurement of the Fast-Neutron Differential Dose Albedo for Concrete," ORNL-TM-1028 (January 1965).

"Differential Fast-Neutron Albedos for Concrete," ORNL-3822

Vol. II: "Results of Monte Carlo Calculations for an Incident Angle of 0 deg" (July 1965).

Vol. III: "Results of Monte Carlo Calculations for an Incident Angle of 45 deg" (July 1965).

Vol. IV: "Results of Monte Carlo Calculations for an Incident Angle of 60 deg" (July 1965).

Vol. V: "Results of Monte Carlo Calculations for an Incident Angle of 75 deg" (July 1965).

Vol. VI: "Results of Monte Carlo Calculations for an Incident Angle of 85 deg" (July 1965).

"Calculation and Measurement of the Fast-Neutron Differential Dose Albedo for Concrete," *Trans. Am. Nucl. Soc.* **7**(2), 365 (1964).

MAIENSCHEIN, F. C.
"Methods of Fast-Neutron Spectroscopy for Reactor Shielding," *Trans. Am. Nucl. Soc.* **7**(2), 368 (1964).

MEHTA, S. K.
"A New Method for the Evaluation of Neutron and Emission Kerma, Kerma Equivalent, and Dose Equivalent, and Spectrum Below 1 MeV for (α,n) Source Using Bonner Spheres," ORNL-TM-1171 (July 1965).

MIHALCZO, J. T.
"One-Velocity Monte Carlo Calculations of Uranium Metal Critical Geometries," *Trans. Am. Nucl. Soc.* **8**(1), 201 (1965).

"Increased Yields from Fast-Burst Reactors. Part I. Effects of Increased Mass on Uranium and Uranium-Molybdenum Critical Cylinders," ORNL-TM-1125 (Apr. 30, 1965).

MIHALCZO, J. T., G. W. MORRISON,* AND D. C. IRVING
"SOURCE, A Neutron Distribution Routine for the O5R Monte Carlo Code," ORNL-TM-1192 (July 8, 1965).

PEELLE, R. W.
"Rapid Computation of Specific Energy Losses for Energetic Charged Particles," ORNL-TM-977 (Apr. 29, 1965).

*Non-Division personnel.

"Determination of Coincidence-Circuit Efficiency by Varying the Input Signal Delay," *Nucl. Instr. Methods* **29**, 293 (1964).

PEELLE, R. W., T. A. LOVE, N. W. HILL,* AND R. T. SANTORO
"Differential Cross Sections by Flight Time Spectroscopy for Proton Production in Reactions of 16-MeV Protons on Nuclei," in *Second Symposium on Protection Against Radiation Hazards in Space, Gatlinburg, Tennessee, Oct. 12–14, 1964,* NASASP-71 (in press).

PENNY, S. K., D. K. TRUBEY, AND M. B. EMMETT*
"Bibliography, Subject Index, and Author Index of the Literature Examined by the Radiation Shielding Information Center," ORNL-RSIC-5 (March 1965).

"Radiation Shielding Information Retrieval System," p. 251 in *Automation and Scientific Communication,* ed. by H. P. Luhn, American Documentation Institute, Washington, D.C.

SANTORO, R. T., W. R. BURRUS, W. A. GIBSON, N. W. HILL,* C. F. JOHNSON,* T. A. LOVE, F. C. MAIENSCHEIN, R. W. PEELLE, J. W. WACHTER, AND W. ZOBEL
"The Space, Time, and Energy Distribution of the Proton Beam of the Harvard University Synchrocyclotron," ORNL-3722 (January 1965).

SANTORO, R. T., AND H. WEAVER
"Method for Making Inexpensive Thick Boron Targets to Obtain Gamma Rays from the $B^{11}(p,\gamma)C^{12}$ Reaction," *Rev. Sci. Instr.* **36**(1), 98 (1965).

SCROGGS, R. J.,* W. ZOBEL, AND F. C. MAIENSCHEIN
"A Multicrystal Gamma-Ray Spectrometer with Time-of-Flight Rejection of Neutron-Induced Background," *IEEE Trans. Nucl. Sci.* **11**, 365 (1964).

SHERWOOD, T. K.,* P. L. T. BRIAN,* R. E. FISHER,* AND L. DRESNER
"Salt Concentration at Phase Boundaries in Desalination Processes," *Ind. Eng. Chem. Fundamentals* **4**(2), 113 (1965).

SILVER, E. G.
"Measurement of the Neutron Diffusion Parameters in Ordinary Ice as a Function of the Temperature by the Method of Time-Dependent Neutron Diffusion," ORNL-TM-1204 (September 1965).

SMITH, W. R.
"Regions of Validity of the (d,p) Coulomb Stripping Approximation," ORNL-TM-1025 (January 1965).

"Distorted Wave Analysis of the $Zr^{90}(d,p)Zr^{91}$ Stripping Reaction," pp. 30–37 in *Nuclear Spectroscopy with Direct Reactions, Contributed Papers,* Vol. I, ANL-6848 (n.d.).

"A General Hauser-Feshbach Nuclear Scattering Program" ORNL-TM-1117 (May 1965).

"DWB Deuteron Stripping Computer Program," ORNL-TM-1151 (June 10, 1965).

"Use of Elastic-Scattering Parameters in (d,p) Stripping Calculations," *Phys. Rev.* **137**, B913 (1965).

TRUBEY, D. K.
"Tabulated Values of Scattered Gamma-Ray Fluxes in Iron Interpolated from Moments-Method Calculations," ORNL-RSIC-7 (May 1965).

"A Calculation of the Neutron Dose in Ordinary Concrete Due to Air-Scattered Neutrons from a Point Fission Source," ORNL-TM-973 (Mar. 15, 1965).

TRUBEY, D. K., AND M. B. EMMETT*
"A Comparison of First- and Last-Flight Expectation Values Used in an O5R Monte Carlo Calculation of the Neutron Distributions in Water," ORNL-RSIC-3 (May 1965); also *Trans. Am. Nucl. Soc.* **7**(2), 357 (1964).

*Non-Division personnel.

"Some Calculations of the Fast-Neutron Distribution in Ordinary Concrete from Point and Plane Isotropic Fission Sources," ORNL-RSIC-4 (June 1965).

VERBINSKI, V. V.
"Angular Distributions of Low-Energy Neutrons Leaking from Various Scattering Materials," ORNL-TM-1078 (May 13, 1965).

"Slowing-Down Spectra of Neutrons in Lithium Hydride," ORNL-TM-1077 (May 1965).

VERBINSKI, V. V., AND J. C. COURTNEY
"Photoneutron Spectra and Cross Sections for ^{12}C and ^{16}O," ORNL-TM-1158 (June 1965).

VERBINSKI, V. V., J. C. COURTNEY, W. R. BURRUS, T. A. LOVE, AND J. G. SULLIVAN*
"Response Functions of an Organic Scintillator to Fast Neutrons," *Trans. Am. Nucl. Soc.* **7**(2), 374 (1964).

WEBSTER, J. W.
"Boundary Conditions for the Cylindricalized Cell of Reactor Lattice Calculations," ORNL-TM-1022 (Dec. 30, 1964).

"The Determination of Neutron Flux in Nuclear Reactors by the Uncollided-Flux Estimator Applied to Monte Carlo Collisions," ORNL-TM-1175 (August 1965).

WEBSTER, J. W., AND E. B. JOHNSON
"Criticality of a Single Unit of Aqueous Uranyl Fluoride Solution Enriched to 5% in ^{235}U," ORNL-TM-1195 (July 23, 1965).

WESTON, L. W., G. de SAUSSURE, R. GWIN, J. E. RUSSELL,** AND R. W. HOCKENBURY*
"Measurements of the Variation of the Ratio of the Capture and Fission Cross Sections of ^{235}U," *Trans. Am. Nucl. Soc.* **7**(2), 270 (1964).

ZOBEL, W., F. C. MAIENSCHEIN, AND R. J. SCROGGS*
"Spectra of Gamma Rays Produced by the Interaction of ~160-MeV Protons with Be, C, O, Al, Co, and Bi," in *Second Symposium on Protection Against Radiation Hazards in Space, Gatlinburg, Tennessee, Oct. 12–14, 1964,* NASASP-71 (in press); also ORNL-3506 (April 1965).

*Non-Division personnel.
**Deceased.

ORNL-3858, Vol. I
UC-34 – Physics
TID-4500 (45th ed.)

INTERNAL DISTRIBUTION

1. L. S. Abbott
2. F. S. Alsmiller
3. R. G. Alsmiller, Jr.
4. H. W. Bertini
5. N. A. Betz
6. J. A. Biggerstaff
7–31. E. P. Blizard
32. T. V. Blosser
33. W. R. Burrus
34. V. R. Cain
35. A. D. Callihan
36. Y. Cassagsnou
37. G. T. Chapman
38. H. C. Claiborne
39. F. H. S. Clark
40. C. E. Clifford
41. W. Coleman
42. R. R. Coveyou
43. G. de Saussure
44. J. K. Dickens
45. L. Dresner
46. R. M. Drisko
47. J. F. Ellis
48. M. B. Emmett
49. R. M. Freestone, Jr.
50. W. A. Gibson
51. L. W. Gilley
52. J. H. Gillette
53. M. Guthrie
54. R. Gwin
55. V. M. Hamrick
56. M. V. Harlow
57. M. P. Haydon
58. K. M. Henry, Jr.
59. L. B. Holland
60. J. L. Hull
61. R. Ingle
62. D. Irving
63. E. B. Johnson
64. W. H. Jordan
65. F. B. K. Kam
66. W. E. Kinney
67. G. A. Kistner
68. C. E. Larson
69. M. Leimdorfer
70. J. Lewin
71. A. Lottin
72. T. A. Love
73. J. J. Lynn
74. H. G. MacPherson
75. R. E. Maerker
76. D. W. Magnuson
77. F. C. Maienschein
78. J. J. Manning
79. B. F. Maskewitz
80. J. W. McConnell
81. J. T. Mihalczo
82. B. McGill
83. H. S. Moran
84. F. J. Muckenthaler
85–86. R. B. Parker
87. R. W. Peelle
88. S. K. Penny
89. C. M. Perey
90. F. G. Perey
91. S. J. Raffety
92. E. R. Rohrer
93. G. R. Satchler
94. R. T. Santoro
95. R. J. Silva
96. E. G. Silver
97. M. J. Skinner
98. E. A. Straker
99. J. T. Thomas
100. D. K. Trubey
101. W. C. Tunnell
102. V. V. Verbinski
103. J. Wachter
104. D. R. Ward
105. J. W. Webster
106. A. M. Weinberg
107. L. W. Weston
108. G. C. Williams
109. G. Young
110. K. J. Yost
111. W. Zobel
112. G. Dessauer (consultant)
113. M. L. Goldberger (consultant)
114. M. H. Kalos (consultant)
115. L. V. Spencer (consultant)

116. Radiation Shielding Information Center
117. Biology Library
118–120. Central Research Library
121. Reactor Division Library
122–123. ORNL-Y-12 Technical Library, Document Reference Section
124–423. Laboratory Records Department
424. Laboratory Records, ORNL R.C.

EXTERNAL DISTRIBUTION

425. Research and Development Division, AEC, ORO
426. V. B. Bhanot, Physics Dept. Panjab University, Chandigarh-3, India
427. Radiation Physics Division, Health and Safety Laboratory, New York Operations Office
428. R. W. McNamee, Union Carbide Corporation, New York
429–798. Given distribution as shown in TID-4500 (45th ed.) under Physics Category (75 copies – CFSTI)